CRUSTAL STRUCTURE OF THE SOUTHWESTERN COLOMBIAN CARIBBEAN MARGIN

Geological interpretation of geophysical data

Dissertation

zur Erlangung des akademischen Grades doctor rerum naturalium

(Dr. rer. nat.)

Vorgelegt dem Rat der Chemisch-Geowissenschaftlichen Fakultät der
Friedrich-Schiller-Universität Jena

von Diplom-Geologin Adriana Maria Mantilla Pimiento
geboren am 7. Februar 1971 in Bucaramanga, Kolumbien

Gutachter

Prof. Dr. Gerhard Jentzsch
Prof. Dr. Jonas Kley
Friedrich-Schiller-Universität Jena, Insitut für Geowissenschaften

Tag der öffentlichen Verteidigung:
28. November 2007

To Carlos Arturo, Richard, Myriam, José Manuel and Monica with love and gratitude.

CONTENTS

LIST OF FIGURES

LIST OF TABLES

ABSTRACT

The active Colombian Caribbean margin has evolved since the late Cretaceous time, resulting in a complex deformation history involving oblique subduction, accretion, extension and tectonic inversion during the Cenozoic period.

The combined interpretation of 2D seismic reflection, gravity and magnetic data provides new insights into the margin configuration (Morrosquillo Gulf area) and the architecture and types of crust present. The margin displays the morphological and tectonic characteristics of a typical accretion-dominated subduction complex. The 3D gravity modelling suggests that the Caribbean Plate is subducting beneath NW Colombia at a low angle of about 5° in an E to SE direction. The major tectonic domains forming the margin include, from west to east: trench, active accretionary prism, outer high and forearc basins.

The trench axis coincides with the toe of the active accretionary prism. The active prism corresponds to the deformation front of the Sinú-Colombia Accretionary Wedge. The outer high domain includes the major structural complex formed by the easternmost part of the Sinú-Colombia Accretionary Wedge and the San Jacinto Fold Belt. It represents the fossil part of the accretionary prism which today acts as a dynamic backstop to the active accretionary prism. The outer high comprises several small sedimentary basins containing post-kinematic Plio-Pleistocene deposits which fossilize the complex outer high structure. The landward boundary of the outer high is marked by the well-developed positive flower structure of the Romeral North or San Jacinto Fault System which represents a structural break between the smaller basins deformed by mud diapirism to the west and the main and deeper forearc San Jorge Basin to the east.

The basement-type present along the outer high-forearc transition (San Jacinto Fold Belt-San Jorge Basin) is still discussed controversially. The results of 3D gravity and 3D magnetic modelling in this study support the presence of an oceanic "basement complex" (mixture of basalts and sediments) underlain by a continental tectonic wedge (CTW) which belongs to the overriding South American Plate. The emplacement of oceanic affinity rocks over continental basement is interpreted as offscraping and backthrusting of Caribbean material onto the continental margin during the initiation of the oblique subduction of Caribbean crust beneath NW South America. The continental crust of the South American arc framework provided the static backstop against which the material of the later dynamic backstop was accreted.

The existence of a continental tectonic wedge (CTW) beneath the oceanic "basement complex" in the San Jacinto Fold Belt (east of the Romeral Zone) indicates that the Romeral North Fault System does not form the tectonic boundary between oceanic crust to the west and continental crust to the east. The Romeral fault and its associated structures form a dextrally transpressive fault system developed within

continental crust (the static backstop) as a result of the oblique convergence between Caribbean and South American plates.

From the crustal model proposed here, two tectonic limits are identified as ocean-continental crust boundaries: an upper one, which represents a major east-directed backthrust that detached oceanic basalts and sediments from the downgoing slab emplacing them over the continental tectonic wedge (CTW), and a lower one, which corresponds to the east-dipping boundary between the downgoing Caribbean and overriding South American plates.

The heat flow distribution in NW Colombia has been controlled by different tectonic uplift and subsidence phases undergone by the accretionary complex during its development. Therefore, the burial and thermal history is very difficult to constrain. Based on general calculations of thermal maturity (vitrinite reflectance) vs. depth and depth-interpretation from the resultant 3D crustal model and a few wells, it can be concluded that a major part of the upper Cretaceous source rocks are overmature, whereas part of the Miocene rocks have not yet reached the mature stage.

ZUSAMMENFASSUNG

Der kolumbianisch-karibische aktive Kontinentalrand hat sich seit der späten Kreidezeit entwickelt und zeigt eine sehr komplexe Deformationsgeschichte, die Subduktion- und Akkretionsprozesse, Extension und tektonische Inversion während des Känozoikums umfasst.

Die kombinierte Interpretation von 2D-reflexionsseismischen Profilen, gravimetrischen und magnetischen Daten erlaubt die Entwicklung eines neuen Strukturmodells und die Bestimmung der Krustenarchitektur und Krustentypen am Plattenrand im Gebiet des Morosquillo-Golfs. Der Kontinentalrand zeigt die morphologischen und tektonischen Eigenschaften eines typischen akkretionsdominierten Subduktionskomplexes. Die 3-dimensionale gravimetrische Modellierung legt nahe, dass die karibische Platte mit einem geringen Einfallwinkel von 5° in E- bis SE-Richtung unter NW Kolumbien subduziert wird. Die wichtigsten tektonischen Elemente des Plattenrandes sind von Ost nach West die Tiefseerinne (trench), das aktive Akkretionsprisma, das äußere Hoch (Outer High) und das Forearc-Becken.

Die Achse der Tiefseerinne fällt mit der Spitze des aktiven Akkretionskeils zusammen. Der aktive Keil bildet den seewärtigen Teil des Sinú-Akkretionskeils. Das äußere Hoch (Outer High) wird vom landwärtigen (östlichsten) Teil des Sinú-Keils und des San Jacinto-Faltengürtels aufgebaut. Das äußere Hoch ist ein fossiler Teil des Akkretionskeils, der heute das dynamische Widerlager (dynamic Backstop) für den aktiven Akkretionskeil bildet. Auf dem äußeren Hoch liegen mehrere kleine Sedimentbecken, die post-kinematische plio- und pleistozäne Ablagerungen enthalten. Diese Sedimente versiegeln die komplexe Struktur des äußeren Hochs. Die Grenze zum Kontinent markiert die ausgeprägte positive Blumenstruktur der nördlichen Romeral- oder San Jacinto-Störungszone. Diese bildet eine wichtige Strukturgrenze zwischen den kleineren und den durch Schlammdiapiren deformierten Becken im Westen und dem größeren und tieferen San Jorge Forearcbecken im Osten.

Die Natur der tieferen Kruste (basement) am Übergang zwischen Outer High und Forearc (San Jacinto Fold Belt und San Jorge Becken) ist Gegenstand einer Kontroverse. Die Ergebnisse der 3-dimensionalen gravimetrischen und magnetischen Modellierung dieser Studie unterstützen die Anwesenheit eines ozeanischen „basement complex" (bestehend aus einer Mischung aus Basalt und Sedimenten), der von einem tektonischen Keil aus kontinentaler Kruste (CTW) der südamerikanischen Platte unterlagert wird. Die Gesteine ozeanischer Herkunft auf kontinentalem Grundgebirge werden als Material interpretiert, das zu Beginn der schiefen Subduktion der karibischen Platte unter NW Südamerika von der ozeanischen Platte abgeschert und auf den Kontinentalrand überschoben wurde. Die kontinentale Kruste der Südamerikanischen Platte bildete das statische Widerlager (static backstop), gegen welches das Material des späteren dynamic backstop angelagert wurde.

Die Existenz eines Keils kontinentaler Kruste unter einem Komplex ozeanischer Affinität im Bereich des San Jacinto-Faltengürtels (östlich der Romeral-Störungszone) beweist, dass der nördliche Teil der Romeral-Störungszone nicht die tektonische Grenze zwischen ozeanischer Kruste im Westen und kontinentaler Kruste im Osten ist. Die Romeral-Störung mit ihren assoziierten Strukturen bildet vielmehr ein dextral transpressives Störungssystem, das durch die schiefe Konvergenz zwischen karibischer und südamerikanischer Platte in kontinentaler Kruste des forearc-Bereichs (static backstop) angelegt wurde.

In dem hier vorgestellten Krustenmodell können zwei Flächen als tektonische Grenzen zwischen ozeanischer und kontinentaler Kruste identifiziert werden: Die obere ist eine große, nach E gerichtete Rücküberschiebung, welche die abgescherten ozeanischen Gesteine der karibischen Platte auf den kontinentalen Keil verfrachtete. Die untere ist die nach E einfallende Grenzfläche zwischen subduzierter karibischer Platte und kontinentaler Oberplatte.

Der terrestrische Wärmefluss in NW Kolumbien wird durch verschiedene Hebungs- und Senkungsphasen bestimmt, die den Akkretionskomplex während seiner Entwicklung erfassten. Eine Bestimmung der Versenkungsgeschichte und der thermischen Entwicklung ist daher sehr schwierig. Ausgehend von allgemeinen Berechnungen der thermischen Reife (dargestellt durch Vitrinit-Reflexionswerte) in Abhängigkeit von der Tiefe sowie von Tiefeninformationen aus dem 3D-Strukturmodell und wenigen Bohrungen liegt ein Großteil der Sedimente aus der oberen Kreidezeit in Bereichen jenseits des Ölfensters, während ein Teil der Sedimente aus dem Miozän noch nicht diesen Bereich erreicht haben.

RESUMEN

El margen activo del Caribe Colombiano ha evolucionado desde el Cretácico superior resultando en una compleja historia de deformación, involucrando subducción oblicua, acreción, extensión e inversión tectónica durante el Cenozoico.

La combinada interpretación de datos sísmicos de reflexión 2D, gravimetría y magnetometría proveen un mejor entendimiento de la configuración del margen (área del Golfo de Morrosquillo), así como de la composición de la corteza presente a lo largo de este. El margen despliega las características morfológicas y tectónicas típicas de un complejo de subducción dominado por acreción. Los resultados del modelamiento gravimétrico 3D sugieren que la Placa Caribe subduce el noroeste de Colombia con un ángulo de aproximadamente 5° en dirección este-sureste. Los mayores dominios tectónicos que forman el margen incluyen de oeste a este: la fosa, el prisma de acreción activo, el alto externo y las cuencas de antearco.

El eje de la fosa coincide con la punta del prisma de acreción activo. El prisma activo corresponde a la parte externa de la cuña accrecionaria de Sinú-Colombia. El dominio del alto externo incluye el mayor complejo estructural formado por la parte más oriental de la cuña accrecionaria de Sinú-Colombia y el Cinturón Plegado de San Jacinto. Este dominio representa la parte fósil del prisma de acreción, el cual actúa como un contrafuerte dinámico para el prisma de acreción activo. Hacia el mar, el dominio de antearco está compuesto por varias subcuencas conformadas por depósitos post-cinemáticos de edad Plio-Pleistocena, los cuales fosilizan el complejamente deformado alto externo. La parte continental del dominio de antearco está marcado por la bien desarrollada estructura en flor positiva del Sistema de Fallas de Romeral Norte o Sistema de Fallas de San Jacinto, el cual representa una interrupción estructural entre las más pequeñas y deformadas por diapiros de lodo subcuencas al occidente y la principal y más profunda cuenca de antearco (Cuenca de San Jorge) al oriente.

El tipo de basamento presente a lo largo de la transición entre alto externo y el dominio de antearco (entre el Cinturón Plegado de San Jacinto y Cuenca de San Jorge) es todavía discutido controversialmente. Los resultados de los modelamientos gravimétrico y magnético 3D obtenidos en este estudio soportan la presencia de un "complejo de basamento oceánico" (mezcla de basaltos y sedimentos), el cual es subyacido por una cuña tectónica de corteza continental (CTW), procedente de la Placa Suramericana. El emplazamiento de rocas de afinidad oceánica sobre la corteza continental es interpretado como material arrancado de la Placa Caribe y cabalgado sobre el margen continental durante la iniciación de la subducción oblicua de la Placa Caribe debajo del noroeste de Suramérica. La corteza continental de la Placa Suramericana proporcionó el contrafuerte estático contra el cual el material del futuro contrafuerte dinámico fue acrecionado.

La existencia de una cuña tectónica de Corteza continental debajo del "complejo oceánico de basamento", en el Cinturón Plegado de San Jacinto, indica que el

Sistema de Fallas de Romeral Norte no corresponde al limite tectónico entre corteza oceánica al occidente y corteza continental al oriente. La Falla de Romeral y sus estructuras asociadas forman un sistema transpresivo dextral de fallas desarrollado en la corteza continental del dominio de antearco (contrafuerte estático) como resultado de la convergencia oblicua entre las placas Caribe y sudamericana.

Dos contactos tectónicos son identificados como limites entre cortezas oceánica y continental: uno superior, el cual representa un mayor retro-cabalgamiento de vergencia oriental que despegó las rocas oceánicas de la placa descendente emplazándolas sobre la cuña de corteza continental, y otro inferior, el cual corresponde al limite (buzando hacia el oriente) entre la descendente Placa Caribe y la colgante Placa sudamericana.

El flujo de calor en NW Colombia ha sido controlado por las diferentes fases de levantamiento tectónico y subsidencia sufridas por el complejo de acreción durante su desarrollo. Por tanto, la historia termal y de enterramiento es difícil de determinar. Con base en cálculos generales de madurez térmica (Reflectancia de Vitrinita) en relación a profundidad y en la profundidad interpretada del modelo gravimétrico 3D resultante e información de pozo, puede asumirse que la mayor parte de la rocas fuente Cretácicas están sobre-maduras, mientras que una parte de las rocas fuente del Mioceno no alcanzaron un estado de madurez.

1. INTRODUCTION AND OUTLINE

1.1 Aims and methods

The main objective of the project is to characterize the crustal structure as well as the structural style of the Colombian Caribbean margin (Morrosquillo area) using a combination of 2D seismic reflection data, surface geology, well data and a large scale 3D density model derived from gravity data. Quantitative magnetic analysis is also incorporated in the interpretation mainly to confirm the definition of the basement-type present along the Romeral Fault Zone obtained from the gravity modelling and to explain local anomalies. The applied methods and results are described in respective chapters.

1.2 Previous works

The Colombian Caribbean margin has evolved since the late Cretaceous resulting in a complex deformation history involving oblique subduction-accretion and tectonic inversion during the Cenozoic. The identification of deep crustal elements as well as the effects of the deformation has important implications for understanding both the regional geological evolution and the hydrocarbon exploration potential of the area.

The Colombian Caribbean area has been the target of hydrocarbon exploration since the beginning of the last century and many geological and geophysical investigations have been carried out. Approximately 28,000 km of 2D and 4,800 km of 3D seismic reflection data have been acquired and about 175 wells in both onshore and offshore areas have been drilled (Luna et al., 2001).

A first overview of the evolution of the Colombia Caribbean area based on surface geology and well information was published by Duque-Caro (1972, 1973, 1975, 1976 and 1979). He proposed the further extension of the Romeral Fault System to the north until the Magdalena fan to separate two distinct geologic environments: a continental one to the east and an oceanic one to the west. He interpreted the Romeral Fault System not only as a simple fault zone but as major structural contact between oceanic and continental crusts along the entire western part of Colombia.

Joint venture projects between the Colombian Oil Company (ECOPETROL S.A) and other oil and gas companies have provided more important integrated geological and geophysical studies.

Gravity anomaly maps of this region have been published by Instituto Geográfico Agustín Codazzi - IGAC (1959), Hayes (1966), Case et al. (1971), Case and McDonald (1973), Case (1974), Bowin (1976), Bermúdez and Acosta (1978) and Briceño-Guarupe (1978). Further gravity maps have been released by the Sierra de Perijá (Kellog, 1980) and the Sierra Nevada de Santa Marta (Bonini et al., 1980).

Kellogg et al. (1983) presented a 2D density model along the Colombian Caribbean Basin, Sierra Nevada de Santa Marta, Cesar Valley Basin and Sierra de Perijá. They proposed a subduction of oceanic crust beneath South America on the Romeral Fault System during the early Tertiary. Romeral is interpreted to be the southeast margin of a late Cretaceous to middle Eocene trench between Caribbean oceanic crust and South America Plate.

Duque-Caro (1984) suggests that the margin of northwestern Colombia has grown by successive westward accretion of the San Jacinto and Sinú Belts from the late Cretaceous to Pliocene time.

Toto and Kellogg (1992) interpreted Sinú and San Jacinto Belts as an up-to-12km thick wedge of sediments which has been accreted to the South American margin throughout the Cenozoic. According to their interpretation, the Romeral Fault System is a paleo-suture zone where a NW-NE directed convergence of up to 1,000 km occurred during the past 45 million years. They also assume that the Romeral Fault System separates Paleozoic continental rocks in the east from oceanic material in the west.

Regional integrated evaluation and hydrocarbon potential projects have been carried out by ESRI-ILEX Ltda (1995) and ICP-ECOPETROL (2000). Laverde (2000) summarized the results from the stratigraphic and structural interpretation from ESRI-ILEX (1995), which indicates that the San Jacinto and Sinú wedges were accreted to the South American continent during the early-middle Eocene and middle Miocene, respectively. The Romeral Fault System is assumed to be an early-middle Eocene tectonic boundary or suture zone between igneous-metamorphic continental crust to the east and Cretaceous to late Paleocene-early Eocene sediments of the San Jacinto Accretionary terrane to the west. The behavior of the continental crust at the San Jorge-Plato Basin is proposed as a tectonic backstop during the accretion of the San Jacinto terrane. However, ESRI-ILEX (1995) and Laverde (2000) did not discuss the relationship of the Romeral Fault System with the tectonic backstop. The main results from the evaluation carried out by of ICP-ECOPETROL (2000) were published by Reyes-Santos et al. (2000) and Reyes-Harker et al. (2000). According to these publications, the San Jorge-Plato Basin is characterized as a group of transtensional and rotating basins which were developed as a result of the oblique collision between Caribbean and South American plates.

Based on the integration of the seismic interpretation and qualitative analysis of the magnetic and gravity anomalies, Ruiz et al. (2000) divided NW Colombia into two zones separated by the Canoas Fault Zone: 1) zone of accretion (south to Cartagena city) and 2) zone of transpression-transtension Caribbean offshore (located between the Canoas and Oca-Santa Marta Fault Systems). The southern zone is underlain by oceanic crust and includes the Neogene Sinú Accretionary Prism and forearc basin. The northern zone is underlain to the west by oceanic crust and by continental crust to the east and includes the Magdalena fan and the offshore area of the Santa Marta Massif and the Barranquilla city. In contrast to all previous studies, Ruiz et al (2000)

proposed a considerably more complex relationship between the continental and oceanic crust along the Colombian Caribbean margin. In the southern zone, the Romeral Fault System is the limit between oceanic and continental crust, while in the northern zone the Romeral cuts a block of continental crust. The presence of continental crust west of the Romeral in the northern zone is explained either by a pre-existing Jurassic-Cretaceous continental margin or by an allocthonous block of continental crust that collided in the early Tertiary. The different structural styles along the Colombian Caribbean margin is caused by the change from more orthogonal convergence in the south to strongly oblique convergence in the north.

Corredor et al. (2002) presented a kinematic model to explain the deformation processes undergone in the offshore portion of the Sinú Accretionary Prism. Forward structural modelling characterizes the observed imbricate fault system as a result of the transpressional collision between the Caribbean and South America plates during Tertiary times. The fold system is further sheared and transported on an Oligocene formed basal detachment (top of oceanic plate?) during Pliocene until present time.

The structural evolution of northwestern Colombia has been also studied by Flinch et al. (2000), Flinch et al. (2002), Flinch et al. (2003) and Flinch (2004), who postulated obduction of the proto-Caribbean Plate above the South American Plate prior to the Cenozoic subduction that lead to accretion along the Colombian Caribbean margin. The San Jacinto and Sinú Fold Belts belong to the same Paleocene to Oligocene accretionary wedge: San Jacinto and the onshore area of Sinú represent the "inner accretionary wedge" of older accreted sediments (Paleocene to Oligocene), whereas the offshore area of Sinú represents the "outer accretionary wedge" of younger sediments (Paleogene to Miocene) including the Neogene offshore prism (Miocene to Pleistocene). The Romeral Fault System offsets the west-ward dipping suture between Cretaceous obducted oceanic crust and the basement of South America, and does not represent the obduction suture. The Romeral Fault system controlled the late Cretaceous-Paleocene trench which later on became the inner accretionary wedge.

A tectonic evolution model for the San Jacinto Fold Belt was proposed by Caro and Pratt (2003), which does not involve accretionary mechanics for the formation of the San Jacinto Fold Belt. These authors suggest that the San Jacinto Fold Belt is an inverted paleo-rift or graben developed on the continental margin of the South American Plate.

Cerón and Kellog (2005) interpreted the northwestern corner of South America as a collage of terranes which include the Chocó-Panama block, Sinú-San Jacinto block, San Jorge-Plato autochthon and Luruaco block. These terranes are underlain by normal to thinned continental crust (transitional crust) with tectonic emplacement of oceanic crust slivers present in the San Jacinto Fold Belt.

Nonetheless, the crustal composition present in northwestern Colombia and the responsible tectonic mechanisms of the current geological setting are still debated.

Most of the works refer to a simple interpretation of the Romeral Fault System as a suture zone separating oceanic from continental crust. Furthermore, extension of the Romeral Fault System from southern Colombia to the north (Colombian Caribbean region) would assume that the tectonic origin and development of rock formation are similar for the Western Cordillera as well as for the San Jacinto and Sinú Fold Belts. One objective of this study is to define the crust type present at the Colombian Caribbean margin (Morrosquillo area) based on qualitative and quantitative interpretation of potential field data.

1.3 Thesis outline

In this thesis, the deformation style present along the Colombian Caribbean margin (Morrosquillo area) is constrained by the 2D seismic dataset. The crustal structure is resolved satisfactorily by 3D gravity modelling. Additional 3D magnetic modelling is used to confirm the basement type (obtained from the 3D gravity modelling) involved along the Romeral Fault System, which has been historically defined as the limit between ocean crust to the west and continental crust to the east. The magnetic modelling also explains the largest discrepancies between the observed and the calculated gravity anomalies of the final 3D density model. An outline of the project is described in the following:

Chapter 2 gives an overview about the origin and evolution of the Caribbean Plate. This chapter presents a synthesis of the tectonic assemblage of the northern Colombian Andes region, describing its geologic domains as well as the fault systems separating them. The geologic map illustrates the main structural and stratigraphic surface characteristics of the study area. In this chapter a stratigraphic framework for the study area is established. It summarizes the sedimentary events which occurred during the convergence between the Caribbean and South American plates and represents a fundamental base for the identification of unconformities or sequence-limits during the seismic interpretation (Chapter 3).

Chapter 3 presents the structural configuration of the Colombian margin (Morrosquillo area) which is well-imaged along a composite seismic profile located at the central part of the study area. About 850 km of seismic information (21 seismic lines) using IESX application were interpreted for the project. Furthermore, the geological map and 22 wells are integrated for this interpretation. The seismic interpretation, which represents important boundary conditions for the 3D gravimetric modelling, is carried out on a very general stratigraphic framework. The main objectives of this interpretation are the characterization of the structural style of the upper crust and the proposal of a new definition of the tectonic domains of the Colombian Caribbean margin.

Chapter 4 deals with the examination of the regional gravimetric and magnetic anomalies that characterize the study area. The basis for understanding these anomalies is the correlation of the Bouguer anomaly map with the major structural features. In order to know the state of isostatic compensation along the margin and

adjacent areas, a general revision of the Regional isostatic anomaly map is made in this chapter. The qualitative interpretation of the magnetic anomalies from the Total Magnetic Intensity and Reduce-to-Pole maps is shown here.

Chapter 5 describes the 3D forward modelling of gravity anomalies and shows that this procedure is a powerful tool to investigate the deep structure along the convergent margins. The 3D gravity modelling represents the major motivation of this project and is carried out with the objective of understanding the current interaction between the Caribbean and South American plates and to determinate the crust type present at the study area. Forward modelling is combined with inversion techniques and is based on the gravity field (Bouguer anomaly) under constraints of seismic and well data as well as surface geology. The resultant 3D model illustrates the crustal structure and density distribution of the Colombian Caribbean margin.

Chapter 6 deals with the quantitative evaluation of the basement present along the Romeral Fault System. This quantitative evaluation is performed through 3D magnetic modelling of 2 areas using as constrains the results of the seismic interpretation, the gravity modelling and depth estimations of Peter's half slope method. The obtained models refine the interpretation from the 3D density model, characterizing the basement which is involved along the Romeral Fault System. Additional to the basement depths calculated for the modelling areas, basement depth for the most prominent anomalies of the study area is estimated.

Chapter 7 integrates and discusses the results of the seismic interpretation (Chapter 3) and the gravity and magnetic modelling (Chapters 5 and 6 respectively). A model of subduction is proposed and the major tectonic units of the margin are defined. The analysis of the current crustal model suggests four main stages of evolution which are also described in this chapter.

Chapter 8 presents some considerations of the resultant crustal model for hydrocarbon maturation. Although this topic does not constitute one of the aims of this work, it is discussed briefly due to the economic importance of the Colombian Caribbean area. The approach presented here could provide the basis for future advanced integrated basin analyses and petroleum system modelling.

Chapter 9 summarizes the conclusions derived from the regional integrated model which can be re-evaluated with the acquisition and interpretation of deep multi-channel reflection seismic data including careful velocity modelling.

2. REGIONAL SETTING OF COLOMBIAN CARIBBEAN AREA

2.1 Caribbean tectonic overview

The history of evolution of the Caribbean Plate began with the breakup of Pangea and with the separation of North America, South America and Africa in Jurassic time. This is the only consensus between two main groups of models in the literature after decades of ongoing discussion about the development of this region since early Cretaceous until today. The pacific models propose an origin of the Caribbean oceanic crust formation in the Pacific region with or without the participation of the Galapagos hotspot (Wilson, 1965; Malfait and Dinkelman, 1972; Burke et al., 1978; Pindell and Dewey, 1982; Burke et al., 1984; Duncan and Hargraves, 1984; Pindell, 1985; Pindell et al., 1988; Pindell and Erikson, 1994; Ross and Scotese, 1988; Pindell and Barrett, 1990; Stephan et al., 1990; Pindell and Kennan, 2001; Pindell and Kennan, 2002a, 2002b and 2003; Kerr and Tarney, 2005), whereas the intra-America models assume that the Caribbean Plate is formed between the two Americas (Ball et al., 1969; Aubouin et al., 1982; Sykes et al., 1982; Donnelly, 1985; Klitgord and Schouten, 1986; Frisch et al., 1992; Meschede et al., 1997; Meschede and Frisch, 1998; James, 2006). Key discussion items for both model-groups are the location of Yucatan and Chortis, the occurrence of plateau basalts (Caribbean B-basalts) and ophiolites, the presence or not of a proto-Caribbean, the time-dependent occurrence of subduction zones as well as relative plate movements of the Americas and Caribbean during this time period.

In the Pacific models (e.g., Pindell and Kennan, 2001), tectonic evolution of the Caribbean starts with the opening of the Gulf of Mexico and a proto-Caribbean seaway by the rotation and accompanying southward motion of Yucatan away from North and South America as those continents diverged in Jurassic-Earliest Cretaceous. The future Caribbean Plate lay southwest of a primary east-facing island arc (Caribbean Great Arc, later the Great Antilles) along the western end of the proto-Caribbean and Mexico and northwest of South America. Spreading of the Proto-Caribbean occurred until Aptian (120 Ma), when a fundamental change of the subduction direction between the Americas occurred. This event was caused by the accelerated spreading of the Atlantic and resulted in a relative east to northeast-directed movement of the Caribbean Plate until the Cenozoic, to a reversal of the subduction-direction between the Americas, and later on in Albian (100 Ma) to the formation of a new east-facing subduction zone between the Caribbean and Farallón plates in the south (later the Central America island arc). A further result of this event was the initiation of the closure of the back-arc basins in Mexico and Andean (NW Colombia). Continued separation of the two Americas and back-arc closures in NW South America led to further eastward motion of the Caribbean Plate, overriding the proto-Caribbean in the NE and starting the convergence with South America. According to these models, a passive margin existed in NW Colombia from 120 until 84 Ma. The situation changed, when spreading of the proto-Caribbean ceased in Campanian (84 Ma). By this change, the boundary between NW Colombia and the Caribbean Plate started to become more compressive, which finally resulted in the formation of the subduction of the Caribbean Plate beneath South America from early Maastrichtian (72 Ma) until late Miocene (9.5 Ma). The changed plate motions

caused also an increased movement of the Caribbean Plate together with the Costa Rica-Panama Arc to the NE as well as further movement of the Caribbean Great Arc towards NE, entering the area of the proto-Caribbean seaway. NE movement did not change until the collision of the Caribbean Plate with the Bahamas in middle Eocene (46 Ma) leading again to a major impact of the plate movements accompanied with the (still) continued westward drift of the Americas; the now easterly directed movement of the Caribbean Plate caused the formation of the Cayman Trough at its northern border and the collision with northern Venezuela with the formation of a flat slab subduction zone beneath the Maracaibo block until late Miocene. In NW Colombia, direction of the subduction changed from formerly NE to a more E oriented one, which lead to the formation of the San Jacinto Accretionary Prism in middle Eocene (46 Ma) and later on to the Sinú Accretionary Prism in early Oligocene (33 Ma). From Oligocene until late Miocene (33 Ma to 9.5 Ma) main developments continued, but at NW South America the Panamanian Arc Ridge entered the Colombian trench causing the emplacement of the northern Andes blocks onto the Caribbean Plate. In late Miocene (9.5 Ma), subduction processes at NW Colombia and northern Venezuela ceased when the Caribbean Plate underwent a change in azimuth of motion relative to the Americas from former E to slightly NE (Pindell and Kennan, 2001). The northeast and southeast boundaries of the Caribbean Plate were affected by this change as the southeastern boundary became transtensional.

The Intra-America models are based on the formation of the Caribbean Plate along with the Gulf of Mexico, the Yucatan Basin and the Cayman Trough via sinistral transtension between North and South America which was initiated by the drift of North America from Gondwana in Jurassic – early Cretaceous. In contrast to the pacific model, the Caribbean Plate ("proto-Caribbean", Meschede and Frisch, 1997) was formed once during the end of the Jurassic until middle Albian (Meschede and Frisch, 1997) or late Cretaceous (James, 2006 and 2005) by a NE-SW oriented spreading process and remained unchanged until Cenozoic. All further developments were caused by the continued westward-drift of the two Americas relative to the Caribbean where plate tectonics were controlled by the movement direction of the Farallón Plate as well as by the relative movements of North America to South America especially in Cenozoic. Major E-W displacement systems such as the Cayman Trough had already been generated during the Jurassic-early Cretaceous and remained active until recent. Larger terranes such as Yucatan and Chortis maintained similar positions as of today. Spreading of the Caribbean occurred from 110 to 95 Ma causing subduction of the Caribbean Plate at its NE and S boundaries and to a postulated beginning of the Costa Rica-Panama Arc at its western border. The spreading ceased with the opening of the South Atlantic in middle Cretaceous, leading to the formation of the Costa Rica-Panama Arc between Chortis and South America as well as the Great Antilles Arc in the north of Cuba and Hispaniola. Continued divergence of spreading trajectories both in the Atlantic and Pacific (James, 2006) resulted in further extension of the Caribbean Plate from 90 to 88 Ma until its present extension. During the Campanian (83 Ma) the motion of the Farallón Plate changed from a northeastward to an almost eastward direction (Engebretson et al., 1985), and the relative movement between North and South America became slightly convergent. The changed plate motion resulted in continued subduction at the Lesser Antilles and initiated the closure of a small basin between the NW boundary of

the Caribbean Plate and the Bahamas, which was terminated by the collision between the two plates in Paleocene (Meschede and Frisch 1997). A major convergent event is identified in Paleocene until middle Eocene which may have been caused by a major change of the motion of the Farallón Plate from E to NE (Engebretson et al., 1985) controlling also the plate configuration of the Caribbean (Meschede and Frisch, 1997). This event affected both the northern and southern Caribbean Plate boundaries and led to the diachronous transpression with the formation of circum-Caribbean wildflysch deposits (James, 2002). Accompanying this event was a middle Eocene orogeny which occurred in northern South America involving crustal shortening, overthrusting and strike-slip faulting in Venezuela and Trinidad. It also caused the separation of the NW South America from the South America Plate allowing the movement northeast along faults parallel to the Eastern Cordillera and to the Venezuelan Merida Andes. Further in the north of South America, separation of the Maracaibo-Bonaire area commenced which later on led to overthrusting of the Caribbean on South America by ongoing relative eastward movement. Continued westward drift of the Americas and the split of the Farallón Plate into the Cocos und Nazca plates, led to the collision of the Panamá Arc with the Western Cordillera of Colombia which caused its northward escape into the Colombian Basin in Miocene. From Oligocene to present, E-W dextral relative motion characterized the plate boundaries: At the northern part of South America, about 300 km of dextral displacement has occurred between the two plates. Similar displacement is also assumed for the plate boundary between North America and the Caribbean.

Both models contain fundamental differences with respect to the presence of subduction at the NW part of South America: Pacific models allow a long term subduction of a significant amount of oceanic plate from 72 Ma to 10 Ma until its current position beneath the Colombian Eastern Cordillera (Pennington, 1981; Kellog and Bonini, 1982; Freymüller et al., 1993; Kellog and Vega, 1995; Taboada et al., 2000; Cortes and Angelier, 2005). From 120 until 84 Ma only a passive margin existed. The pacific models are suitable to explain the time-dependent occurrence of accretionary prisms and ophiolites at NW Colombia.

On the other hand, only very limited subduction occurs according to Intra-America models. It is restricted to the very early opening of the Proto Caribbean in Jurassic-early Cretaceous time. During the spreading of Proto Caribbean the continental margin was passive until its cease in middle Cretaceous. From Paleocene onwards, the region is characterized by orogeny, thrusting and activation of NE-oriented fault systems. The models fail to explain the occurrence of accretionary prisms as they occur in the Colombian Caribbean margin.

Both models consider the occurrence of plateau basalts ("horizon B-basalts"), which cover large areas of the Colombian Basin (as well as the Caribbean Plate) and which were caused either by a "jumping hot spots" event or by decompression melting due to excessive plate extension. Subduction of such thickened oceanic plate is difficult or even impossible as assumed by Meschede and Frisch (1997).

The plate reconstruction from the early Jurassic to late Miocene according to the Pacific model (Pindell and Kennan, 2001) is comprised in attachment 1. Notice that for the area discussed here, the new interpretation presented in Chapter 7 differs from the evolution proposed in the large-scale model.

Figure 1 shows the present plate boundaries of the Caribbean region. The Caribbean Plate is limited by subduction zones in the west and east, the first one by the Costa Rica-Panama and the second one by the Lesser Antilles subduction zone. The boundaries in the north and south are less well-defined: Burke and others (1978) identified strike-slip fault systems from central Guatemala to the Puerto Rico trench in the north and from the northern part of Colombia to Trinidad in the south. The plate boundary at the NW corner of the South America plate is a broad diffuse zone containing many independently moving blocks on the south and east of the Colombian and Venezuelan Basins (Case et al., 1984).

The geodetic observations indicate that convergence along the Colombian Caribbean margin is still taking place. The calculated rates of convergence are 1.7 cm/yr (Kellog and Bonini, 1982), 1 cm/yr (Freymüller et al., 1993) and 1.3 ± 0.3 cm/yr (Van der Hilst and Mann, 1994). Seismicity studies (Pennington, 1981; Kellog and Bonini, 1982; Malavé and Suárez, 1995) suggest that the Caribbean Plate is subducted amagmatically under the South American Plate. Taboada et al. (2000), and Cortes and Angelier (2005) also favor the subduction of the Caribbean and Nazca plates beneath the NW and W wedges of the northern Andes which is based on integrated interpretation of focal mechanisms of earthquakes and tomographic images. Both publications assume a shallow N-NE trending subduction of the Caribbean Plate at latitudes north of 5° or 7°N. Southward of 7˚N moderately steep N-S trending subduction of the Nazca plate occurs. Between these latitudes an overlapping of the two subducting slabs is assumed where the Nazca Plate is subducting below the Caribbean Plate. In contrast, the interpretation from tomography images (Van der Hilst, 1990; Van der Hilst and Mann, 1994) indicates that no significant convergence between the Caribbean Plate and the entire South America Plate can be identified. These authors conclude that the principal motion between these plates is right-lateral strike-slip where the Caribbean Plate is underthrusted beneath the Maracaibo Block due to its northward directed movement. Nevertheless, it must be noted that the discussion is restricted to the interaction between the Caribbean Plate and the Maracaibo Block only. The identified subducted "Bucaramanga slab" is interpreted to be a part of the oceanic Nazca Plate, but which can be seen only in the tomographic images for latitudes from 7°N to 10°N. The type of continental margin at the Sinú-San Jacinto area is not discussed by these authors.

2.2 Tectonic framework of northern Colombia

Figure 2 shows the tectonic assemblage of the Northern Colombian Andes region according to the most recent integrated synthesis and interpretation published by Cediel et al. (2004). Based on this regional reconstruction, a description of geologic domains as well as the fault systems separating them is summarized below.
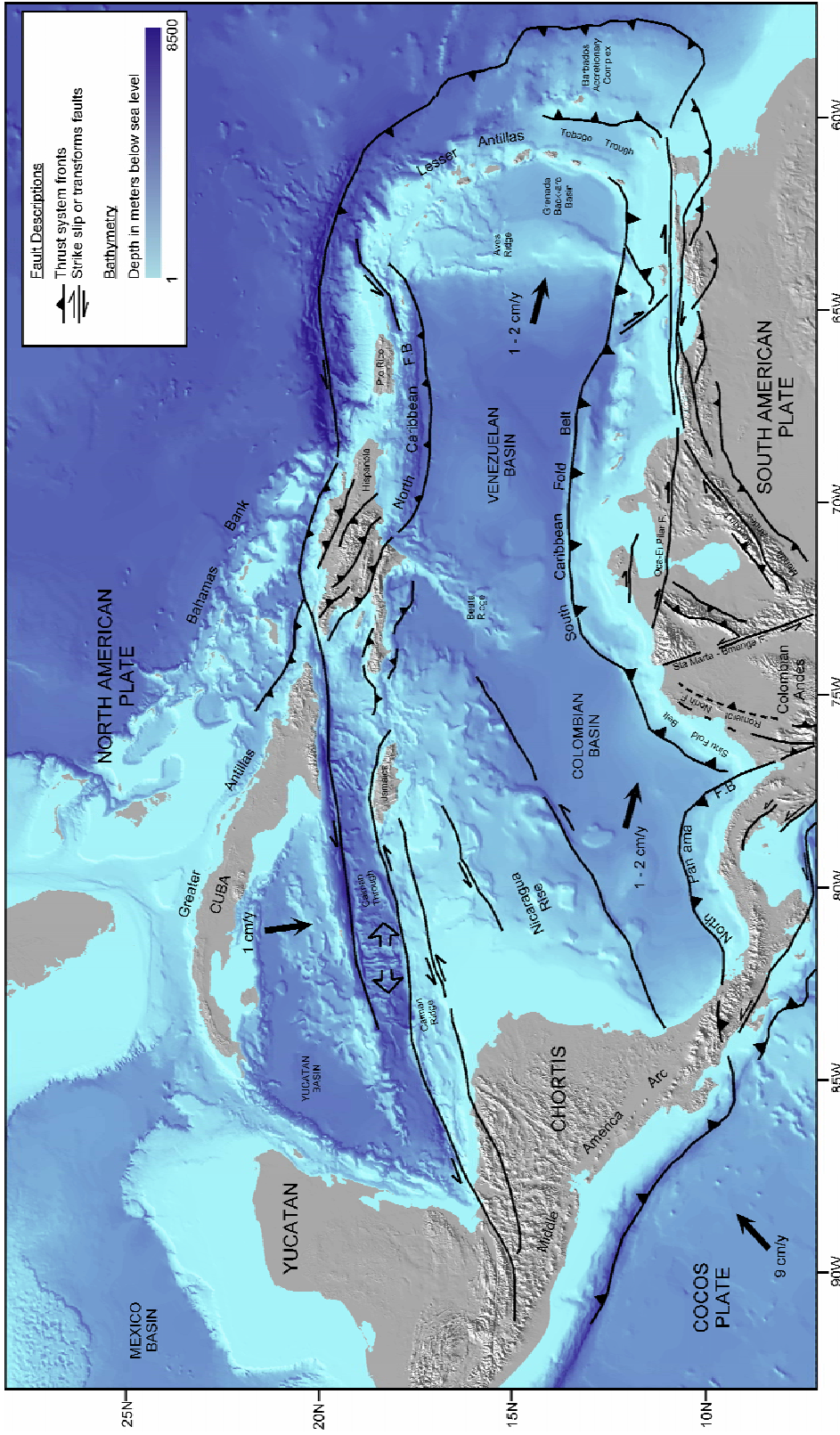
Figure 1: Present day tectonic map of the Caribbean region indicating the plate boundaries and main fault systems. Map sources: Pindell and Barrett (1990); Taboada et al. (2000); French and Schenk (2004); Giunta et al. (2006). Bathymetry from French and Schenk (2004).
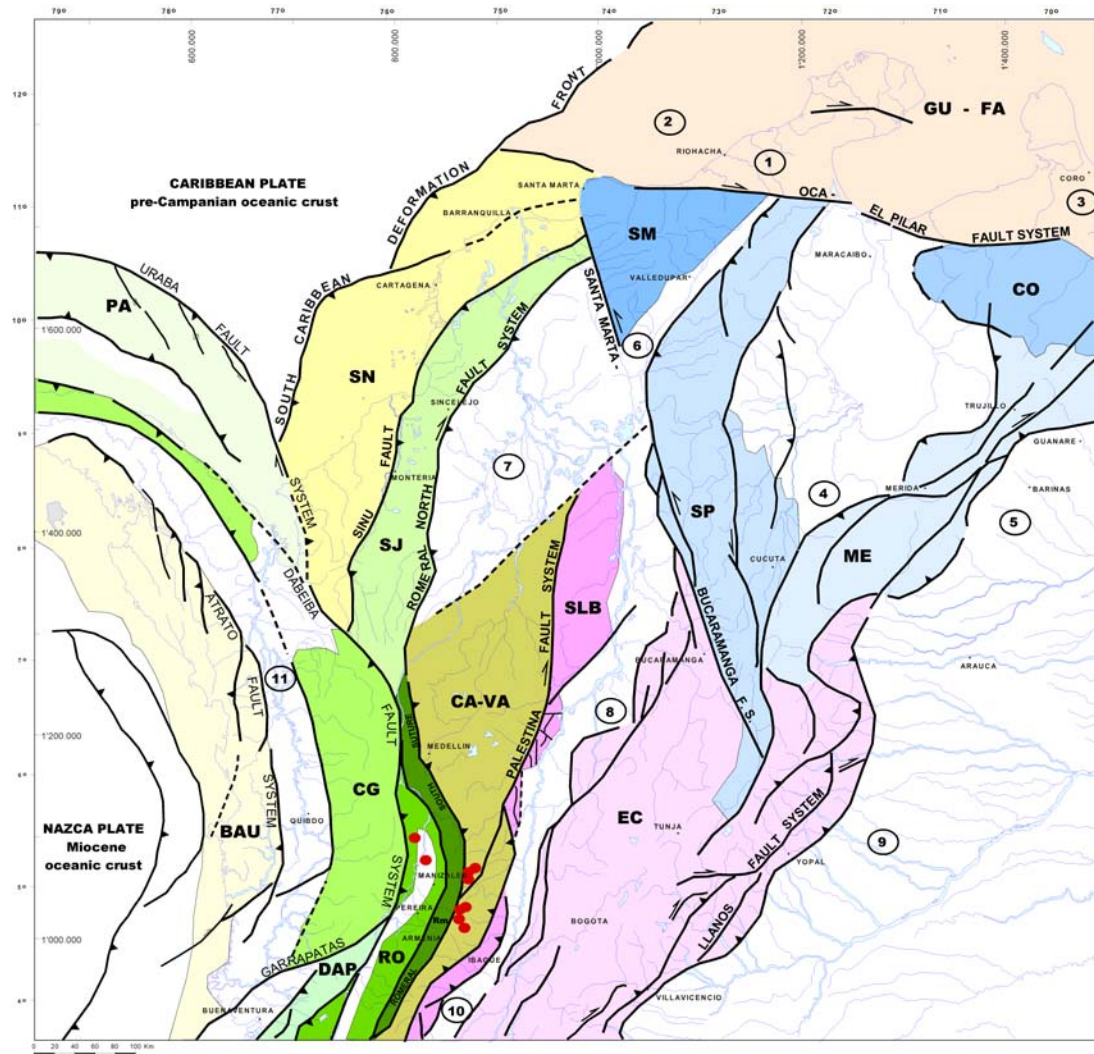
Figure 2: Lithotectonic and morphostructural map of north Colombia (simplified from Cediel et al., 2004). (SM) Santa Marta Massif, (CO) Carora Basin, (SP) Santander Massif-Serranía de Perijá, (SN) Sinú terrane, (SJ) San Jacinto terrane, (CA-VA) Cajamarca-Valdivia terrane, (SLB) San Lucas block, (PA) Panama terrane, (CG) Cañas Gordas terrane, (BAU) Baudó terrane, (RO) Romeral terrane, (Rm) Romeral mélange, (DAP) Dagua-Piñon terrane, (EC) Eastern Cordillera, (1) Guajira Basin, (2)Ranchería offshore and Chuchupa-Ballena Basins (3) Falcon Basin, (4) Catatumbo/Maracaibo Basin, (5) Barinas Basin, (6) Cesar-Ranchería Basin, (7) Lower Magdalena Basin, (8) middle Magdalena Basin, (9) Llanos Basin, (10) Upper Magdalena Basin, (11) Atrato (Chocó) Basin. Red dots indicate the location of Pliocene-Pleistocene volcanoes.

The Guajira-Falcón (GU-FA) and Caribbean Mountain (Venezuela) terranes consist of fragments of Proterozoic and Paleozoic continental crust, Jurassic sediments and Cretaceous oceanic crust. Because of its age and composition it is assumed that these terranes were originally a part of Pacific-Caribbean-Chocó assemblage and accreted to the northwestern coast of South America 100 Ma ago.

12

Detachment in Albian and dextral transport along the Romeral-Peltetec, San Jacinto and Oca-El Pilar fault systems led to their present position since late Paleocene. The passage is recorded by the assemblage of slivers of different sequences. Here, the Jurassic sequence of this terrane seems to correspond with contemporaneous deposits which are exposed in the Yucatan Peninsula (Pindell, 1993). The Caribbean Mountain terrane (Venezuela) represents a part of the Guajira-Falcon (GU-FA) terrane which was decoupled and obducted onto the Maracaibo block during the Eocene.

The Santa Marta Massif (SM), the Sierra de Mérida (ME), the Sierra de Perijá together with the Santander Massif (SP), and the Cesar-Ranchería and Catatumbo-Maracaibo basins form the Maracaibo block which represents the northwestern portion of the Guyana Shield. This autochthonous continental block has migrated since the middle to late Cretaceous to the northwest along the Santa Marta-Bucaramanga and Oca-El Pilar fault systems, developing the Sierra de Mérida, the Santander-Perijá Belt, and the Sierra Nevada de Santa Marta. The movement led to a forced underthrusting of the Caribbean Plate below the apex of the Santa Marta Massif in Miocene to Holocene. The lack of subduction-related volcanism indicates a low interaction angle between Caribbean Plate and the Maracaibo block.

The Chocó Arc contains the Cañas Gordas (CG) and Baudó (BAU) terranes and constitutes the eastern segment of the Panamá Double Arc. Cañas Gordas represents the north part of the Western Cordillera and is built up of volcanic-arc related rocks and sediments of middle to late Cretaceous age, whereas the Cretaceous to Paleogene-aged tholetiitic basalts and pyroclastic to siliciclastic sediments of the Baudó segment indicate an origin in an oceanic plateau. The Chocó Arc is limited to the south by the Garrapatas Fault which in combination with the Dabeiba Fault in the north facilitated the obduction of the Cañas Gordas terrane (CG) on the South America Plate in Miocene. Cañas Gordas (CG) and Baudó (BAU) terranes are separated by the Atrato Fault System which consists of a series of east-vergent en echelon rotated thrust faults of Miocene to Pliocene age. The Baudó terrane (BAU) was accreted onto Cañas Gordas (CG) terrane through this fault system.

Sinú (SN) and San Jacinto (SJ) represent the Colombian Caribbean terranes. The San Jacinto terrane (SJ) includes a complex of basalts and ocean-floor sediments of upper Cretaceous - Paleocene (?) age (Cansona Formation) where paleomagnetic (Brock and Duque-Caro in Cediel et al., 2004) and geochemical data (Kerr et al., 1996) suggest an origin southwest to its current position as well as an association with the tholeiitic MORB-type basalts of the Pacific Dagua-Piñón terrane (DAP). The Paleocene to Eocene turbiditic sequences of continental affinity and the middle Eocene erosional unconformity indicates the pre-Oligocene accretion of the San Jacinto terrane (SJ) to the South American Plate along the Romeral North or San Jacinto Fault System. Accretion of Sinú terrane (SN) on the San Jacinto terrane (SJ) took place since Miocene. In Chapter 3 a new definition of the tectonic domains of the Sinú and San Jacinto areas as well as the characteristic structural style in each of them is presented.

The Cajamarca-Valdivia terrane (CA-VA) and the San Lucas block (SLB) represent the north part of the Central Cordillera. The Cajamarca-Valdivia terrane (CA-VA) is composed of metamorphic rocks (greenschist to low amphibolite metamorphic grade) of intraoceanic-arc and continental-margin affinity (Restrepo-Pace, 1992), whereas the San Lucas block (SLB) consists of metaluminous, calc-alkaline, dioritic to granodioritic batholiths of Triassic-Jurassic age which were situated on a modified basement of the Chicamocha (see Fig. 3 of Cediel et al., 2004) and Cajamarca-Valdivia (CA-VA) terranes. Subduction related calc-alkaline magmatism occurred in the Cajamarca-Valdivia terrane (CA-VA) during the late Cretaceous, Paleogene, and Neogene. The event is indicated by the presence of I-type batholiths which may be a result of the oblique and low-angle subduction of the Dagua oceanic crust prior to the collision of the Dagua oceanic plateau. Recent volcanism in the Northern Andes started in the late Pliocene and is forming a 1000 km long north to northeast trending belt of strato-volcanoes. It has been caused by the current subduction of the Miocene-aged Nazca oceanic crust beneath the South America plate. The Palestina Fault System, which was active from the middle to late Paleozoic, is considered as the suture between the Cajamarca-Valdivia (CA-VA) and Chicamocha terranes (see Fig. 3 of Cediel et al., 2004). The dextral reactivation of this fault system was documented by Feininger (1970) as a right-lateral strike-slip movement which was related with activity along the Romeral Fault system during Aptian-late Cretaceous.

The Eastern Cordillera (EC) which overlies the Chicamocha terrane (see Fig. 3 of Cediel et al., 2004) represents an inverted sedimentary basin that records culminant, deep, crustal rifting in the northern Andes and along the continental margin of northwestern South America during the late Jurassic to middle Cretaceous (Cediel et al., 1994). This rifting resulted in the invasion of the Cretaceous seaway from the northwest and the deposition of thick sequences of predominantly early Cretaceous transgressive marine and lesser Cenozoic continental strata (Cooper et al., 1995). Incipient basin inversion began in the Paleogene (Sarmiento, 2002) and accelerated during the late Miocene-Pliocene. Uplift mechanisms involved a unique form of transpressive pop-up resulting from the combined tectonic movements of the Maracaibo block and Pacific-Caribbean-Chocó assemblage.

The Romeral terrane (RO) is located between the Dagua-Piñón (DAP) terrane to the west and the Romeral Fault system to the east. It is characterized by mafic-ultramafic rocks, ophiolites and oceanic sediments of Jurassic to early Cretaceous age as well as the complete absence of a continental basement. All tectonic and geologic elements within this complex are highly deformed and fragmented, and considered as mélange (Rm). The presence of fragments of Paleozoic schists and Proterozoic gneiss in the northern part indicate an autochthonous continental margin, whereas in the southern part (Peltetec mélange) the presence of calc-alkaline and MORB lithologies may represent an intra-oceanic arc environment. It is suggested that the Romeral Fault System together with the Peltetec Fault in Ecuador and the San Jacinto Fault in the north represent the continental margin of the northwestern South American Plate where the Romeral terrane was transported and accreted highly obliquely 130 Ma ago. Nevertheless, in the case of the San Jacinto Fault System (Romeral North) important differences occur in the absence of any mélange as well as in the lack of subduction related volcanism.

14

2.3 Geology of study area

The Colombian Caribbean area extends from the Urabá Gulf (Panama border) in the SW to the Guajira Peninsula (Venezuela border) in the NE. The area, which is commonly defined as northwestern Colombia, represents the Caribbean coast of Colombia situated in the north of the culmination of the Colombian Andes and southwest of the Sierra Nevada de Santa Marta (Fig. 3). The area of interest of the present work is located between the cities of Cartagena and Montería, including the Lower Magdalena Valley Basin, and both lowlands and offshore areas of the San Jacinto and Sinú fold belts. It is denominated herein as the Colombian Caribbean margin.

2.3.1 Sinú Fold Belt

The Sinú Fold Belt corresponds to the Sinú-Colombia Accretionary Wedge which lies between the present day offshore Colombia trench and the San Jacinto Fold Belt. The Sinú Fault marks the western boundary of the belt, separating it from the San Jacinto Fold Belt. Duque-Caro (1979) defined this limit by its surface expression, controlling the Sinú River, and by the change of the structural style between the Sinú and San Jacinto Fold Belts. Additionally, there is no presence of mud diapirism in the San Jacinto area.

The Sinú Fold Belt is more than 500 km long and approximately 125 km wide. Structurally, the belt is characterized by narrow and steep anticlines separated by broad synclines and which can be observed between the Urabá Gulf and the southern part of the Morrosquillo Gulf (Fig. 3). In this zone, a complicated structural pattern, which includes thrusts following the trend of the Sinú Fault and strike-slip faults, can be observed. The exposed rocks (onshore area) are mostly of late Miocene to Pliocene age. Active mud volcanoes are present in both areas - Sinú River to the south and Cartagena-Barranquilla to the north. This phenomenon is well described and discussed by Case (1974), Duque-Caro (1979), Vernette (1986), Toto and Kellog (1992), Vernette et al. (1992) and others. The age assigned to this mud is late Oligocene to early Miocene based on foraminifera determinations from the heterogeneous mixture extruded at the surface (Duque-Caro, 1979).

2.3.2 San Jacinto Fold Belt

The San Jacinto Fold Belt is located between the Lower Magdalena Valley Basin and the Sinú Fold Belt, which is separated by the Romeral Fault System and Sinú Fault respectively. The belt is approximately 360 km long and 60 km wide, trending N20°E on the surface (Fig. 3), it is mainly characterized by narrow and elongated anticlinal structures commonly faulted along strikes and separated by less deformed synclines. The more elevated topography (about 1270 m) is related to the anticlinal structures where in general the oldest units are exposed in their cores (Duque-Caro, 1984).
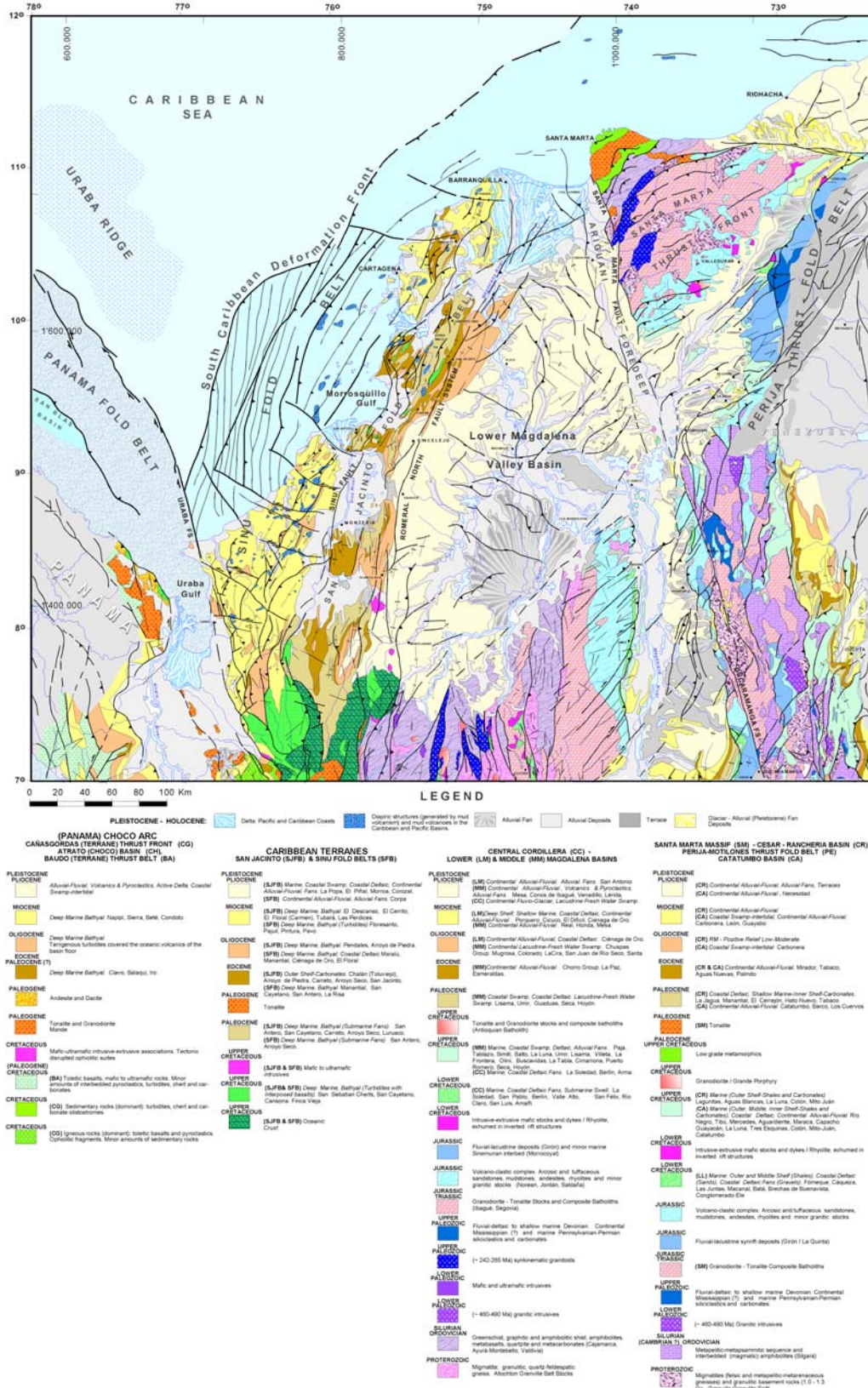
Figure 3: Geologic Map of NW Colombia (Cediel and Cáceres, 2000).

The oldest sedimentary rocks exposed are cherts and siliceous mudstones of late Cretaceous age and turbidites of Paleocene to middle Eocene age (Duque-Caro, 1979).

2.3.3 Lower Magdalena Valley Basin

The dominant geographic feature and name-holder of this geologic province is the Magdalena River which flows to the Caribbean Sea. The basin is limited by the Romeral Fault System to the west, by the Santa Marta-Bucaramanga Fault to the east, by the Santa Marta Massif to the northwest and by the Cordillera Central foothills and Serranía de San Lucas to the south (Fig. 3). The Lower Magdalena Valley Basin is conformed by the Plato and San Jorge depocenters which are separated by the Cicuco or Magangué High. Due to relatively undeformed Plio-Pleistocene sediments, which are exposed in the most part of the basin (Fig. 3), the definition of the structural style and the lithologic record has been recorded by the oil and gas companies using sub-surface data (seismic and wells).

2.3.4 Romeral Fault System

The Romeral Fault System has been considered as a major paleo-suture which separates the Lower Magdalena Valley and the San Jacinto Fold Belt. The Romeral Fault System was initially recognized by Grosse (1926) in the southwestern of the Antioquia State. Barrero et al. (1969) assigned this name to the west-vergent fault system, which separates the Western and Central Cordilleras, as well as the contact between oceanic crust to the west and continental crust to the east. This fault system extends from southwestern Ecuador where it has been mapped as the Peltec-Giron-Portovelo faults (CODIGEM, 1993a in Cediel et al., 2004) to Montelibano area. Several interpretations include strike-slip system (Campbell, 1968; Case et al., 1971), west-vergent thrust of high angle (McCourt and Millward, 1983), right-lateral strike-slip system (McCourt and Aspden, 1983), left-lateral transtensional fault system (Kellog et al., 1983) and transpressional system with compressional and strike-slip components (Alfonso et al., 1994).

The use of the Romeral name in the Colombian Caribbean area (north of the Colombian Andes) is due to the fact that Duque-Caro (1975, 1976 in Duque-Caro 1979) projected this fault system 140 km further to the north to indicate a "suture" that separates the San Jorge-Plato Basin to the east and the accreted San Jacinto "terrain" to the west. This fault system has no significant surface expression in this region because Quaternary deposits cover most part of it (Fig. 3). However, Duque-Caro (1979) proposed its identification from the following observations: a) the change from high deformation present in the San Jacinto Fold Belt to the relative undeformed San Jorge Sub-basin, b) the presence of mafic volcanism and mafic, ultramafic and tonalitic plutonism associated with cherts and turbidites of late Cretaceous to middle Eocene age which are located to the west only and are completely absent in the east, c) the serpentinization of mafic and ultramafic intrusives along the western side, which is clearly visible south of Planeta Rica, d) the occurrence of a low-grade metamorphic belt (greenschist facies) along the eastern side of the Romeral Fault System, which has been recognized in wells, and

which correlates with the lower Tertiary Gaira Schist of the Santa Marta Massif (Irving, 1971) and e) s-shaped structural closures along the Romeral Fault System, possibly related to a north-south transcurrent movement.

The Romeral Fault System has later been interpreted in the Colombian Caribbean region as the early-middle Eocene tectonic boundary or suture between continental crust on the east and the accreted San Jacinto terrain to the west (ESRI-ILEX, 1995; Laverde, 2000). The obduction model presented by Flinch et al. (2000) and Flinch (2003) shows the Romeral Fault as a structure with a poliphasic transpressional and transtensional evolution that offsets the west-dipping obduction suture. Cediel et al. (2004) use the San Jacinto Fault name to refer to the "Romeral North Fault", interpreting it and its associated structures as a dextral-oblique accretion record of the San Jacinto and later Sinú terranes to the continental margin. Based on the combined analysis of the seismic, gravity and magnetic data, a new interpretation of the fault system at the Caribbean region in Chapter 7 is presented.

2.4 Stratigraphic framework

The definition of the stratigraphic framework allowed the identification of the major unconformities or sequence-limits from the seismic data (Chapter 3). The unconformities are surfaces of erosion or non-deposition which represent gaps in the geologic record and which generate seismic reflections separating strata with different physical properties or attitudes, thus providing a density/velocity contrast (Brown, 1985).

To generate the stratigraphy framework for the study area, a general revision of the surface geology, available well data, technical reports and recent publications was realized. The chronostratigraphic chart shown in Table 1 summarizes the stratigraphic framework of the study area.

The sedimentation in Northwestern Colombia was strongly controlled by the complex interaction between Caribbean and South American plates, resulting in a complex stratigraphic setting along the Colombian Caribbean margin.

The continental basement has been drilled by several wells in the San Jorge and Plato sub-basins to the east of the Romeral Fault System. This basement includes metamorphic rocks of Precambrian to Paleozoic age, locally intruded by lower Jurassic granodiorites (INGEOMINAS, 1997).

The basement of oceanic affinity is exposed as fragment fault flakes in the San Jacinto Fold Belt westward of the Romeral Fault System and consists of upper Cretaceous basalts and serpentinites. Associated with this oceanic basement appear intercalations of cherts, organic-rich shales, siltstones and limestones, denominated as Cansona Formation and interpreted as ocean-floor sediments of late Cretaceous age (Duque-Caro, 1979; ESRI-ILEX, 1995; Laverde, 2000).

The late Paleocene-early Eocene San Cayetano Formation overlies discordantly the Cansona Formation (INGEOMINAS, 1994 in ESRI-ILEX, 1995). This unit is exposed

in the core of anticlinal structures of the San Jacinto Fold-Belt and consists of lithic-arkosic sandstone, hemipelagic shales and some cherts intervals. The sandstones form thick packages and are considered as submarine fan turbidite (Laverde, 2000).

Table 1: Chronostratigraphic Chart of the Colombian Caribbean area (compiled from ESRI-ILEX , 1995; Laverde, 2000; ICP, 2000).

m.y	EPOCH	AGE		DEPOSITION ENVIROMENT	ONSHORE SINU	SAN JACINTO	SAN JORGE-PLATO BASIN
1.8	Quaternary	Holocene		San Jorge-Plato Basin: Lacustrine. Sinu-San Jacinto Area: Fluvio-deltaic facies to the west and Fluvio-alluvial facies to the east.	POPA	SINCELEJO/BETULIA	CORPA
		Pleistocene					
5.3	Neogene	Pliocene	Late	San Jorge-Plato Basin: Shallow marine. Sinu-San Jacinto Area: Littoral and fluvial toward the east, and turbitic toward the west.	ARJONA (PAJUIL)	CERRITO/ZAMBRANO-RANCHO	TUBARA
11.2			Early				
		Miocene	Late				
16.4			Middle	Deep water		CARMEN SUP	PORQUERO MEDIO SUP
23.8			Early	San Jorge-Plato Basin: Deltaic to shallow water sedimentation. Sinu-San Jacinto Area: Deep water sedimentation.	FLORESANTO LISETA	PERDICES/CARMEN INF	PORQUERO INF CALIZA DE CANTAGALLO
33.7	Paleogene	Oligocene	Late	Shallow marine to deltaic	PAVO	CIENAGA DE ORO	
			Early	Shallow water	MARALU		
		Eocene	Late		MANANTIAL	SAN JACINTO	?
			Middle	Shallowing-upward plataform deposits	CHERT DE LA CANDELARIA	TOLUVIEJO/CHENGUE/MACO	?
53.8			Early				
		Paleocene	Late	Submarine fans deposits	SAN CAYETANO		
65			Early				
	Cretaceous	Late	Maastrichtian	Abyssal Slope sedimentation	OCEANIC "BASEMENT" COMPLEX/FINCA VIEJA/CANSONA		
			Campanian				
	Pre-Cambrian to Jurassic						CONTINENTAL "BASEMENT" COMPLEX

The Upper Cretaceous-early Eocene sequence represents trench and deep water sediments which were deposited at the Colombian Caribbean margin, but are absent in the San Jorge-Plato Basin because this part of continent, already emerged, was occupied by the Cordillera Central-Santa Marta Massif block for this time (Duque-Caro, 1979).

A complex of siliciclastic and carbonate deposits which is exposed in the San Jacinto Area and which has been drilled by several wells in the most-western part of the San Jorge-Plato Basin represents the middle-late Eocene sequence. The siliciclastic deposits unconformably overlay the San Cayetano Formation, pinching out toward the east by onlapping basement. These deposits consist of intercalations of shales with some interposed phacoidal blocks of sedimentary breccias to irregular-bedded

calcareous sandy conglomerates forming clasts of different lithology (basalts, cherts, quartz, metamorphics, granodiorites, mudstones and limestones). This heterolithic assemblage denominated as the Maco Formation has been interpreted by Laverde (2000) to be a tectonic mélange. The middle Eocene carbonate facies are known as Chengue Formation and include mudstones, marlstones and micrites, which grade upward to "Toluviejo" algal packstone and calcareous sandstones. Deep water and siliceous sediments of middle Eocene have been recognized in the Sinú Region, forming dome structures and small ridges. These sediments are named "Chert de la Candelaria" by ESRI-ILEX (1995).

Duque-Caro (1979) documented a progressive marine invasion from the northwest during the late Eocene-early Oligocene. In this period of time a sedimentation change from deep water to shallow water environment occurred. The sediments of this age in the San Jacinto Fold-Belt correspond to the San Jacinto Formation and in the Sinú area to the Manantial and Maralú formations. These units consist essentially of fining-upward successions of conglomeratic sandstones to mudstones with local intercalations of late Eocene-early Oligocene limestones (Laverde, 2000).

The late Oligocene-early Miocene sequence was deposited in the shallow marine to deltaic environment and is denominated Ciénaga de Oro Formation in the San Jacinto Fold Belt, and Pavo Formation in the Sinú Area (ESRI-ILEX, 1995). The equivalent sequence (Ciénaga de Oro Formation) in the San Jorge-Plato Basin was deposited in the shallow marine to deltaic environment and consists mainly of quartz sandstone with calcareous cement, locally conglomeratic, with interbedded limy siltstone, carbonaceous and silty shale and occasional limestone and coal beds (ESRI-ILEX, 1995).

According to the drilled wells in the San Jacinto Fold-Belt, a highly variable lithology characterizes this unit; towards north the sequence is mainly composed by sandstone, while in the middle to south the unit is dominantly middy with some scarce sandy interbeds. The sediments exposed in the Pavo Formation in the Sinú Area include coarse-grained and conglomeratic, whitish or buff-colored, friable and lithic sandstones, interbedded claystones to siltstones and some lignitic coal seams, (Laverde, 2000).

At the beginning of the early Miocene an important transgressive event occurred. This event is characterized by the development of platform deposits which, according to the paleotopography, acquired a reefal disposition. These deposits include biomicrites and packstone of bivalves, gastropods, foraminifers and corals, which have been drilled by several wells in the San Jorge-Plato Basin, and which are denominated as "Caliza de Cantagallo". This unit has a reefal character in the basement highs, while the carbonate facies are associated with deeper water sediments (ESRI-ILEX, 1995). Haffer (1963) recognized these calcareous deposits in the Sinú area as "Caliza de Liseta".

Shales of deep water environment present in the San Jorge-Plato Basin and San Jacinto area indicate that the shallow deposits were covered by a flood during the early-middle Miocene (ESRI-ILEX, 1995). These deep water sediments correspond

to the Porquero Formation in the San Jorge-Plato Basin, Carmen Formation in the San Jacinto Area and Floresanto in the Sinú region. In the San Jorge-Plato Basin the sequence consists of varicolored and lightly calcareous claystone to siltstone, locally with gypsum; intercalation of sandstone, occasionally micrite and lignites; intercalation of claystone-siltstone calcareous fossiliferous (ESRI-ILEX, 1995). The sediments exposed in the San Jacinto Area (Morrosquillo Gulf) include mud-dominated layers interbedded with somewhat calcareous siltstones and thin beds of lithic sandstones (Laverde, 2000).

A regional unconformity is registered in the middle Miocene, generating the change of deep to shallow facies (ICP, 2000; Reyes-Harker et al, 2000). A thick siliciclastic sequence of middle Miocene-early Pliocene age overlies this unconformity. This sequence is denominated as the Tubará Formation in the San Jorge-Plato Basin, as the Cerrito/Zambrano-Rancho Formation in the San Jacinto Fold Belt and as the Pajuil Formation (Arjona Formation by INGEOMINAS 1994) in the Sinú Area (ESRI-ILEX, 1995). This unit in the San Jorge-Plato Basin has a marine to non-marine character and includes fossiliferous, lithic and fine- to medium-grained sandstone. This sequence in the San Jacinto-Sinú area consists of an intercalation of fine- to medium-grained lithic-sublithic sandstones grading upward to siltstones and mudstones interpreted as littoral and fluvial sediments to the east, that prograded westward forming turbidite deposition during the late Miocene to early Pliocene time (Laverde, 2000).

The strong change in the sedimentation from marine to continental is represented by the intra-Pliocene unconformity which is overlain by fluvio-alluvial and fluvio-deltaic deposits of the late Pliocene-Holocene age. This sequence is denominated in the Sinú area as the Popa Formation which is composed by reefal limestones, calcareous shales, and fine- to coarse-grained sandstone. The Sincelejo and Betulia formations correspond in the San Jacinto Fold-Belt to younger deposits including mudstone, claystones and siltstone interbedded with a sandy sequence. The sequence present in the San Jorge-Plato Basin was deposited in the lacustrine non-marine environment and is represented by claystones and siltstone with occasional sandstone beds, denominated Corpa Formation (ESRI-ILEX, 1995).

3. 2D STRUCTURAL CONFIGURATION

The interpretation of 850 km of 2D seismic reflection data throughout the study area, integrating the surface geology and well-log data, allows the identification of the morphological elements and tectonic domains of a typical subduction complex. Figure 4 indicates the location of the three composite 2D seismic profiles. Each of them is on average 250 km long and covers both offshore and onshore areas of the Colombian Caribbean active margin (Morrosquillo area). Four major tectonic domains from west to east can be defined (Attachment 2):
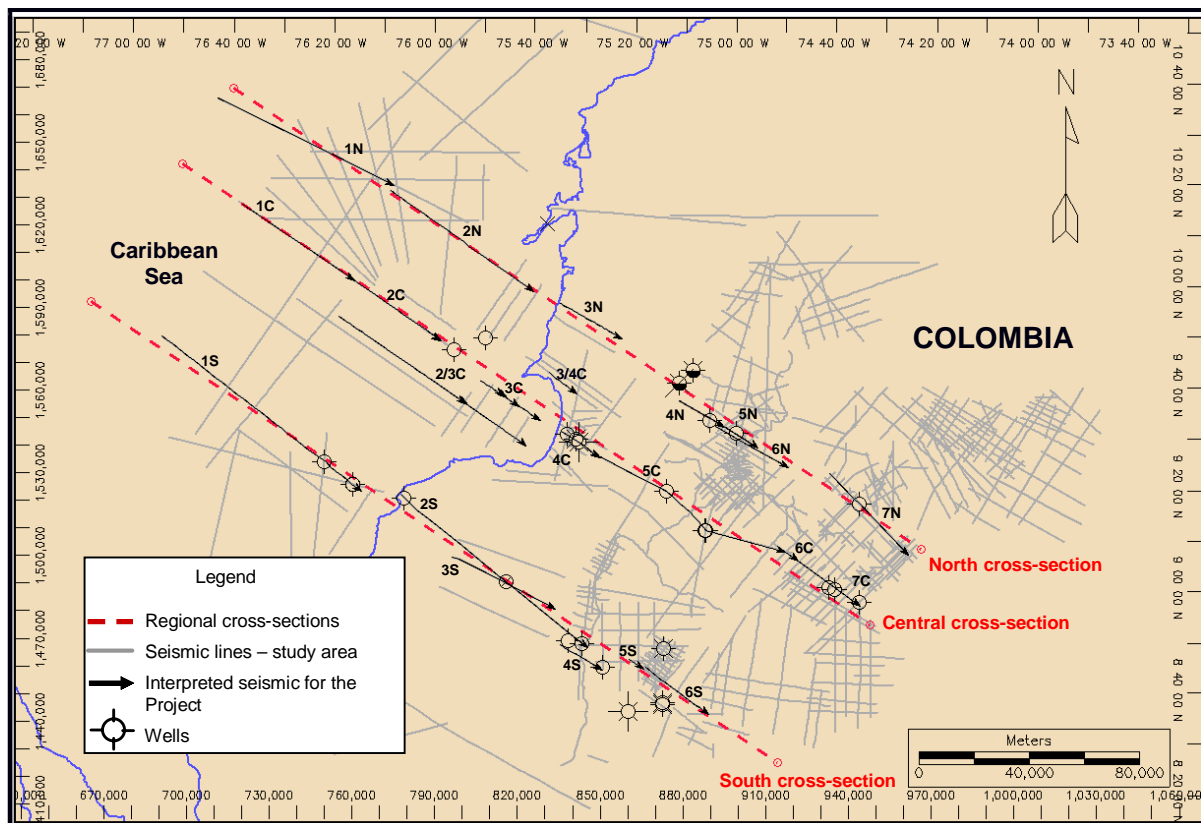
Figure 4: Seismic base map and location of the composite seismic profiles (2D structural cross-sections).

3.1 Colombian Caribbean Basin (trench domain)

The trench domain is particularly well-defined in the westernmost part of the northern composite profile (Fig. 5). The trench axis coincides with the toe of the active accretionary prism. The Colombian Caribbean Basin extends from the structural front of the accretionary prism. The basin infill is characterized by subparallel, subhorizontal, continuous and landward-divergent reflections that onlap the interpreted basement. The top of the oceanic plate can be traced in this domain as a relative strong, landward-dipping reflection from 6 to 7 seconds (TWT) displaying a

23

good lateral continuity. Several normal faults cut deep into the lower sedimentary layers and the interpreted oceanic basement.

Seismic-stratigraphy analysis of the multi-channel seismic-reflection profiles (Bowland, 1993) and DSDP sampled sediments (in Bowland, 1993) suggest that a very thick sedimentary sequence, locally over 6 km thick, was deposited on the top of the oceanic basement. This sequence includes late Cretaceous-Eocene biogenic pelagic sediments, Eocene-late Miocene clastic turbidity flows and late Miocene-Holocene clastic sediments from turbdite-fan systems (Bowland, 1993).
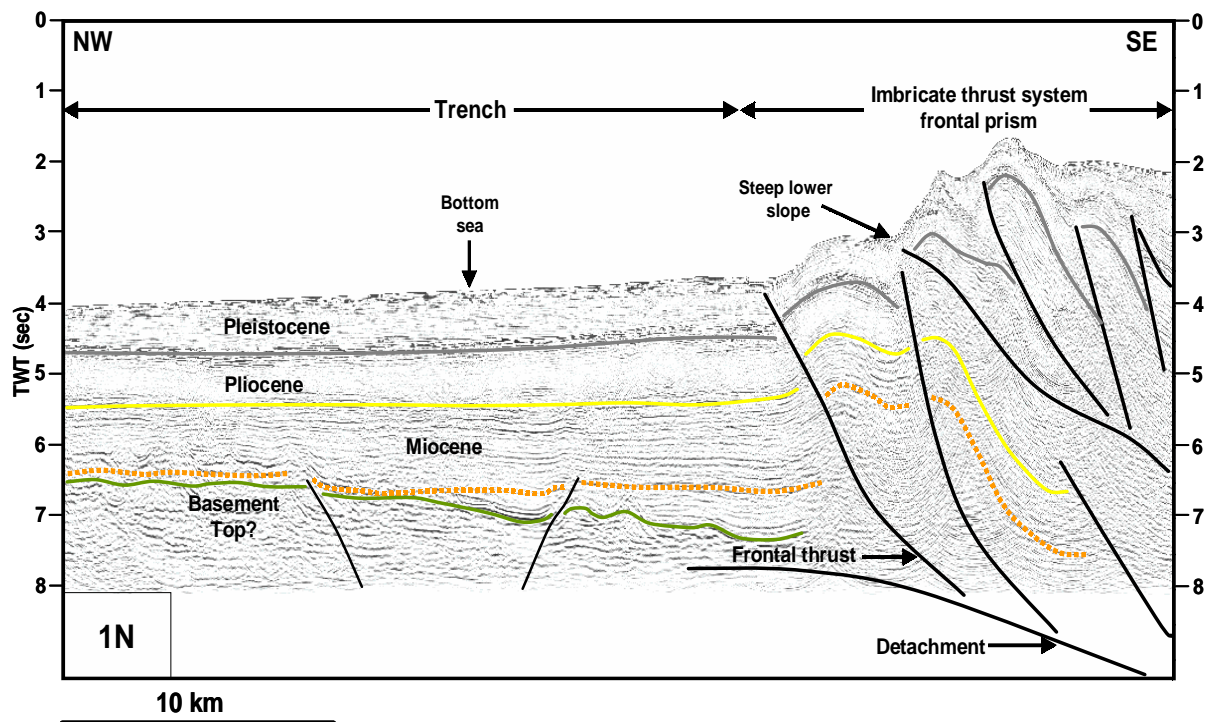
Figure 5: Seismic image of the trench domain in the western part of the seismic line 1N (see location in Fig. 4). The trench infill is characterized by sub-parallel, sub-horizontal, continuous, landward-divergent reflections that onlap the interpreted basement indicated by green reflector.

3.2 The active accretionary domain (frontal prism)

A clear image of the front prism is shown in Figures 5 and 6. This domain is limited seaward by the trench and landward by the outer high domain and represents the younger part of the Sinú-Colombia Accretionary Wedge. The area is characterized by a zone of active deformation and strong shortening, resulting in a complex seaward-vergent imbricate thrust system of short wavelength folds and complicated patterns of syn-depositional deformation. This imbricate thrust system involves the complete sedimentary sequence. Its basal detachment could be localized near to the top of the oceanic basement. Because this detachment is deeper than the seismic data (more

than 8 seconds) its definition is supported by structural modelling and geometrical constrains.

A very steep slope characterizes the sea floor topography at the frontal structures of the active accretionary prism. Several small basins can be recognized. Pelagic sediments cover the thin-skinned structures and pounded Pleistocene sediments are trapped in these small basins which becomes visible at the slope trend.

The seismic information shows a change in the structural style of the active front structure, which varies from an imbricate thrust system (Fig. 5) to a triangle zone (Fig. 6) along the strike. These geometric structural changes could be the result of some mechanical stratigraphic or any deeper heritage structural control.
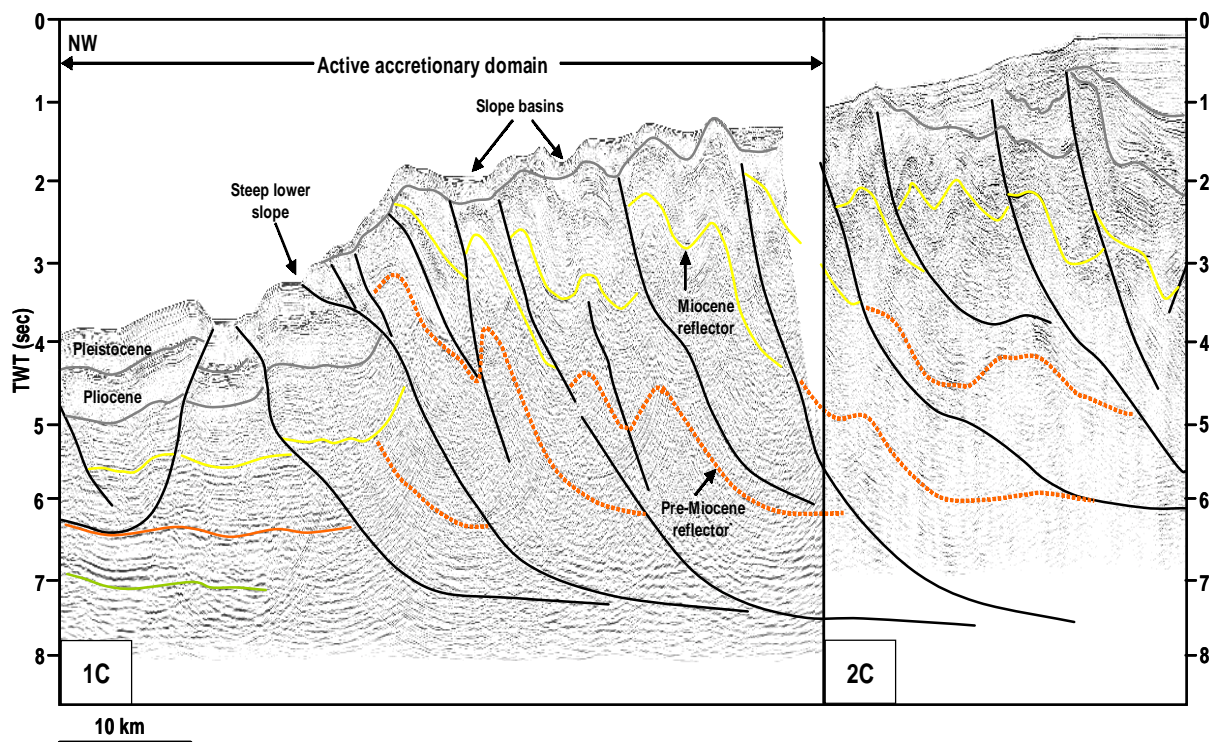
Figure 6: Seismic expression of the active accretionary domain in the seismic line 1C (see location at the Fig. 4). This domain represents the younger part of the Sinú-Colombia Accretionary Wedge and is limited seaward by the trench and landward by the outer high domain.

3.3 Outer high (older accretionary domain)

The transition between the active accretionary prism and the forearc domain is marked by the outer high domain (Byrne et al., 1993). A seismically well-imaged deformation zone is located 80 km from the trench in landward direction (Attachment 2). This zone coincides with the more elevated zone and the slope break at the seafloor topography and is interpreted as the boundary between the active

accretionary prism and the outer high. Structurally, this boundary is characterized by a west-vergent imbricate thrust system and by a backward breaking out-sequence thrust. Some thrusts forming these systems cut through to the top of the forearc basin deposits (Fig. 7). Younger deformation is evidenced by faulting and folding present in the forearc sedimentary fill.
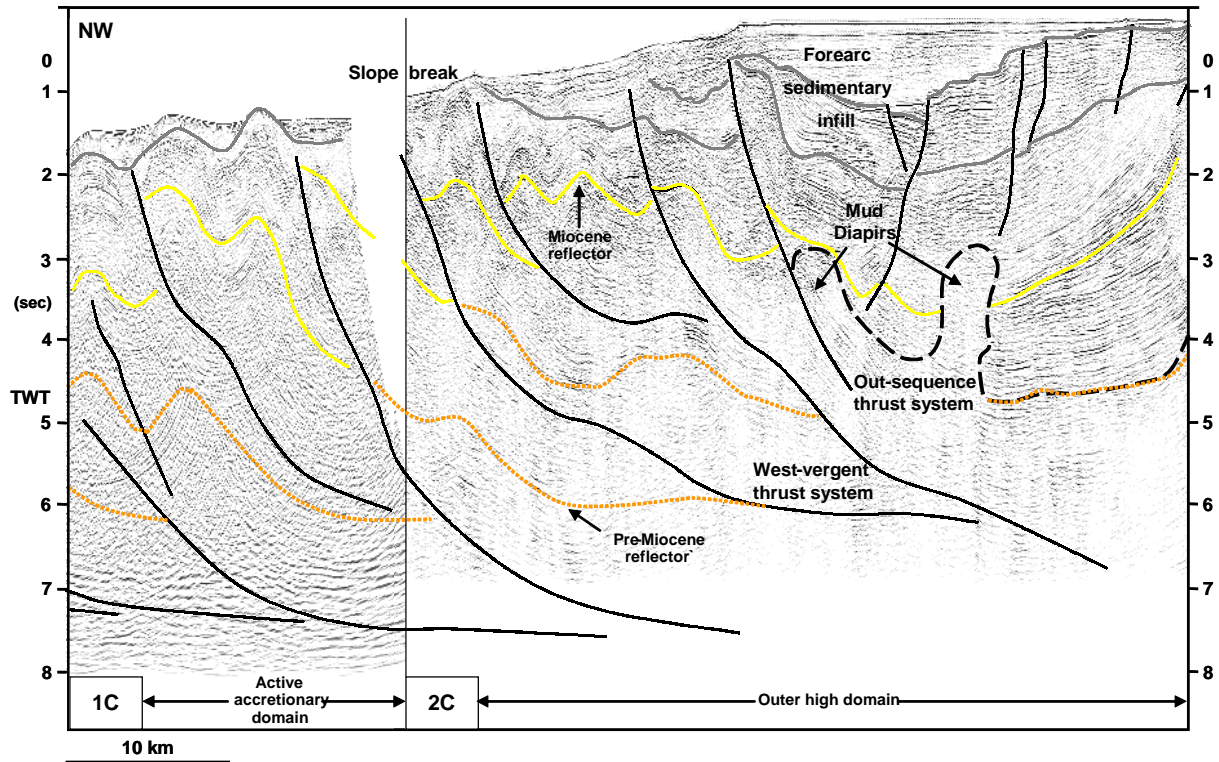
Figure 7: Seismic expression of the boundary between the active accretionary and outer high domains in the seismic line 2C (see location in the Fig. 4). A west-vergent imbricate thrust system and a backward breaking out-sequence thrust system characterize this zone.

Towards the east, the zone of this boundary is characterized by normal faulting, growth folding and mud diapirism (Fig. 8). The geometry of the pre-kinematic sedimentary units (beneath yellow reflector) is relatively well defined but the high deformation and mud diapirism masks the lower units which characterize the internal structure of this domain. Shortening is concentrated into some anticlines where the underlying ductile mud can flow towards the anticline cores leading to the formation of compressional diapirism. These mud diapirs do not necessarily extrude up to the surface but can be stopped and sealed by further sedimentation (forearc basin sedimentary fill). Flanked to the compressional diapirism structures, syn-tectonic sedimentation can be recognized. The layers of syn-tectonic strata (middle Miocene-Early Pliocene) deposited during uplift of the anticlines and diapirism display fan-like patterns with progressive onlaps onto the limbs of anticlines, leading to syn-tectonic unconformities with overlying sediments. Normal faulting is present 15 km landward

26

from the slope break. These faults show a typical fan-like pattern of deposition, indicating a contemporaneous fault-control subsidence and syn-tectonics deposition.

Landward, where the limit between the Sinú-Colombia Accretionary Wedge and San Jacinto Fold Belt has been defined, the seismic character changes from well-defined reflection geometry of the San Jacinto Fold Belt to chaotic seismic patterns of the Sinú Fault (Fig. 8 and 9). This loss in resolution indicates the high degree of deformation undergone in this zone. Just as was mentioned in the previous chapter, Duque-Caro (1979) interpreted the Sinú Fault as the feature that marks a change in the structural style between the Sinú Fold belt in the west and the San Jacinto Fold Belt to the east as well as the east-limit of the mud diapirism which is only present at the Sinú Area.
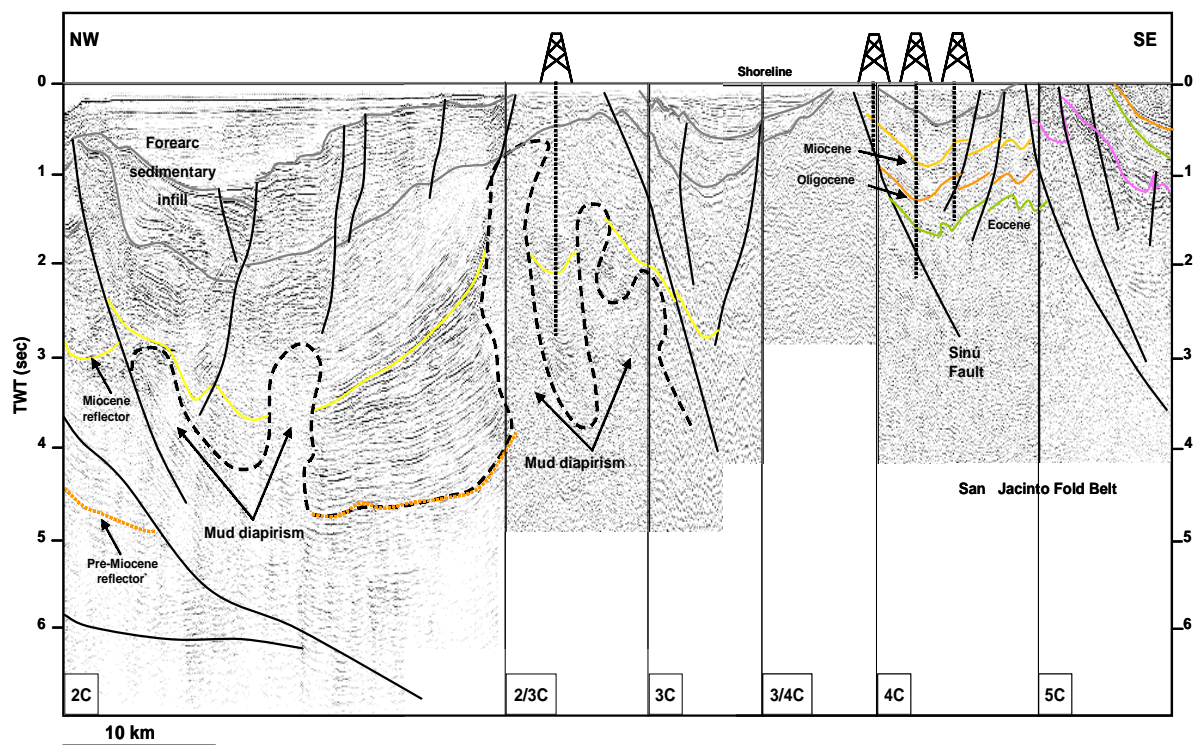
Figure 8: Outer high domain displayed in the central composite seismic profile (see location in Fig. 4). Normal faulting, growth folding and mud diapirism characterize this domain.

Because the San Jacinto Fold Belt is poorly defined by existent seismic images, it was only possible to identify the middle Eocene, middle Miocene and intra-Pliocene unconformities but not the basement top (Fig. 9). Normal faults affecting the pre-middle Miocene sequence are common, while the compressional deformation is represented by steep thrust faults and some inversion structures.

The most eastern part of the Sinú-Colombia accretionary wedge and the San Jacinto Fold Belt conforms a major structural complex which is interpreted here as the outer

high domain at the Colombia Caribbean margin. The outer high represents part of an older accretionary prism which acts as a backstop to the frontal active accretionary prism of the Sinú-Colombia Accretionary Wedge (Attachment 2).
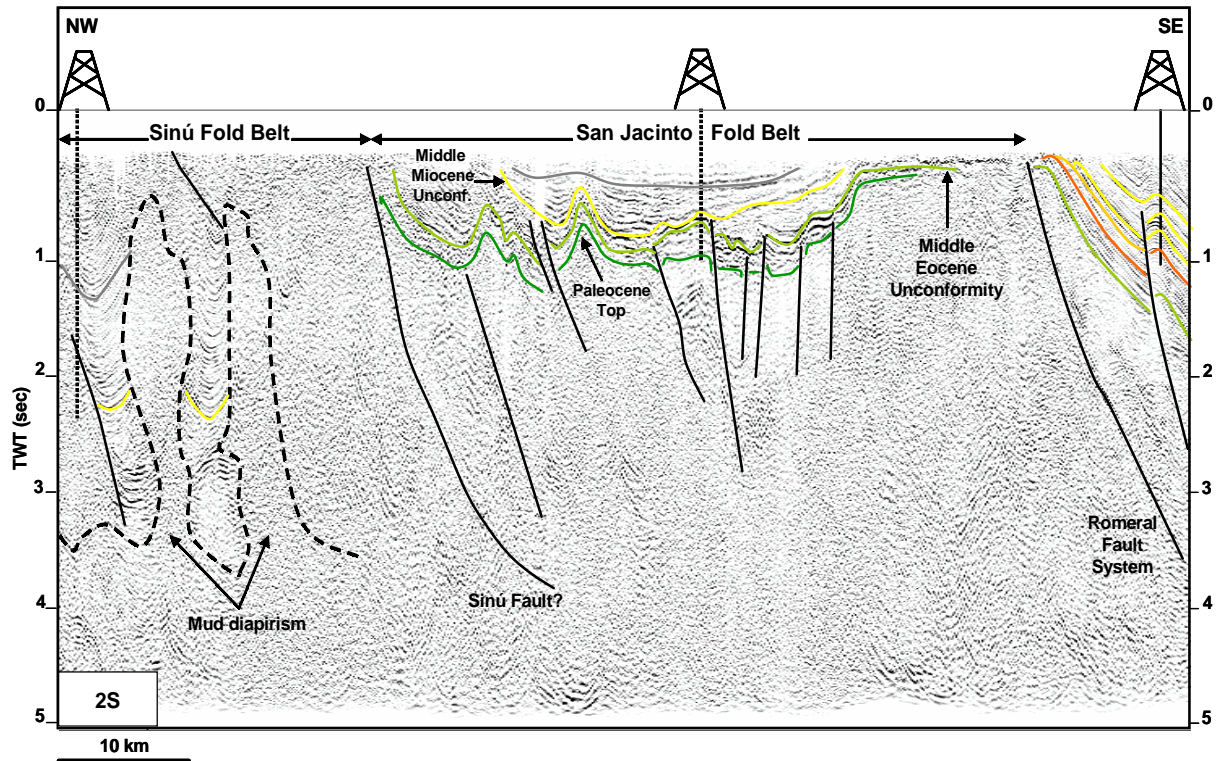
Figure 9: Seismic line 2S (see location at the Figure 4) displays the best seismic image of the San Jacinto Fold Belt. Normal faults affecting the Pre-middle Miocene sequence, steep thrust faults and some inversion structures characterize this zone.

3.4 Forearc domain

Oceanographic investigations and experimental modelling has revealed that the process of tectonic accretion in active margins is an efficient mechanism to develop the forearc basins (Larroque et al, 1995). These basins are bounded seaward by the structural high of the accretionary system and landward by a relative rigid backstop against which their sediments are deformed (Dickinson, 1973, and 1974; Karig & Sharman, 1975). Examples of these forearc basins have been recognized in western Colombia (Mountney and Westbrook, 1997), northern Colombia (Hardy, 1991), the Tobago Trough forearc basin off the Lesser Antilles (Westbrook, 1995), the Sunda Margin (Kopp et al, 2001), the Hikurangi Basin - New Zeland (Larroque et al, 1995) and the Tosa Basin adjacent to the Nakai Trough (Nasu, 1982).

Along the Colombian Caribbean margin, a seismically well-imaged series of depocenters in the shelf sector fossilizing the outer high domain can be recognized (Attachment 2). These depocenters have a wide spread surface extension over

hundreds of square kilometers with an over-1km-thick sedimentary cover. They are elongated, oriented parallel to the regional structural trend, and they are particularly developed behind the Neogene accretionary prism and characterized by a series of forearc sub-basins. These sub-basins are conformed by post-kinematic Plio-Pleistocene deposits which are seismically characterized by parallel to sub-parallel and lightly continuous reflectors onlapping the intra-Pliocene unconformity (Attachment 2). Growth folding and deformation caused by mud diapirism are evident. The deformation phase that generated the development of the active accretionary prism in the front of the Caribbean convergent margin was contemporaneous with the deposition of the upper Miocene-Lower Pliocene (?) sequence and had little effect on the post-kinematic forearc deposits, resulting in the preservation of almost flat-lying sequences of Pliocene-Pleistocene strata.

Vernette et al. (1992) and Ruiz et al. (2000) previously recognized some of these depocenters (e.g. San Bernardo Sub-basin) indicating the influence of oblique-slip deformation along its trend within the Sinú Fold Belt. Within the forearc basins recent tectonic movements are documented by folded sedimentary strata and active faults, some of which crop out at the sea floor and seem to be active because the sediments of the sea floor are affected. A well-defined active extensional fault trend characterized the sector near to the present shoreline (Attachment 2).

The landward part of the forearc domain is characterized by a bulge which coincides with that zone where the Romeral Fault System has been traced (Fig. 10). The structural uplift generated by the development of the Romeral Fault System (RFS) is the most prominent characteristic that marks the transition between the highly deformed forearc domain to the west and the deep San Jorge-Plato Basin to the east (Attachment 2).

As was mentioned in the last chapter, the Romeral Fault System has been interpreted as the Early-middle Eocene tectonic boundary or suture between continental crust on the east and the accreted San Jacinto terrain to the west (Duque-Caro, 1979; ESRI-ILEX, 1995; Laverde, 2000).

Upon the evidence on hand the Romeral Fault System is characterized by a seismically well-defined, regional scale, asymmetric, positive flower structure (Fig. 10). The thinning of the Early Miocene strata toward the western border of the San Jorge-Plato Basin indicates the rotation and uplift along the fault zone which could be contemporaneous with the Miocene sedimentation (Fig. 9, 10 and 11).

Seismic stratigraphy investigations (ICP, 2000) indicate a late Paleogene age for the oldest sediment layers in the forearc basins corresponding to Eocene-Oligocene strata which are thickening progressively to the west through the Romeral structural uplift. The Pliocene to recent deposits reveal that the development of the Plato-San Jorge Basin is characterized by continuous sedimentation and related subsidence. As in the adjacent basins, more than 4 km of sediments have accumulated. The San Jorge-Plato Basin infill consists largely of horizontally layered strata, roughly parallel

and mainly undisturbed (Figure 11). Exploratory drilling has penetrated alternating sequences of sand, silty mudstone and limestones as well as metamorphic and igneous rock of continental basement. Structurally, the basin is characterized by initial extensional structures and later by thrusting and inversion generated by a major transpressional tectonic regime. Interpreting the Plio-Pleistocene sequence of the San Jorge-Plato Basin as forearc sedimentary fill, the Romeral Fault System represents a major structural break separating the smaller, mud-diapirism-deformed basins from the main Plato-San Jorge Basin in the forearc domain (Attachment 2).
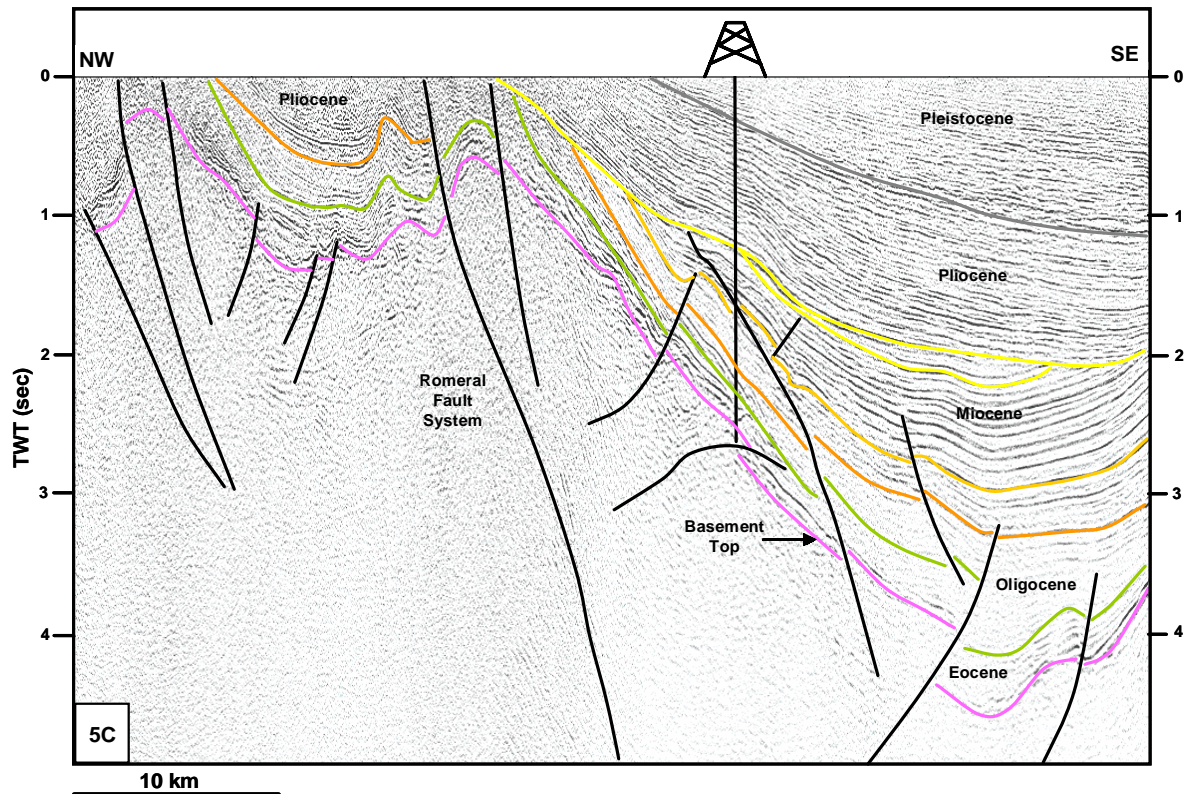
Figure 10: Line 5C (see location in Figure 4) displays the seismic expression of the Romeral Fault System. A regional scale, asymmetric and positive flower structure is well defined.

According to weak reflections present beneath the basin infill, which show low frequencies and high amplitudes, the continental basement continues westward through the Romeral Zone and probably below the entire forearc basin.
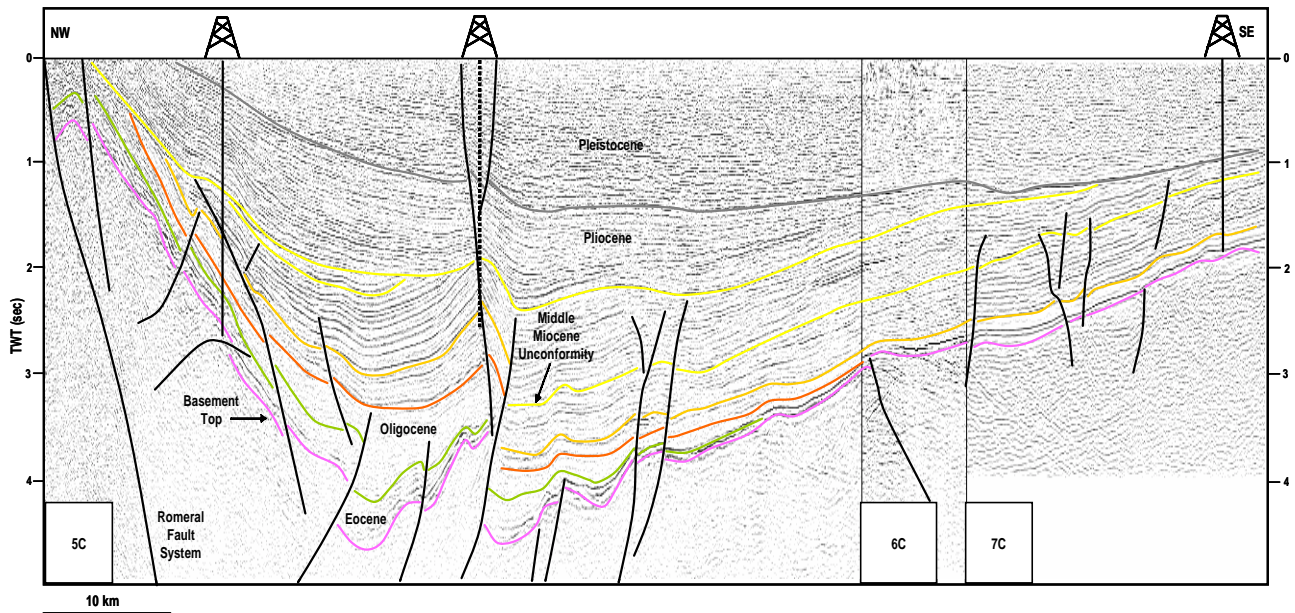
Figure 11: Seismic lines 5C, 6C and 7C (see location in Figure 4) cover fully the San Jorge Basin. Structurally, the basin is characterized by initial extensional structures and later by thrusting and inversion.

4. GRAVITY AND MAGNETIC ANOMALIES

For this study, gravity and magnetic data were provided by the Colombian Oil Company (ECOPETROL S. A). All data was mapped in the Bogotá coordinate system with the Colombia Datum (TM projection) using Surfer mapping software. For the presentation of the Isostatic anomaly the Gauss coordinate system was used.

4.1 Bouguer anomaly map

Prerequisite for gravity modelling is a uniform Bouguer map of the area under investigation (Hoffmann et al., 2003). The gravity data set for northwestern Colombia was compiled from available land surveys from Colombia, gravity marine surveys acquired on the Colombia platform and adjacent areas, and complemented with satellite-derived gravity data for offshore area (Cerón, 2002). The available data set for this project covers an area of 350 x 650 km^2. Spatial resolution is better than 2 km (half-wavelength) onshore and up to 5 km in some areas offshore. The data set was reduced to complete Bouguer anomaly using a density of 2.67 x 10^3 kg/m^3 onshore and 2.2 x 10^3 kg/m^3 offshore (GETECH, 2001).

Figure 12 shows the Bouguer anomaly map in conjunction with the major structural features of northwestern Colombia.

The strong positive Bouguer anomalies, which decrease toward the continental margin, characterize the Colombian Caribbean Basin. These positive values indicate that the oceanic rocks have higher densities than the continental rocks. This is supported by measured densities of less altered basalts and gabbros which are 2.8 to 3.0 x 10^3 kg/m^3 (Case et al., 1969b in Case et al., 1971).

Adjacent to the Colombian Caribbean Basin follows the South Caribbean deformation front. The region east of this tectonic feature is characterized by local high and low gravity anomalies which follow the trend of the Sinú and San Jacinto fold belts. The Sinú Fault (Duque-Caro, 1979), which separates the two fold belts, does not show a significant gravity expression, which indicates that rocks on both sides of the fault have similar average densities.

The Romeral Zone, which is considered to be the limit between San Jacinto Fold Belt and San Jorge-Plato Basin (Duque-Caro, 1979), corresponds to a NE-SW striking positive anomaly.

The Plato and San Jorge sub-basins are characterized by gravity lows down to -90 mGal. These basins are separated by a local gravity high (-30 to 10 mGal) which correlates with the Cicuco High.

The Sautatá Arc at the Panamá-Colombian border is characterized by positive anomalies with values of up to 90 mgals which decrease SE toward the Urabá Basin and NW toward the Sinú Accretionary Wedge.
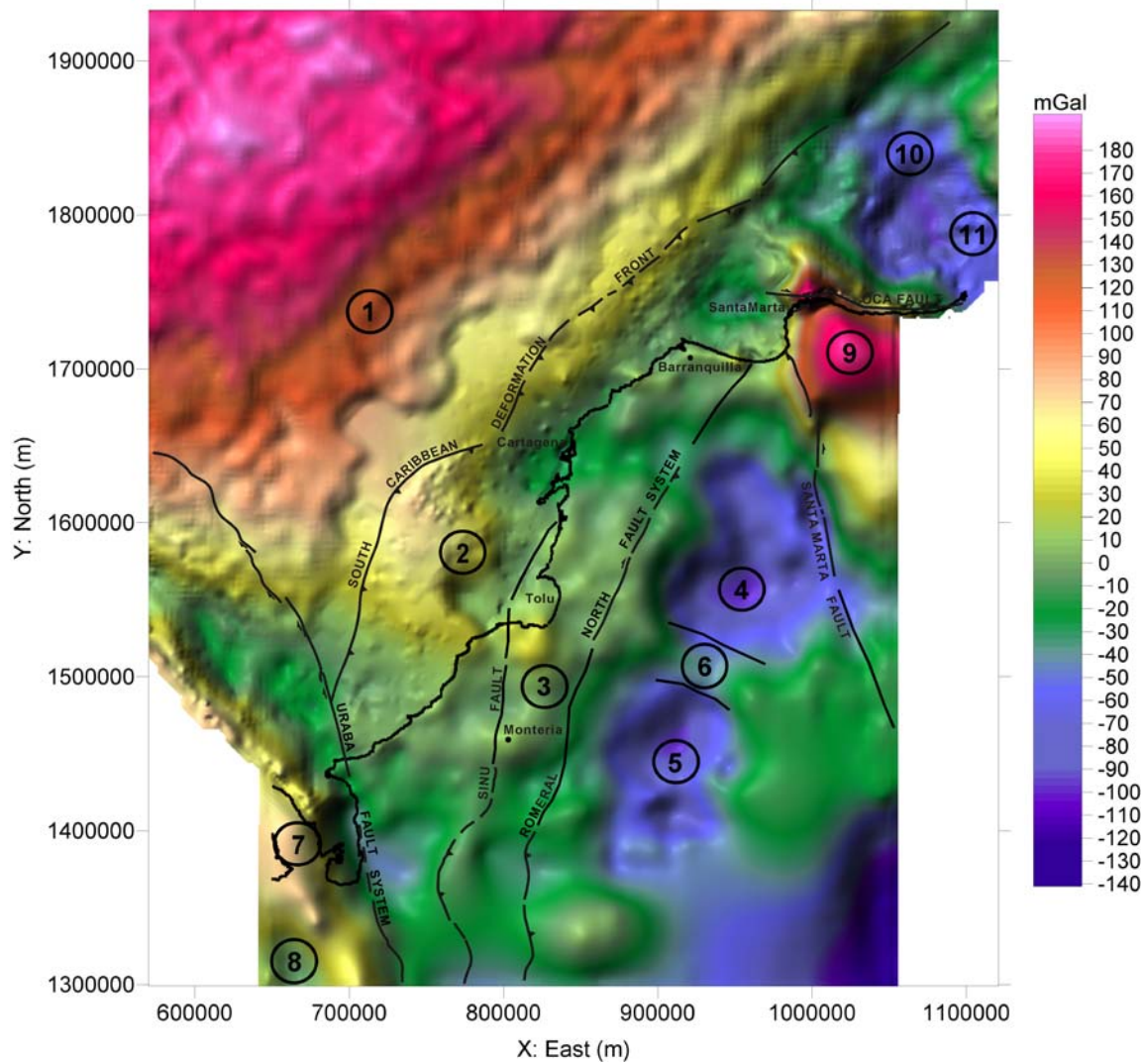
Figure 12: Bouguer anomaly map of NW Colombia and major structural features. (1) Colombian Caribbean Basin, (2) Sinú Accretionary Wedge, (3) San Jacinto Fold Belt, (4) Plato Sub-basin, (5) San Jorge Sub-basin, (6) Cicuco High, (7) Sautatá Arc, (8) Urabá Basin, (9) Santa Marta Massif, (10) Ranchería Offshore Basin and (11) Chuchupa-Ballena Basin.

A steep gradient is found along the Uramita (Urabá) Fault which was interpreted by Duque-Caro (1990) as the structural boundary between the Urabá Basin and the Sinú Accretionary Wedge.

Anomalies up to 180 mGals occur at the Santa Marta Massif. These strongly positive values may be caused by relatively dense metamorphic rocks, but more likely they indicate a thin continental crust. Therefore, the massif is out of isostatic equilibrium (see Fig.13). The massif is limited to the north by the Oca Fault which is correlated

34

with a steep gradient that marks the density contrast between the crystalline rocks of the Santa Marta Massif and sedimentary deposits of the Ranchería offshore and Chuchupa-Ballena basins. Another very steep gravity gradient characterizes the western limit of the massif. This gradient coincides with the mapped trace of the Santa Marta-Bucaramanga Fault Zone, which represents the boundary between the massif and the San Jorge-Plato Basin, where the anomaly values decrease substantially.

4.2 Regional Isostatic anomaly map

Isostatic anomalies provide valuable insight into active structures and tectonic processes that produce them. Isostatic anomalies are computed from free-air anomalies using corrections for topography, for water depth, and for changes down to the assumed depth of a compensating level (an arbitrary depth above which Archimedean mass-balance is assumed) as a function of elevation according to models such as those of Airy, Pratt or Heiskannen. From comparison of topography, free-air, Bouguer anomalies, and computed isostatic anomalies, subjective interpretations can be made of the extent of regional isostatic balance. Isostatic anomalies that average about zero over large areas suggest that columns are in approximate mass balance. Negative isostatic anomalies may indicate mass deficiencies as compared with "standard" columns and such areas should tend to rise. Positive anomalies indicate mass excesses and should tend to sink. Where the mass excesses or deficiencies are sustained, horizontal forces are overriding vertical forces. Many negative or positive isostatic anomalies have intra-crustal sources, as determined from steep gradients; thick, low-density sedimentary basins may produces lows, or thick sequences of mafic volcanic rocks, for example, may produce highs (Case et al., 1990).

The regional Isostatic anomaly of north Colombia (Fig. 13) was compiled from the maps available on Land and Marine Gravity CD-ROMs (1999). A very general interpretation of it is presented below.

In the Colombian Caribbean Basin the anomalies have values near zero suggesting approximate isostatic equilibrium. Large negative anomalies occur along the South Caribbean Deformed Belt from northwestern Colombia to north Venezuela as well as over the Panama Deformed Belt. These lows are related to more than 10 km of deformed sediments of accretionary prisms developed by Neogene convergence between the Caribbean and South American Plates. This trend of negative anomalies from northern Panama to northern Venezuela is interrupted by local positive anomalies ranging from -10 to up to 30 mGal, which could indicate a minor sedimentary load when compared with the rest of the accretionary prism.

Regional isostatic anomalies of San Jorge-Plato, Ranchería Offshore-Chuchupa-Ballena-Baja Guajira, Middle Magdalena Valley and Catatumbo basins are as low as – 60 mGal. These values are consistent with thick and low-density sediment layers deposited in these basins.
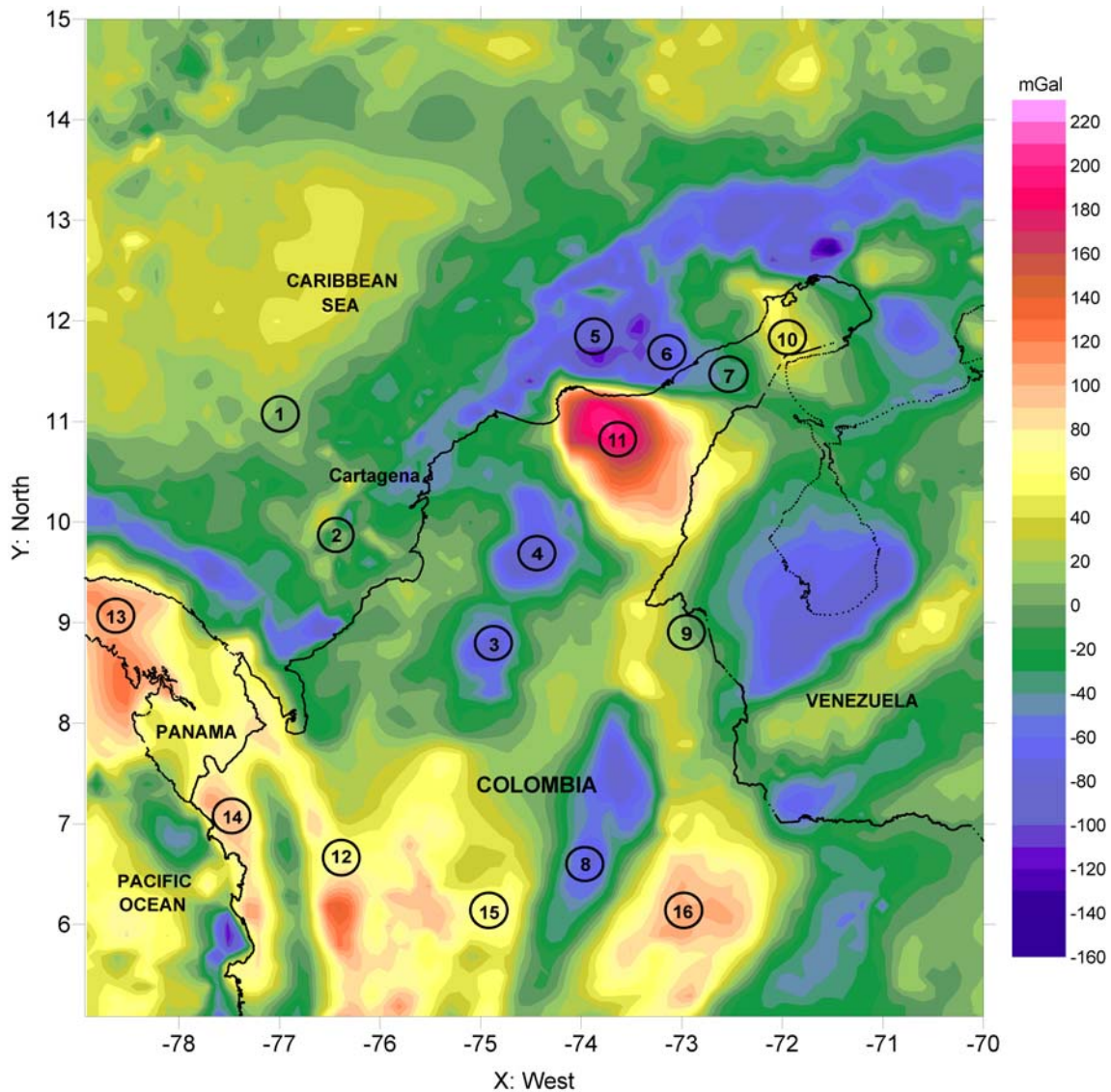
Figure 13: Isostatic anomaly map of NW - South American corner (Land and Marine Gravity CD-ROMs, 1999). Contour interval 10 mGal. (1) Colombian Caribbean Basin, (2) Local positive anomalies interrupting trend of negative anomalies from Panamá to Northern Venezuela, (3) San Jorge Sub-basin, (4) Plato Sub-basin, (5) Ranchería Offshore Basin, (6)Chuchupa-Ballena Basin, (7) Baja Guajira Basin, (8) Middle Magdalena Valley Basin, (9) Catatumbo Basin, (10) Guajira Peninsula, (11) Santa Marta Massif, (12) Western Cordillera, (13) Eastern Panamá, (14) Serranía del Baudó, (15) Central Cordillera, (16) Eastern Cordillera.

The positive isostatic anomalies present in the Guajira Peninsula could represent a thin continental crust or the area has been non-isostatically uplifted (Case and McDonald, 1973).

The strong positive anomalies of up to 190 mGals at the Santa Marta Massif, which rises to 5.776 m, indicate that the area is out of isostatic balance. An uncompensated excess mass must exist under the massif at relatively shallow depth (Case and McDonald, 1973).

The Western Cordillera (Colombian Andes), the Serranía del Baudó and eastern Panamá are characterized by strong positive anomalies ranging up to 120 mGals. The area is out of isostatic equilibrium with an excess of mass, probably sustained by convergence between the Nazca and South America plates (Case et al., 1990).

Positive anomalies, up to 100 mGal, north of the Central and Eastern Cordilleras (Colombian Andes) can be observed. These values are generated by an up-to-45 km thick continental crust that underlies these mountain ranges (Case and McDonald, 1973).

**4.3 Qualitative interpretation of magnetic anomalies**

Analysis of the characteristics of the magnetic contours by visual inspection of the magnetic map helps to determine the basic geologic nature of its buried source as well as the presence of major faults involving the basement. Because magnetic relief is controlled by the lithology and is almost independent from topography and sedimentary cover, all observed magnetic anomalies are either related to the crystalline basement or to mafic rocks of the oceanic crust. For instance, in areas where the hard rocks are shallow and uniformly magnetized such an assumption might give useful qualitative information on the structure of the rocks, particularly when linear trends are observed (Dobrin, 1976). The qualitative evaluation of the magnetic anomaly map of the Study Area is described below.

4.3.1 Magnetic total-field intensity map

Magnetic surveys both from aerial and marine platforms were compiled into a single grid using a leveling technique to bring different data patches to a common equivalent elevation of 1000m barometric at average sea level and a common epoch for 2004 (Cerón, 2002). The compiled data set was complemented offshore using the Geophysics of North America data (Finn et al. 2002).

The data coverage at the Colombian Caribbean Basin (offshore region) is not sufficient to analyze the character of the anomalies in this area. Therefore, the description presented below is restricted to the onshore portion and the most eastern offshore part of the study area.

From the magnetic map (Fig. 14) two areas can be identified where the anomalies have different tendency, amplitude and magnetic-relief. These two areas are separated by a NE-SW striking lineament of narrow and elongated magnetic anomalies which coincide with the Romeral zone.
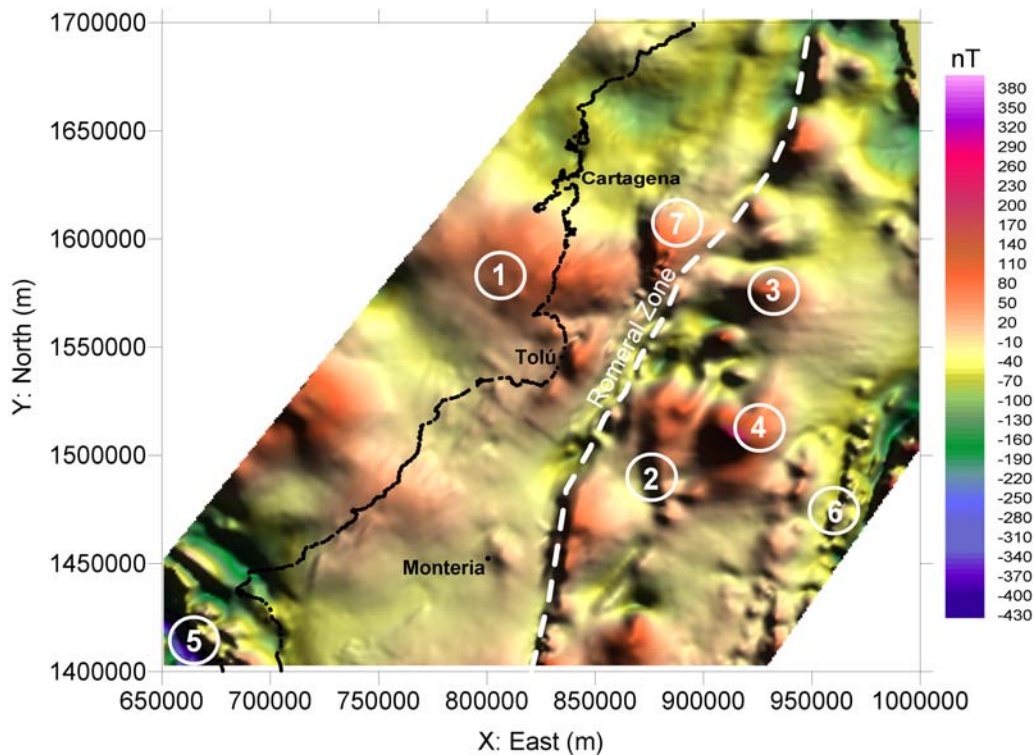
Figure 14: Magnetic total-field intensity map of NW Colombia (compiled by Cerón, 2002). (1) E-W oriented Caribbean magnetic anomalies, (2) and (3) low amplitude and high-relief anomalies in the San Jorge and Plato sub-basins, (4) NW-SE linear, strong and positive anomalies in the Cicuco High, (5) strong negative to slightly positive magnetic anomalies in the Sautatá Arc, (6) low amplitude and high relief anomalies at the eastern part of the San Jorge Basin, and (7) high amplitude and high relief anomaly southeast of Cartagena city.

Large scaled anomalies are the dominant magnetic characteristics west of the Romeral Zone. They could be part of the easterly oriented magnetic lineation observed in the Colombia Basin which are interpreted by Christofferson (1973) as a record of ancient geomagnetic field reversals resulting through the seafloor-spreading process.

East of the Romeral Zone, magnetic anomalies have restricted extensions and show high variation of magnetic intensity (Fig. 14). They reflect the lateral contrast of magnetic susceptibility of the basement because sedimentary rocks normally do not show such a magnetic expression.

Anomalies of medium to high amplitude and high-relief, trending NW-SE and E-W are present across the San Jorge and Plato sub-basins (east of the Romeral Fault System). The Cicuco High, which separates the San Jorge and Plato sub-basins, follows NW-SE linear, strong and positive anomalies. The anomalies present east of the Romeral Zone must be generated by the basement (intra-basement source) that

underlies the San Jorge and Plato sub-basins which have been drilled by several wells. The basement consists of Silurian to Paleozoic metamorphic rocks (greenschists, amphibolites, metabasites, granulitic migmatites and gneisses), which were intruded by Paleozoic mafic to ultramafic rocks and Cretaceous stocks of tonalities and granodiorites. Ultramafic to mafic intrusions occur frequently in the western part of the Cordillera Central (see Fig. 3: Geologic map). It can be assumed that the high amplitude and high relief anomalies (in Fig. 14 designated with 3 and 4) are caused by these local rock variations within the basement as these rocks contain higher amounts of magnetic minerals.

The Gulf of Urabá region is partially present in the southwestern corner of the map. The Sautatá Arc is the major feature of this region which is built up of basic Cetaceous volcanics. In Fig. 14, the arc can be recognized as parallel chains of strong negative (-400 nT) to medium positive anomalies (+50 nT). The observed correlation of the negative anomalies with the topography were interpreted to be caused by a polarization low which is related to the igneous rocks along the crest of the Sautatá Arc (Case et al., 1971).

Linear trends of low amplitude and high relief anomalies occur at the eastern part of the San Jorge Basin, which are very different to the anomalies observed from the anomalies under the basin and near to the Romeral Fault Zone. Assuming that the basement consists of the lithologies of the Cordillera Central as well as of the Serranía de Lucas, it can be suggested that the observed anomalies are caused by lower Cretaceous mafic stocks and dikes. These intrusives are exposed in the northern part of the Cordillera Central (see Fig. 3: Geologic map).

The San Jacinto Fold Belt, west to the Romeral Fault Zone, is generally characterized by large positive to negative anomalies of medium magnetic relief with smooth gradients. Small local positive anomalies present to the east of the cities of Monteria and Tolú could be related to highs of oceanic basement which is exposed in the southern part of the San Jacinto Fold Belt (see Fig. 3: Geologic map).

The high amplitude and high relief anomaly present southeast of Cartagena is more similar to the anomalies from the continental basement of the San Jorge and Plato basins than to the anomalies from the oceanic basement of the San Jacinto Fold Belt.

4.3.2 Reduced-to-Pole map (RTP)

However, and due to the individual components of the magnetic field, in the Magnetic total-field intensity map (Fig. 14), the anomalies do not appear directly above the causative bodies; to the magnetic latitude these bodies appear as significant pairs of positive-negative anomalies. The method to remove the distortion effects of magnetic data from varying inclination and azimuth of the magnetization vector is called "Reduced to Pole" (Baranov and Naudy, 1964). The application of this method converts data which have been recorded in the inclined Earth's magnetic field to what

the data would have looked like if the magnetic field had been vertical. Reduction to pole removes the anomaly asymmetry caused by the inclination and locates the anomalies above the causative bodies (Sheriff, 1984).

LCT-software was used for the reduction to pole process (RTP) to obtain the map shown in Figure 15. The parameters of the Earth's regional magnetic field are determined from a 13th order polynomial approximation of magnetic satellite readings and calculated for the time of the survey. The value for the Earth's magnetic intensity of 28400 nT and the magnetic inclination and declination for the survey area of 39.5°N and 3.5°W respectively were used as magnetic parameters for the merged onshore and offshore area.
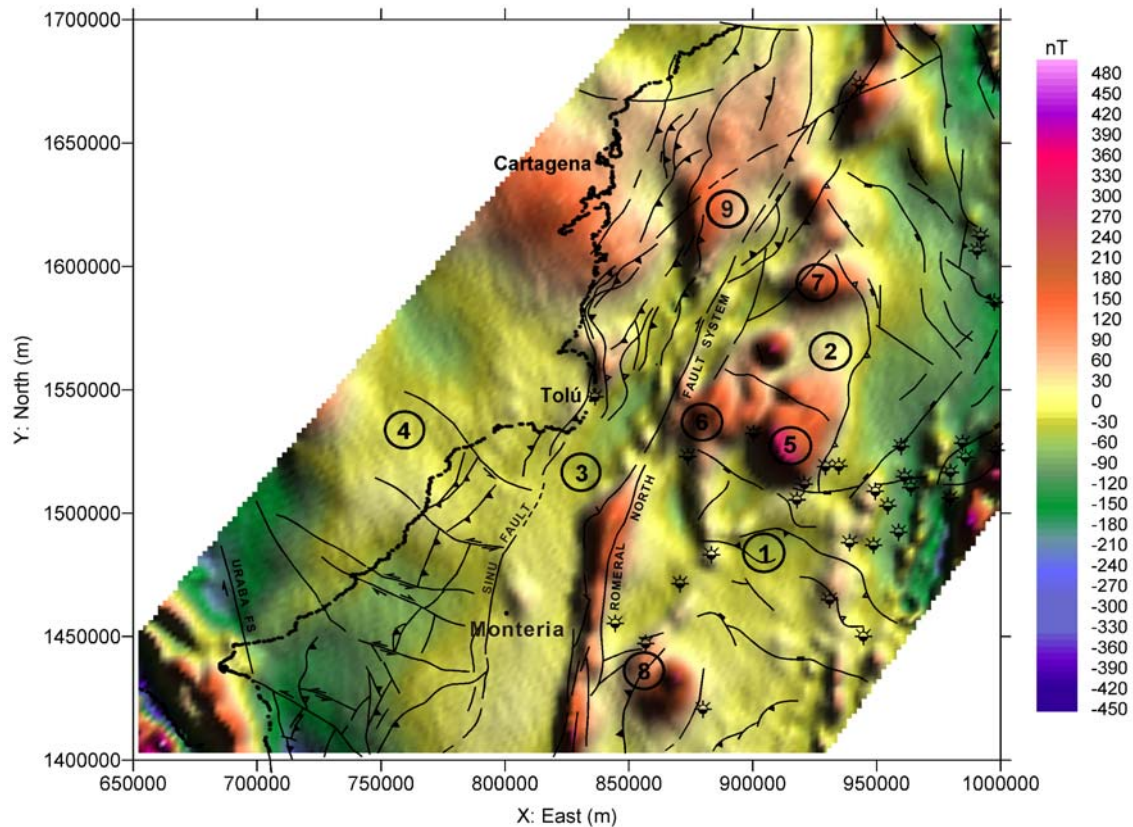
Figure 15: Magnetic Reduced-to-Pole anomaly map of NW Colombia with the structural map (Cediel and Cáceres, 2000) superimposed. (1) San Jorge Sub-basin, (2) Plato Sub-basin, (3) San Jacinto Fold Belt, (4) Sinú Accretionary Wedge, (5) Cicuco High, (6) Ayhombe High (7) Apure High, (8) Cábano-Tablón High, and (9) positive anomaly southeast to Cartagena city. The symbols indicate the location of some wells which have drilled the basement.

Smooth contours and low magnetic relief characterize the San Jorge and Plato sub-basins and San Jacinto Fold Belt and Sinú Accretionary Wedge. This indicates higher sediment load where the magnetized rocks of the basement are very deep. In these

zones the magnetic relief reflects the lithology of the basement rather than irregularities at the basement surface. Minima of the magnetic anomaly coincide with the maximum depth of the San Jorge and Plato sub-basins, whereas its outer borders show moderate positive values of about 120 nT.

In the RTP-map, the location of the Romeral Fault System can be much better identified when compared with the TMI-map (Fig. 14). The Romeral Zone is characterized by long, NE-SW striking anomalies where steep gradients occur at their borders. The strong positive anomalies indicate that this fault system has displaced strongly magnetized rocks near to the surface. As mentioned above (Chapter 4.3.1), the basement of the area is the only rock source containing higher amounts of magnetic minerals. Therefore, the Romeral Fault System led to an uplift of igneous-metamorphic rocks near to the surface. This assumption is confirmed by the occurrence of positive magnetic anomalies at the Cicuco, Ayhombe and Apure highs where wells have been drilled shallow basement. Reyes-Santos et al. (2000) interpreted the region east to the Romeral Fault System as a group of transtensional and rotating basins, conformed by basements blocks, which are related to normal and thrust faults and which have controlled the thickness of the overlaying sedimentary units. The structural uplift generated by the development of the Romeral Fault System is one of the most spectacular features which are observed from the seismic data (see Chapter 3.4).

As mentioned above, the positive anomaly up to 190 nT located southeast of Cartagena city is interpreted to be related with the continental basement present in the San Jorge and Plato basins. This would indicate that toward north, the Romeral Fault System is propagating to the west and its frontal structures also involve continental basement here.

5. 3D FORWARD GRAVITY MODELLING

The 3D gravity modelling was carried out with the interactive modelling program IGMAS (Schmidt and Götze, 1995). The modelling is based on the interactive modification of an initial 3-dimensional model which consists of various bodies with defined geometry and physical properties. Because magnetic effects can be treated in a similar way as gravity, the IGMAS program can be used for magnetic modelling as well. The principles of forward gravity modelling are described below.

5.1 Theory

The modelled area is divided into vertical sections (planes) which should be oriented vertically and rectangularly to the main strike direction. It is not necessary that all planes are equidistant to each other, but it must be taken into consideration that all of them have to be parallel (Figure 16). It should also be noted that the plane-number depends on the complexity of the observed geology and gravity anomalies. In areas with complex structures additional planes are necessary to avoid misinterpretation due to spatial aliasing (Figure 16). In order to avoid any impacts by edge-boundaries on the modelled density distribution, the model area has to be extended to 1000 km in x- and y-directions. On these planes, the 2-dimensional polyhedrons are modelled. The polyhedrons are constructed with numerous vertices which are triangulated automatically by the software to form a triangle net.

Figure 16: Example of the presentation of a simple two-layer substructure in data structure. $S_1…S_{12}$ = triangles, $EB_1…EB_3$ = vertical sections, $L_1…L_4$ = lines, and $V_1…V_{13}$ = model vertices. Earth vertical section is both a cross-section and a working area on the graphical terminal (Götze and Lahmeyer, 1998)

The effect of gravity on these polyhedrons is calculated by transforming a volume integral into a sum of line integrals. Following Götze and Lahmeyer (1988) and

applying Gauss's und Green's theorems on potential theory, the gravity potential is given by:

$$U(P) = G \iiint \frac{dm}{R}$$

(eq. 1)

with: U(P) = potential at P, R = distance between P and dm, G = gravitation constant, dm = ρ · dx · dy · dz = ρ · dV.

The derivation of the potential U gives the gravity g:

$$g(P) = \frac{dU}{dz}(P) = G\rho \iiint \frac{\partial}{\partial z}\left(\frac{1}{R}\right)dv$$

(eq. 2)

By using the Gauss formula this is transformed into:

$$g(P) = \frac{dU}{dz}(P) = G\rho \oiint_{surface} \cos(n,z)\left(\frac{1}{R}\right)dS$$

(eq. 3)

with n = outer surface normal vector.

This surface integral is calculated for the whole polyhedron surface. The term cos(n,z) describes the direction of the surface element dS in the Cartesian coordinate system. The attraction of the whole polyhedron may be expressed as a superposition of the attractions emanated by its single plane surfaces S_j .

$$g(P) = G\rho \sum_{j=1}^{m}\left[\cos(n_j,z)\iint_{Sj}\left(\frac{1}{R}\right)dS_j\right]$$

(eq. 4)

m is the number of plane surfaces.

Equation (4) is transformed into a linear integral using the polygon P_j which comprises the surface S_j. The polyhedron is built of the vertices V_j. The parameters $h_{j,i}$, $r_{j,i}$, $a_{j,i}$ and $b_{j,i}$ describe the distances of the different vertices in a surface oriented coordinate system. The gravity g in point P, caused by a polyhedron, is described by:

$$g(P) = fp\left(\sum_{j=1}^{m}\cos(n_j,z)\left\{\sum_{i=1}^{Kj}h_{j,i}\left[\ln\frac{b_{j,i}+\overline{PV_{j,i-1}}}{a_{j,i}-\overline{PV_{j,i}}}+\frac{\left|\overline{PP_j^*}\right|}{h_{j,i}}\left(\arctan\frac{\left(r_{j,i-1}\right)^2+b_{j,i}\,\overline{PV_{j,i-1}}}{\left|\overline{PP_j^*}\right|\left|h_{j,i}\right|}-\arctan\frac{\left(r_{j,i-1}\right)^2+a_{j,i}\,\overline{PV_{j,i}}}{\left|\overline{PP_j^*}\right|\left|h_{j,i}\right|}\right)\right]+2\pi\left|\overline{PP_j^*}\right|\delta\varepsilon\right\}\right)$$

(eq. 5)

with:

$$\delta = \begin{cases} 1 \text{ for } P^* \in S_j \\ \\ 0 \text{ for } P^* \notin S_j \end{cases}$$

ε: factor

P_j: polygon j containing surface S_j

The matching of the modelled curve with the observed Bouguer anomaly or the magnetic field can be achieved by "trial and error": geometries of the polyhedrons and to a lesser degree also densities are changed by an interactive process in order to achieve a best fit between the calculated and observed gravity response. Additionally, the "inversion" option also helps to find an optimum of the modelled gravity.

5.2 3D modelling area and starting model

The 3D gravity modelling region covers an area of 258.7 x 163 km^2 and strikes with S56°E approximately parallel to the direction of the tectonic transport. Eleven planes build up the 3D model. Figure 17 shows the location of these planes in the Bouguer anomaly map.

Planes 4, 8 and 10 correspond to the south, central and north 2D structural cross-sections (Chapter 3) for which seismic and well information are available. The interpreted time cross-sections were converted to depth sections using a velocities scheme generated from the integration of the available velocity logs and rms velocities. The resultant depth structural cross-sections were adjusted with the unit-tops information from graphic composite logs. A simplified structural interpretation was the base to define the upper crust polygons of the initial density model. The assigned densities for these sedimentary polygons were taken from density logs. The densities applied to middle and lower crustal bodies were preliminarily estimated using the information from other published geophysical studies (Case et al., 1971; Case and McDonald, 1973; Case et al., 1984; Kellog et al., 1983; Case et al., 1990; Stern, 1998) and then were modified by inversion parameters during modelling. The downgoing slab configuration of the Caribbean Plate has been initially inferred from seismicity cross-sections shown in the publications of Pennington (1981), Kellog and Bonini (1982) and Malavé and Suárez (1995).

Due to the complexity of the study area, additional planes had to be constructed in between the sections 4, 8 and 10. This is necessary to avoid misinterpretations by unconsidered gravitational anomalies (see Chapter 5.1). By numerical modelling of the Bouguer anomaly under constrains of all available geophysical and geological data it is also possible to derive the geological structure between the seismic sections.

5.3 3D density model

The large scale 3D density model was constructed to characterize the crustal structure and density distribution of the Colombian Caribbean margin. The elevation profile at the top of the model is based on a grid of the satellite bathymetry data and

the gravity station elevations. The model extends from sea level as a reference down to a depth of 50 km.
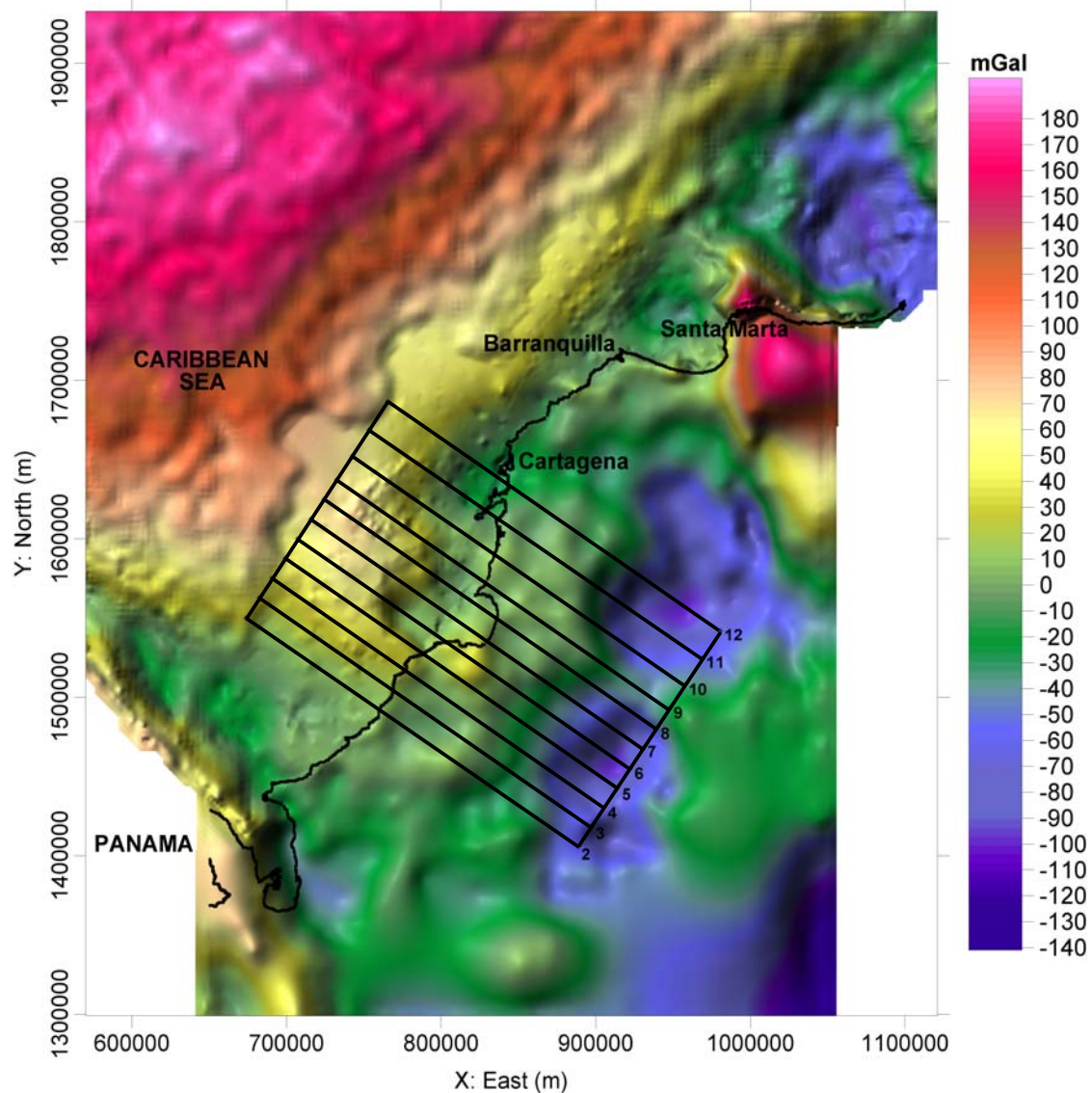
Figure 17: Location of the 3D modelling area in the Bouguer anomaly map. The black lines depict the planes of the gravity modelling.

A very good fit between the observed and calculated curves was obtained for each plane along the different tectonic domains. Figure 18 shows a comparison between the calculated and the observed gravity field. The differences between the modelled and the observed anomalies are displayed in Figure 19. The distribution of gravity differences (Figure 20) indicates that the residues are well distributed around zero (0) and remaining differences are less than 10 mGal. Furthermore, its standard deviation is less than 2 mGal which is comparable to the data-resolution.
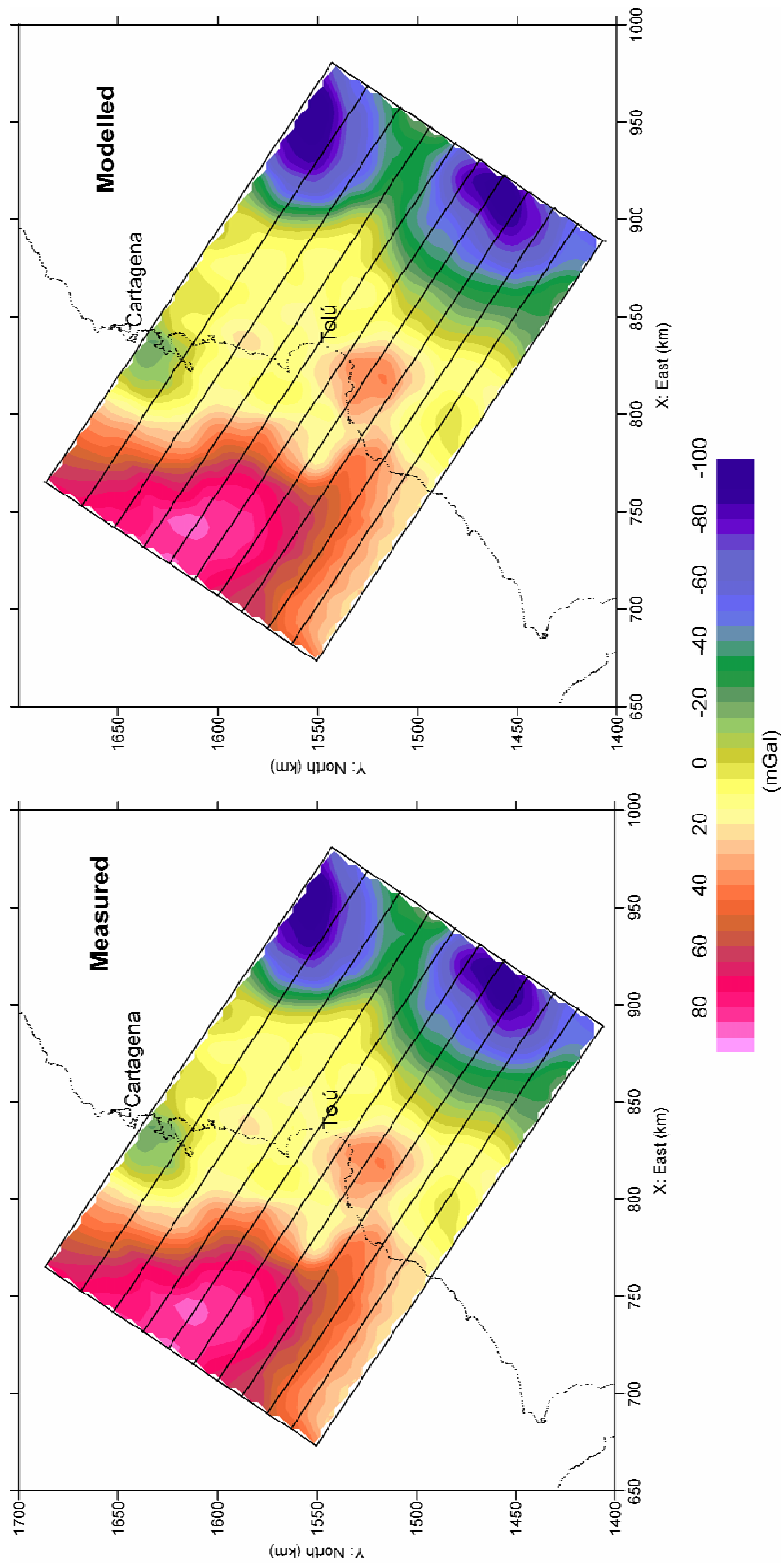
Figure 18: Observed and calculated gravity fields in the 3D modelling area (contour interval 5 mGal).
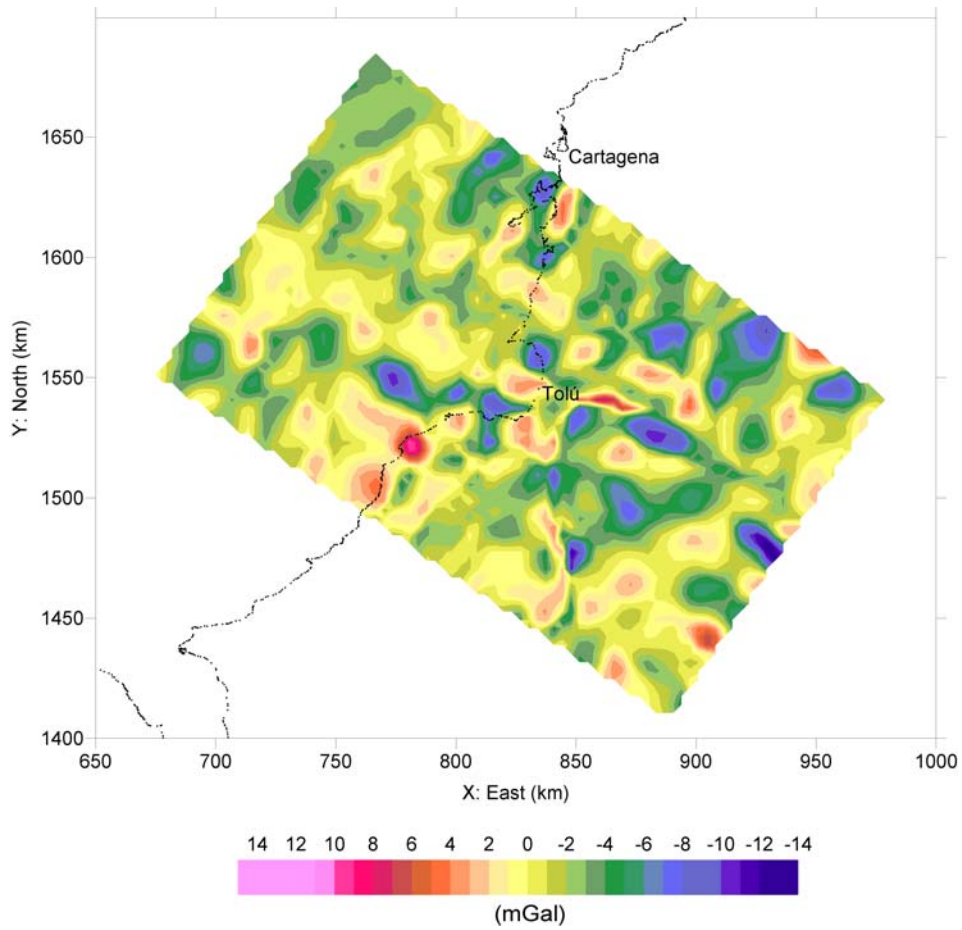
Figure 19: Residual map of final model (contour interval 2 mGal).

Mean: -1.3 mGal
std-dev.: 1.8 mGal
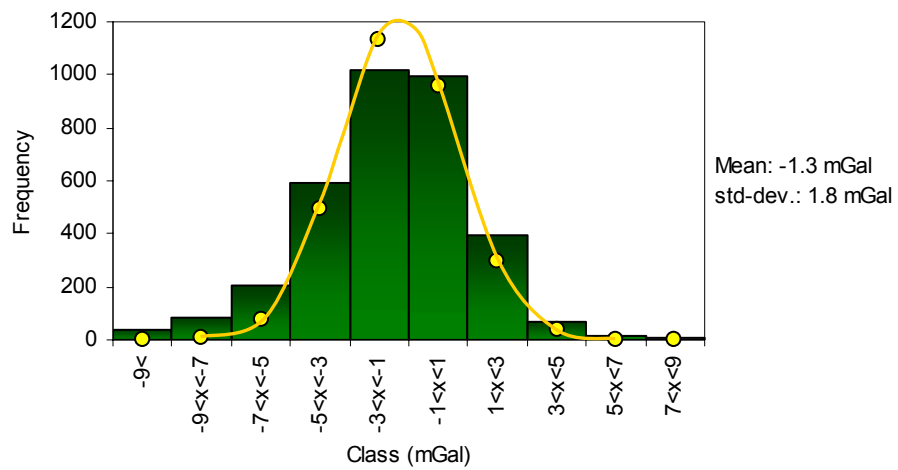
Figure 20: Distribution of residuals. Yellow line indicates normal distribution.

5.4 Interpretation of the 3D density model

The model illustrates very well the current subduction complex where the Caribbean Plate dips at a low angle of about 5° in ESE direction (Figure 21).
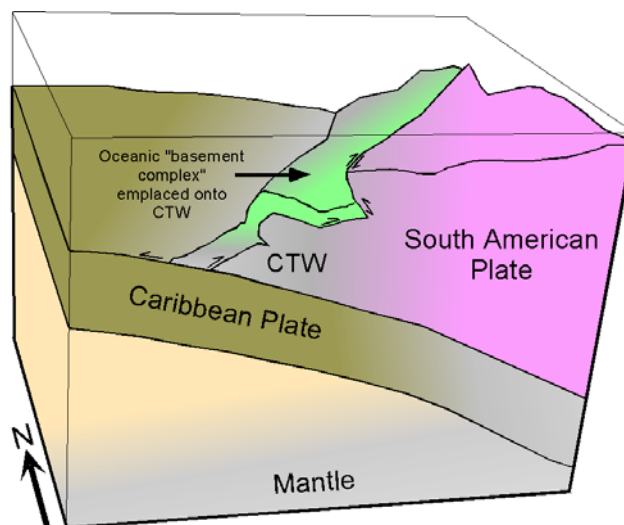
Figure 21: Distribution of crust-types along the Colombian Caribbean margin (3D view of the density model). CTW: continental tectonic wedge.

Figures 22a, 22b, 22c show planes 4, 8 and 10 of the model respectively. Due to use of the complete Bouguer anomaly in both offshore and onshore areas, the density of the water is replaced by the reduction density at the ocean side (Nettleton, 1971) which is 2.2 x 10^3 kg/m^3 as described in Chapter 4.1.

The Caribbean Plate was assumed to be normal oceanic crust in origin and was modelled with a density of 2.9 x 10^3 kg/m^3. The 3D density model shows that more than 6 km of sediments overlie the oceanic basement of the Caribbean Plate which is consistent with interpretations of Edgar et al. (1971), Lu and McMillen (1982) and Bowland (1993) of refraction and multi-channel reflection seismic data realized in the Colombian Caribbean Basin (CCB).

A density of 3.3 x 10^3 kg/m^3 was selected for both oceanic and continental lithospheres. The depth of the crust-upper mantle boundary of ≈25 km was initially taken from the publications of Case et al. (1984, 1990). However, the exact location of the Moho-boundary could not be determined by this modelling. Any changes of the lower continental crust by granulite-eclogite transition, ultramafic underplating or intrusions were not considered because these changes lead to a rise of the density from 3.0 to 3.3 x 10^3 kg/m^3; no separation between crust and lithosphere can be seen by the gravity modelling without further information. Nevertheless, assuming an average thickness of the lower crust of 5 to 8 km, the Moho-limit in this model would be located at 23 to 26 km.
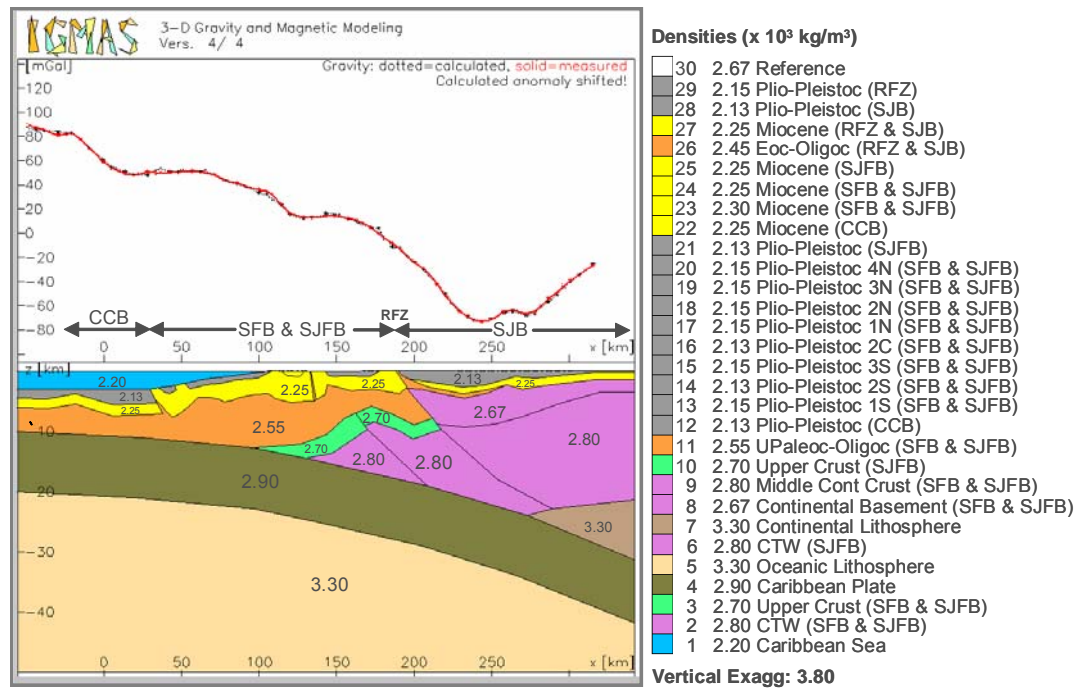
Figure 22a: Plane 4 (2D structural south cross-section) of the 3D density model.
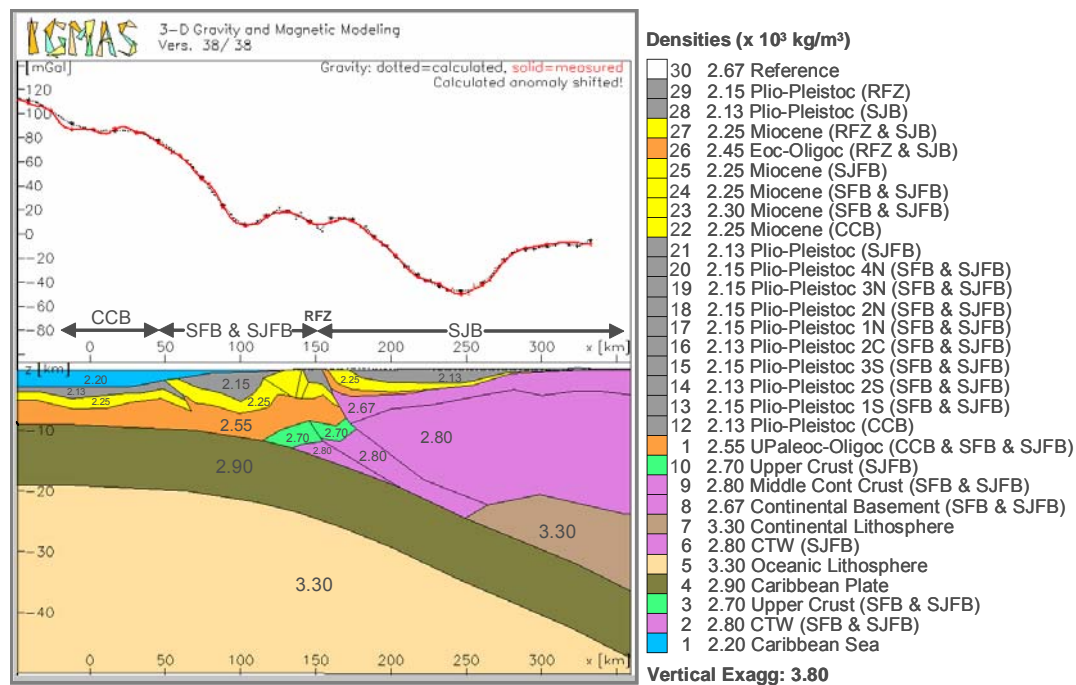
Figure 22b: Plane 8 (2D structural central cross-section) of the 3D density model.
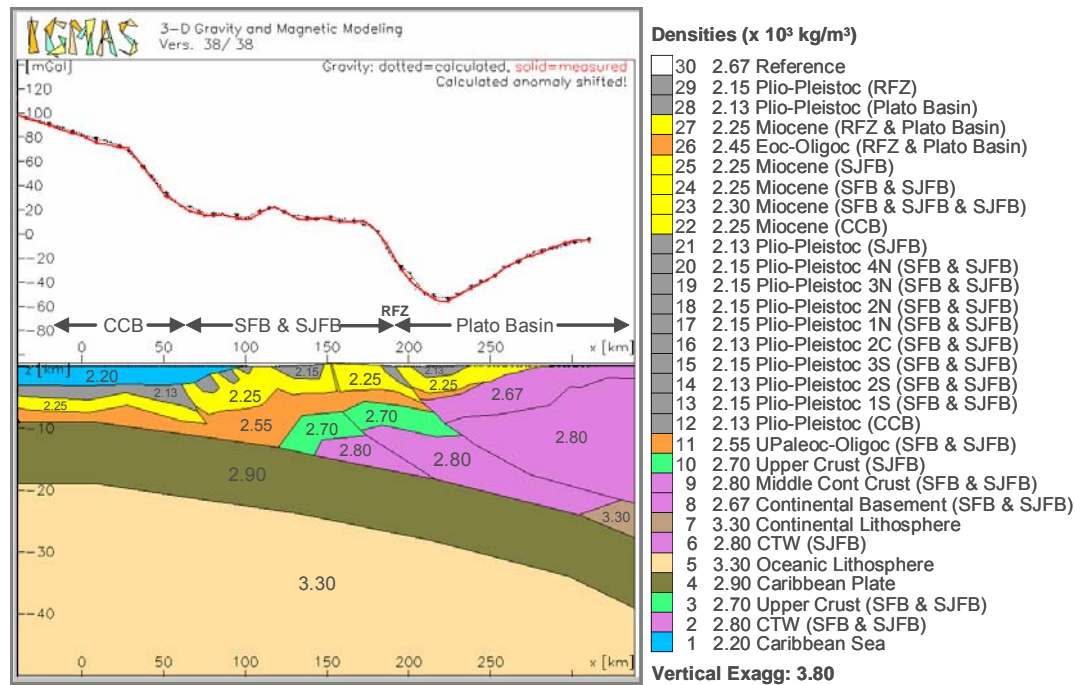
Figure 22c: Plane 10 (2D structural north cross-section) of the 3D density model.

According to seismic interpretation and well data, the upper crust in the San Jacinto and Sinú Fold Belts (SFB & SJFB) as well as in the San Jorge (SJB) and Plato Basins was divided in three sedimentary layers which correspond to late Paleocene to Oligocene (San Jacinto and Sinú Fold Belts), Eocene to Oligocene (San Jorge and Plato Basins), Miocene and Plio-Pleistocene sequences (see Chapter 2.3). As was previously mentioned, the applied densities for these polygons were initially taken from density logs. The computed gravity anomaly was then compared with the observed data and the densities and boundaries of the layers were adjusted until a satisfactory fit was achieved. Thus, in the resultant model a density gradient for the sedimentary cover can be observed which increases from 2.13 to 2.55 x 10^3 kg/m^3.

Average densities of 2.8 x 10^3 kg/m^3 for middle crust and 2.67 x 10^3 kg/m^3 for upper crust in the San Jorge (SJB) and Plato Basins were used. The gravity modelling confirms that the basement present in this basin is of continental type.

The San Jacinto and Sinú Fold Belts (SFB &SJFB) correspond to a local positive anomaly which decreases towards the San Jorge (SJB) and Plato Basins in the east. The variations of the gravity response between 100 and 200 km (Fig. 22a, b and c) suggest a more complex deformation of the basement in the Sinú and San Jacinto Fold Belts (SFB & SJFB).

The Plato and San Jorge basins are marked by regional lows, reaching values down to -60 and -50 mGal respectively. Some local gravity highs (e.g. in Fig. 22a: plane 4)

in the San Jorge Basin (SJB) are observed which are related to different configurations of basement-blocks.

Just as can be seen in the Bouguer anomaly map (Fig. 12), the Sinú Fault can also not be resolved in the modeled planes because no density differences occur between the two areas. Therefore, location of this lineament is based on surface geology and seismic data only.

Several different interpretations of the composition of the basement were tested for the San Jacinto Fold Belt (SJFB), west of the Romeral Fault Zone (RFZ). Finally two crustal bodies were included: an upper one, which represents lithologies of oceanic affinity with an average density of 2.70 x 10^3 kg/m^3 and the other lower one (CTW) with a density 2.8 x 10^3 kg/m^3, which is modelled as a block that contains middle continental crust.

The upper layer presumably consists of a mixture of deep ocean floor sediments and oceanic crust, and therefore has an average density of 2.70 x 10^3 kg/m^3 which is lower than that of pure basalt. This oceanic affinity layer includes the upper Cretaceous "oceanic basement complex" and the deep ocean floor sediments of the Cansona Formation (see Chapter 2.3). The emplacement of the mixture nature oceanic basement over continental basement (CTW) can be interpreted in two ways: 1) Offscraping of materials from the upper Caribbean Plate during the initiation of east-dipping subduction of Caribbean crust beneath northernwestern South America, or 2) Obduction of proto-Caribbean oceanic crust over continental basement of the South American margin as is proposed by Flinch (2004). The density model does not allow the differentiating of these two cases. Flinch (2004) assumes obduction of the proto-Caribbean oceanic crust during the upper Cretaceous (Campanian – Maastrichtian), followed by subduction and accretion. This author identified ophiolites thrust onto the basement of the South American Plate which are interpreted as obducted fragments of the Great Caribbean Arc of Burke (1988) or even parts of the over-thickened Caribbean Plateau crust. In their interpretation, the Romeral Fault System offsets the west-ward dipping obduction suture. However, the 3D gravity modelling results obtained here do not support the presence of layers with oceanic crust-density east of the Romeral Fault Zone in the San Jorge-Plato Basin. Apart from the discussion of the emplacement-mechanism of these basalts (either obduction or early subduction related), the absence of rocks with oceanic affinity east of the Romeral Fault Zone (San Jorge-Plato Basin) could be explained by erosion of them caused by the hanging wall uplift of subduction system during the earlier development-phase of the Romeral Fault System.

The minimum and maximum depth of the top of the upper oceanic layer (ρ = 2.70 x 10^3 kg/m^3) is 5.5 and 13 km, respectively. This unit has a minimum thickness of about 2.6 km in the San Jacinto Fold Belt (Fig. 22a: plane 4) and it extends westernmost into the Sinú Fold Belt with an approximate maximum thickness of 4 km (Fig. 22c: plane 10). Because these lower boundaries cannot be identified from the seismic

data, the approximation of them is based solely on the results of the gravity modelling.

The lower layer consists of middle continental crust and is interpreted as a continental tectonic wedge (CTW) which is part of the overriding South American Plate. This is partially in accordance with the interpretation from Ruiz et al. (2000): according to their interpretation, continental crust is present west of the Romeral Fault System at the northern area of the San Jacinto Fold Belt, whereas the role of the Romeral Fault System as an oceanic-continental crust boundary is restricted to the south of the Canoas Fault Zone. However, the results of the 3D gravity modelling from this study show that continental crust underlies the oceanic "basement complex" of the San Jacinto Fold Belt along the whole modelled region which includes the south area of the Canoas Fault Zone. The lack of any density contrast between middle continental crust of the CTW and the continental crust of the South American Plate, which occurs almost at the same depths, indicates that both together form the continental margin.

According to the modelling results, the Romeral Fault Zone (RFZ) coincides with an east-dipping limit which separates the upper continental crust (2.67×10^3 kg/m^3) to the east from the upper oceanic crust (2.70×10^3 kg/m^3) to the west at least to a depth of 10 km. The presence of blocks that contain middle continental crust beneath a layer of oceanic type rocks in the San Jacinto Fold Belt (SJFB) indicates that the Romeral Fault System does not represent a paleo-suture to which oceanic crust has been accreted. Apparently, the Romeral Fault System had cut the block of continental crust on which the San Jacinto Fold Belt (SJFB) was formed. Therefore, the Romeral Fault System is not an oceanic-continental crust boundary as has been interpreted in other publications (see Chapter 1.2), but represents a transcurrent fault system which is developed on the continental side. This implies a new definition of the ocean-continental crust boundary. Two tectonic limits are identified: an upper one which represents the west-ward dipping contact between the continental tectonic wedge (CTW) and oceanic basalts decoupled from the downgoing slab, and a lower one which represents the east-ward dipping boundary between the downgoing Caribbean Plate and overriding South American Plate.

6. QUANTITATIVE INTERPRETATION OF MAGNETIC ANOMALIES

A complete quantitative interpretation of magnetic field data estimates three types of information about sources of geological interest: the depth, dimension and contrast in physical property. Unfortunately, such a quantitative interpretation suffers from inherent ambiguity when no other prior information is available. Due to the lack of information about the magnetic properties of rocks within the study area, applicability of forward modelling is very limited. Application of methods and quantitative interpretation is therefore restricted to some particular anomalies.

6.1 Maximum slope map (second derivate)

In general, and because of its practical application, prism-like rectangular parallelepipeds with infinite lateral extent and parallel sides are used to establish criteria for the interpretation of magnetic data. Each magnetic anomaly and even data point is interpreted in such a way. The deeper the top of such a body, the lesser the gradients of the magnetic field over and beyond its edges. It is therefore possible to make depth-estimations from the study of the observed magnetic gradients applying different filters and calculation methods. Filters commonly applied include gradient and derivate filters as well as band-pass filters and wave filtering. Figure 23 shows the second derivative at each point of the RTP-grid. In literature this filter is also known as "maximum slope analysis" or "profile curvature". The second derivate produces highs where the gradient (rate of change) is greatest. Through magnetic modelling it can be shown that the magnetic field changes most rapidly over the edges of causative bodies. The method is, therefore, very useful to define the edges of magnetic anomalies (Dobrin, 1976; Sharma, 1997).

In Figure 23, the maximum rates of positive slope-change are shown in red colors which in general represent the limits of magnetic bodies. Four different types of anomalies can be distinguished. The first type includes prominent N-S and SW-NE elongated regions of same gradients following traces of faults involving the magnetized rocks. Gradients are always positive at their western side and negative at the eastern parts. The second type are circular shaped gradients which represent borders of bodies with limited spatial extension. These anomalies may not relate with fault systems and may represent intrusions. Elongated gradients of positive to negative slope changes characterize the third type. The anomalies are restricted to the eastern part of the San Jorge Basin and the Sautatá Arc (Southern Panamá), whose interpretation is presented in the Chapter 4.3.1. The fourth type cannot be identified in Figure 23, but can be recognized in figure 15 where medium positive magnetic anomalies occur west from Cartagena (offshore area) at the Ayhombe High and at the Montería area. All of them are completely absent in the gradient map (Fig. 23) because of their low slope change.
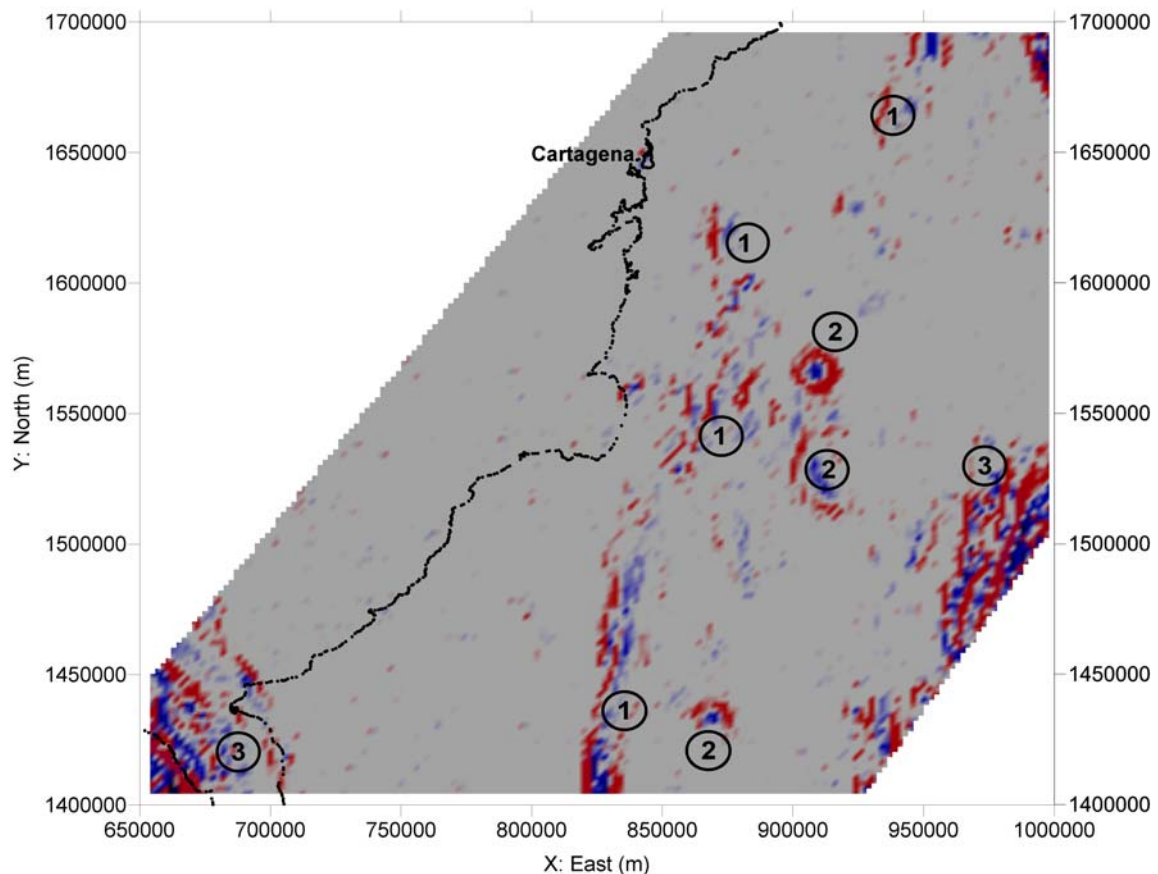
Figure 23: Maximum slope or profile curvature map. (1) Prominent N-S and SW-NE oriented gradients, (2) circular gradients and (3) negative to positive elongated gradients at mountain ridges. Red colors represent strong positive gradients, while the blue colors indicate stronger negative gradients. Positive gradients of type 1 are always accompanied with negative gradients on their eastern side.

6.2. Estimation of depth

Different techniques have been developed during the last decades to estimate the magnetic depth. These techniques are independent of the susceptibility contrast and work for different simplified source geometries (dimensions). All of them are based on the correlation between the depth of a magnetic body and the magnetic gradient which is measured on the surface above the body. Two methods are widely used for initial depth estimations of magnetic anomalies. The first method determines the depth to the top of the anomaly using the maximum slope of the magnetic profile over a magnetic body as a depth-indication (straight slope). This method is known as the maximum slope method. Depth-results of this method are very sensitive to the quality of the measured profile as well as to the difficult determination of the upper and lower inflection points of the magnetic profile. The second method was developed by Peters (1949) which is less subjective than the former one. The depth is estimated by finding the horizontal distance between two parallel lines that pass through the maximum

and minimum of the magnetic profile and have a slope equal to one half of the maximum horizontal gradient of the anomaly. This distance, the so-called half-slope parameter P, is usually between 1.2 to 2 times the depth to the top of the anomaly (Fig. 24). Experience in working with these depth-indices has shown that the errors in depth estimation are within 7% of the real depth (Nettleton, 1962).
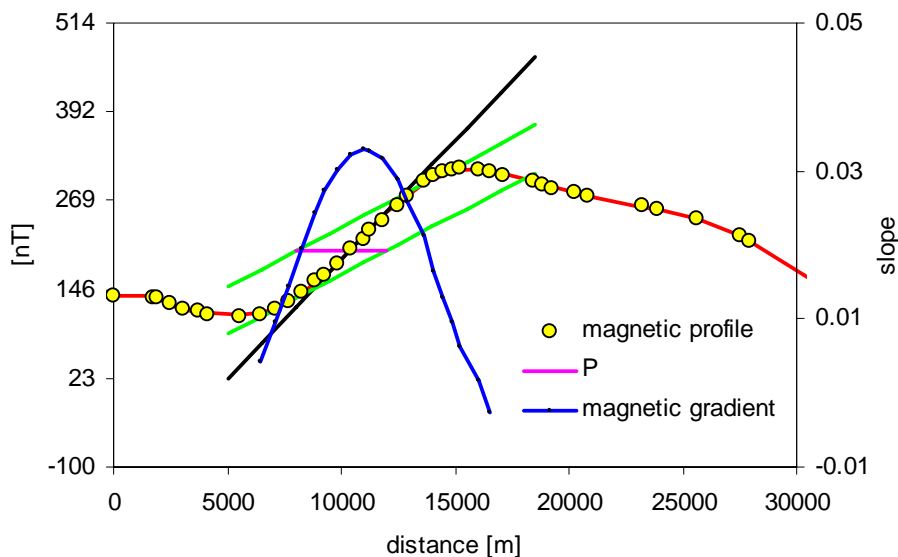
Figure 24: Application of Peter's half slope method. Yellow circles represent measured magnetic values, the red line the fit-curve through the magnetic profile based on 15th order polynomial, the blue line denotes the variation of the magnetic gradient (slope); the thick black line indicates the maximum slope (m_{MAX}) of the profile within the interval from 5 to 20 km; this line intersects the magnetic fit curve at the point with the maximum slope; the two thick green lines have a slope of $m=\frac{1}{2} m_{MAX}$ and intersect the magnetic fit curve at points where the slope is equal to $\frac{1}{2} m_{MAX}$; Peter's parameter P is the horizontal distance between these two green lines.

The terrain slope map indicates the location of the profiles used to estimate the depth of most prominent anomalies in the study area (Fig. 25). It can be shown that the maximum slope is located near to the edges of bodies causing the observed magnetic anomalies on the surface. Therefore, the map can be used in general to identify the anomaly borders and body-geometry: faults such as the Romeral Zone appear as elongated tabular-shaped bodies, whereas circular anomalies indicate column-like shaped bodies. The classification of the body-geometry is necessary to select the correct factor for the depth calculation from Peter's Half Slope parameter P. It must be noted that assumptions of body-geometries from the discussion above are very general and influenced by unknown parameters which may significantly affect the observed magnetic anomaly. This problem cannot be resolved without further information. For the application of Peter's Half Slope an Excel-based Visual-Basic application was developed which calculates the depth for different body-geometries from the observed profiles. Final selection of the correct depth dependent

on the shape-parameter was done manually. Table 2 summarizes the results of the depth calculation.
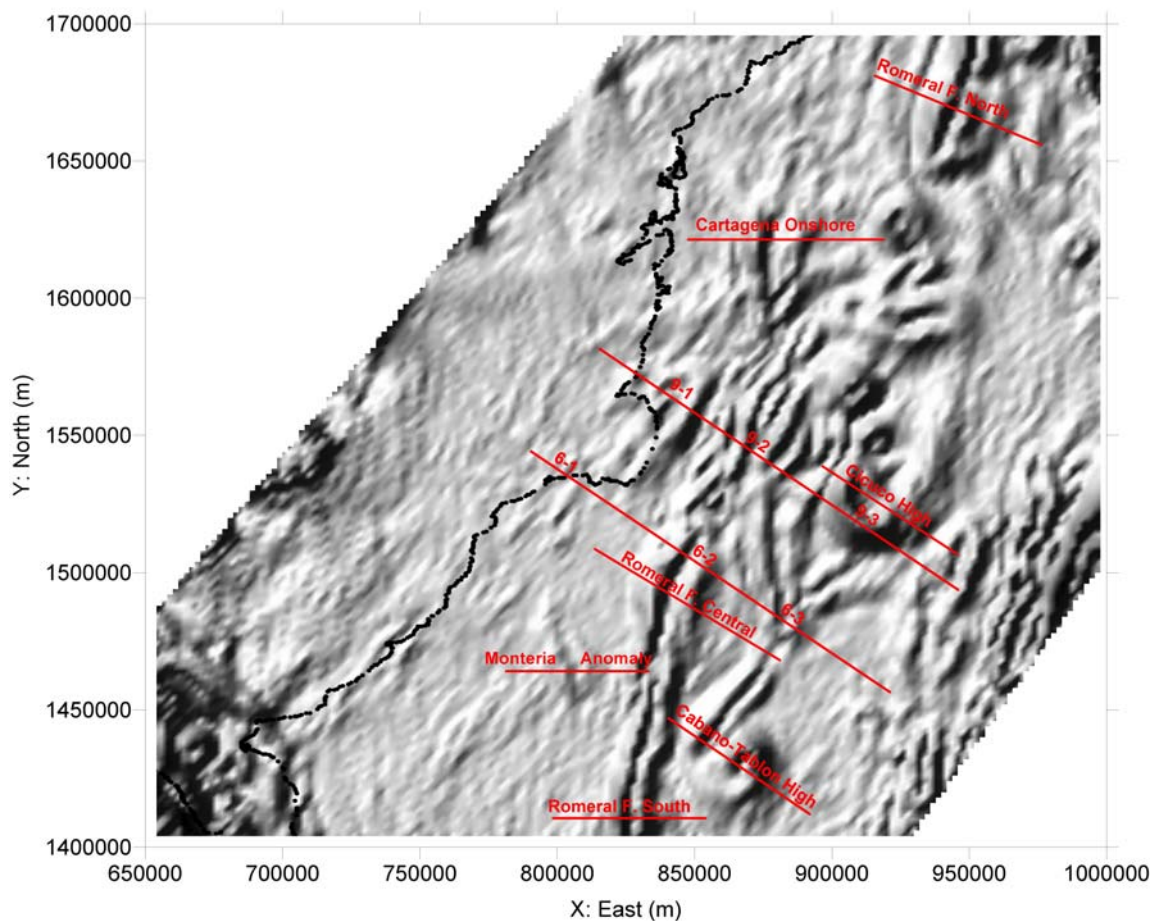
Figure 25: Terrain slope map based on the first derivate of any point of the RTP-map. The regions with high slope and slope changes appear as high relief, regions with constant slope as smooth surface; the red lines indicate selected profile locations for depth estimations.

Magnetic anomalies can be generally classified into three different types (Bird, 1997). This classification is based on their intensities, amplitude and frequencies (broad-narrow peaks). Anomalies with high amplitudes (> 100 nT) indicate intrabasement sources where the causative body has a thickness of the same order or greater than its depth to the surface. Such anomalies are related to lithologic variations in the basement or igneous rocks with the sedimentary section. Anomalies with amplitudes of a few 10 nT are related to basement features and are known as suprabasement sources. Such causative bodies are thin compared to their depth, but more important than intrabasement structures as they indicate deformations of the basement-surface which may have affected the overlying sediment cover. Anomalies with amplitudes less than 10 nT are related to variation of the magnetic properties within the same causative body (e.g. local inhomogeneities of magnetic minerals in crystalline rocks

58

leading to local variation of the susceptibility). Amplitudes in the order of 1 nT indicate sedimentary magnetization contrasts.

Depth-values of each anomaly from Figure 25 are summarized in Table 2 and represent the minimum depth of the causatives bodies of the observed anomalies. The values are compared with the basement-top information from two wells and from the 3D density model (Chapter 5). Table 2 also summarizes the origin of the magnetic anomalies. All depth estimations from different methods are close to each other. Because magnetic field varies one power faster with respect to the distance from an anomaly, shallow, intermediate and large basement depths, basement features and lithological contrasts can be resolved more accurately than with gravity data. The estimated depth-values for each observed magnetic anomalies as well as their relationship to the basement sources are the constraints for the forward magnetic modelling.

6.3 3D magnetic modelling

The IGMAS software is used to obtain a 3D magnetic model for two selected model areas. As explained in Chapter 5, this application supports both forward and inverse modelling of the model-polygon geometries, densities, and magnetic susceptibilities. Magnetic effects can be modelled by using either Poisson's theorem or a slight modification of the formulas derived for gravity modelling (Götze and Lahmeyer, 1988).

6.3.1 Modelling areas and procedure

Two areas were selected for modelling. The location of the larger differences in the residual map of the 3D density model was the fundamental aspect for the definition of modelling areas. The explanation of these differences and the confirmation of the basement-type involved by the Romeral Fault System constitute the aims of the magnetic modelling. The modelling areas are designated into north and south models according to their geographic location (Fig. 26). They correspond to planes 9 and 6 of the 3D density model (Fig. 27 and 28, respectively).

Because remnant intensities as well as the direction of magnetization are unknown for the rocks in the study area, only estimations for the apparent susceptibility can be done (sum of induced and remnant rock magnetization). Constraints from the 3D density model (Chapter 5.3) and seismic interpretation as well as the basement-depth information from some wells and magnetic data (Chapter 6.2) are used. For the sedimentary cover, apparent magnetic susceptibility is set to 0. This value is supported by the general observation from the TMT-map (Fig. 14) as magnetic intensity is inversely correlated with the sediment load on the basement surface. Therefore, contribution to the magnetic profiles from sediments is negligible.

For the continental basement, only the depth-values previously calculated by Peter's method are set to be constant during modelling with the IGMAS software. The

remaining geometry of the basement-surface and the magnetic susceptibilities are modified until a satisfying fit between calculated and observed anomalies is achieved.

Table 2: Calculated depths for each defined anomaly in Fig. 25, 27 and 28. IB: intrabasement source; SB: suprabasement source; see also Chapter 6.3.2 for further explanation.

Anomaly index	Depth (km) Peter's method	Depth from 3D density model (km)	Depth from well (km)	Anomaly type	Basement type
Cábano-Tablón High	2.75			IB	igneous metamorphic
Cicuco High	2.2			IB	igneous metamorphic
Cartagena onshore	4.4			IB	RFZ
RFZ-north	4.5			IB	RFZ
RFZ-Central	5.6			IB	RFZ
RFZ-south	3.3			IB	RFZ
Monteria	2.1			SB	Basalts + sediments
6-1	3.9			IB	Basalts + sediments
6-1-1	5.1	7.1		SB	Basalts + sediments
6-1-2	3.9			SB	Basalts + sediments
6-1-3	4.1			SB	
6-2	2.4	4.7		IB	RFZ
6-2-1	2.4			IB	RFZ
6-2-2	4.2			SB	igneous metamorphic
6-3	3.7	4.5	3.69	SB	igneous metamorphic
9-1	3.4	9.8 (?)		IB	Basalts + sediments
9-1-1	3.8			SB	Basalts + sediments
9-1-2	3.4			SB	Basalts + sediments
9-1-3	4.4	4.6		SB	Basalts + sediments
9-2-1	5.0			IB	RFZ
9-2-2	3.7			SB	RFZ
9-2	2.0	1.8		SB	igneous metamorphic
9-2-3	2.7			SB	igneous metamorphic
9-3-1	4.0	3.5		IB	igneous metamorphic
9-3-2	2.2	2.2	2.14	SB	igneous metamorphic

Apparent susceptibility of the "oceanic basement complex (basalts + sediments)" layer of the San Jacinto Fold Belt is adjusted without modifying the basement geometry which is controlled by depth estimations (Table 2) and the 3D density model. The susceptibility value of this layer is lower than the average value of pure basalt. This is in accordance with the assumption that this layer represents a mixture between deep-ocean sediments and offscraped basalts from the Caribbean Plate. Position of the Caribbean Plate is not changed from that of the 3D density model. An apparent susceptibility of average basalt is assumed. Nevertheless, impact on the calculated anomaly is very small due to its depth. The oceanic-continental crust boundaries are taken from the 3D density model and only small adjustments are done.

Surface configuration of the basement polygons is refined from the depth estimations (Table 2) of the low-amplitude peaks. A limitation of the model is due to the fact that the IGMAS software cannot resolve all observed low amplitude anomalies.
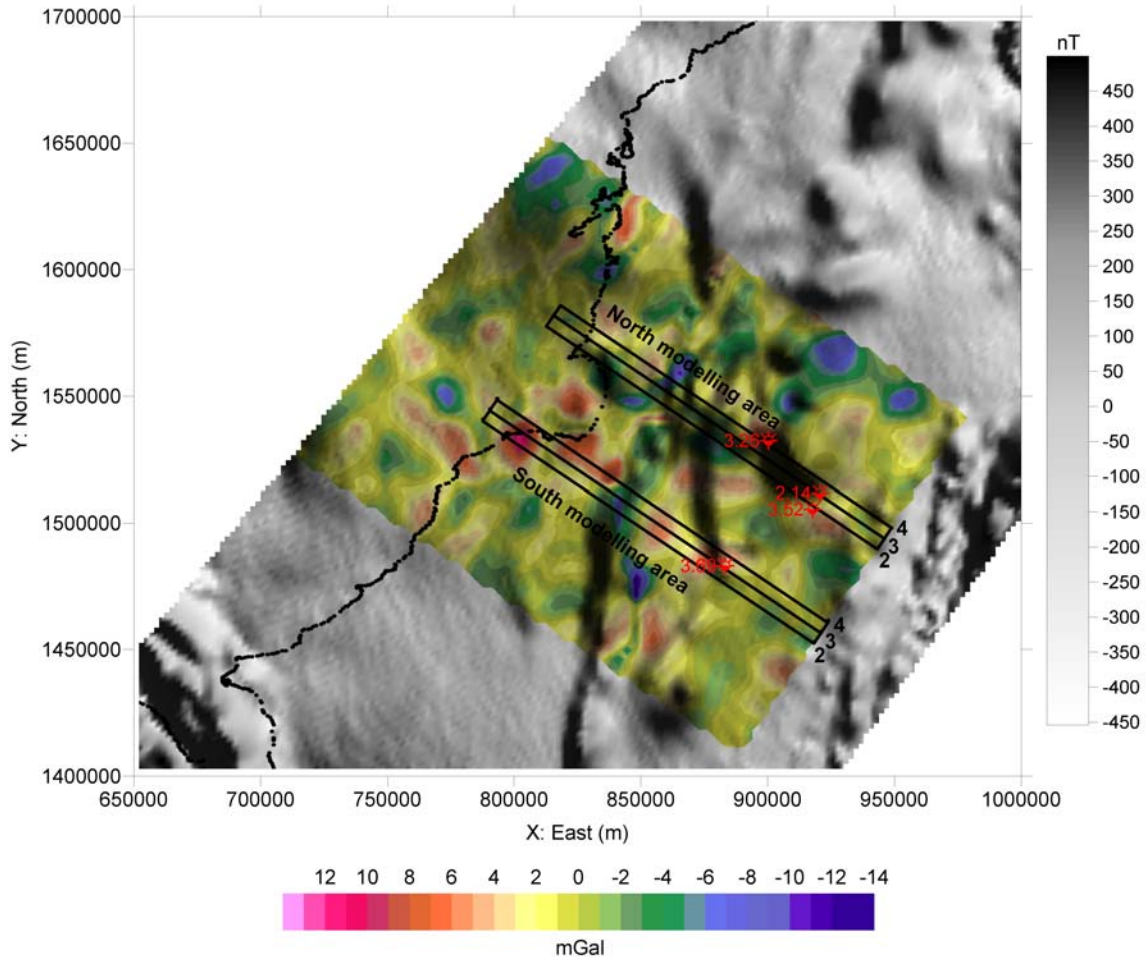
Figure 26: Combination of the RTP-map (Fig 15) and residual map of resultant 3D density model (Fig. 19). The black lines depict the planes of the magnetic modelling areas; the red symbols indicate the location of wells used for the modelling with their respective basement-top depth in km.

6.3.2 Interpretation of the 3D magnetic north model

The magnetic profile of plane 9 shows three high amplitude anomalies with positive magnetic intensity which are indicated by the numbers 9-1, 9-2 and 9-3 in Fig. 27. They are correlated with particular characteristics of the crustal structure of this profile: anomaly 9-1 corresponds to the layer "basalts + sediments", anomaly 9-2 to the Romeral Fault System and the Ayhombe High to its eastern part, and anomaly 9-3 to the Cicuco High (Fig 29).

61
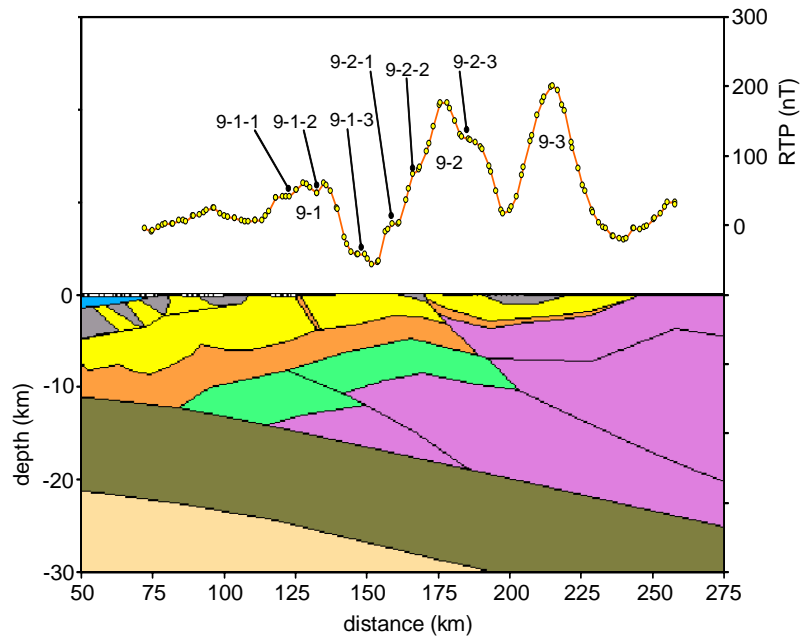
Figure 27: Combined diagram showing in the lower part the modelled crustal structure based on gravity data (plane 9) and in the upper part as red line the corresponding magnetic intensity profile. Two different kinds of magnetic anomalies can be distinguished: 9-1, 9-2 and 9-3 have high amplitudes of up to 230 nT, whereas superimposed secondary peaks are in the range of a few 10 nT (indicated as 9-1-1 to 9-2-3).
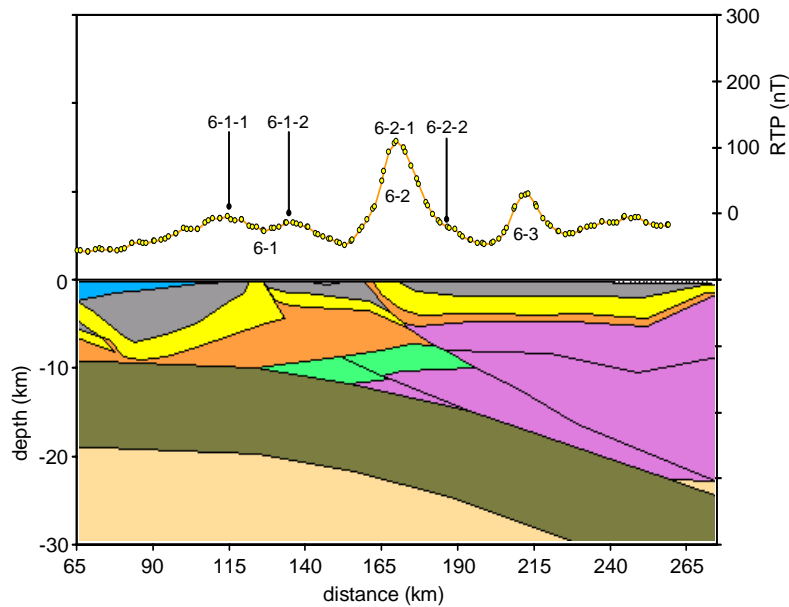
Figure 28: Combined diagram, refers to explanation of Fig. 27, but corresponds to plane 6 from 3D density model. Yellow points indicate magnetic stations; peaks 6-1, 6-2 and 6-3 are roughly correlated with the "basalts + sediments" layer, Romeral Zone and continental basement-surface configuration.

The Romeral Fault Zone (RFZ) appears as a fault zone with a width of more than 20 km which is wider than the identified east-dipping limit of this fault zone from the 3D density model. Several small amplitude peaks of anomaly 9-2 reflect the complex configuration of the continental basement which is involved in this fault system. From seismic images (e.g. Attachment 1) and the resultant north magnetic model, it can be assumed that the most frontal structures of the Romeral Fault System are developed at the San Jacinto Fold Belt. A further conclusion is that continental basement is present beneath this fold belt as in the 3D density model. Several small anomalies of peak 9-1 are caused by suprabasement features and indicate the significant deformation of the "basalts + sediments" layer containing slices of basalts and sediments. Modelling of this magnetic feature also indicates the presence of continental basement below this layer. Anomaly 9-3 is probably caused by an intrusion-like body with high susceptibility. This body is not present in the 3D density model which may be an effect of its limited size or its small density contrast to the surrounding metamorphic basement. It has been found that a single value for the magnetic property of the metamorphic basement is not able to explain this prominent anomaly. Because depth estimation shows no difference to the general depth of the Cicuco High, this anomaly cannot be caused only by a basement high. Also, its high amplitude is contradictory to a suprabasement source. In order to obtain a fit, an additional polygon is implemented into the profile containing higher susceptibility than the surrounding metamorphic basement. Lower Paleozoic mafic to ultramafic intrusives occur frequently in the Silurian to Ordovician metabasalts of the Central Cordillera (Cediel and Cáceres, 2000). These rocks are building up the western part of the basement of the San Jorge Basin and Cicuco High. It can be concluded that this prominent anomaly is related to the occurrence of such a mafic intrusion. This is also supported in the maximum-slope map in Fig. 23 as it appears as a local anomaly with limited spatial extension. As only the width of the body can be determined from the magnetic data (Fig. 23: maximum slope or curvature map), an average susceptibility value for ultramafic rocks is selected to obtain the depth extension of this polygon. Without further investigations, the emplacement and displacement of this body within the metamorphic basement by faults cannot be solved because magnetic modelling is at its limit here. However, the conclusion from above would indicate that most of the anomalies of type 2 in Fig. 23, which are restricted to the eastern part of the San Jorge-Plato Basin, may be caused by mafic to ultramafic intrusion-like bodies.

6.3.3 Interpretation of the 3D magnetic south model

A 3D model is created with use of the depth estimations from peaks 6-1, 6-2 and 6-3 (Fig. 28). Similar to the modelling of plane 9, low amplitude peaks are used to determine details of the basement-surface. All medium to high anomalies are correlated to the polygons of the 3D density model and similar interpretations as for the north-model are done: anomaly 6-1 corresponds to the layer "basalts + sediments", anomaly 6-2 to the Romeral Zone and anomaly 6-3 to a special basement feature of the San Jorge Basin (Fig. 30). Anomaly 6-1 is very similar to that one from plane 9 and contains a superposition of three low amplitude anomalies.
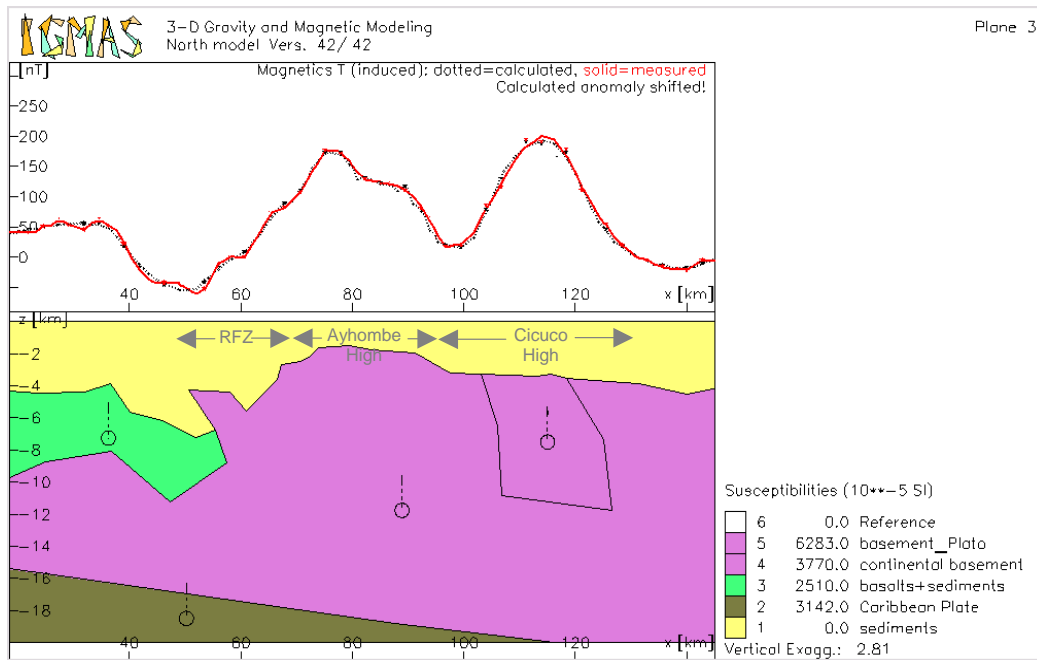
Figure 29: Plane 3 of north model (corresponding to plane 9 from 3D density model).
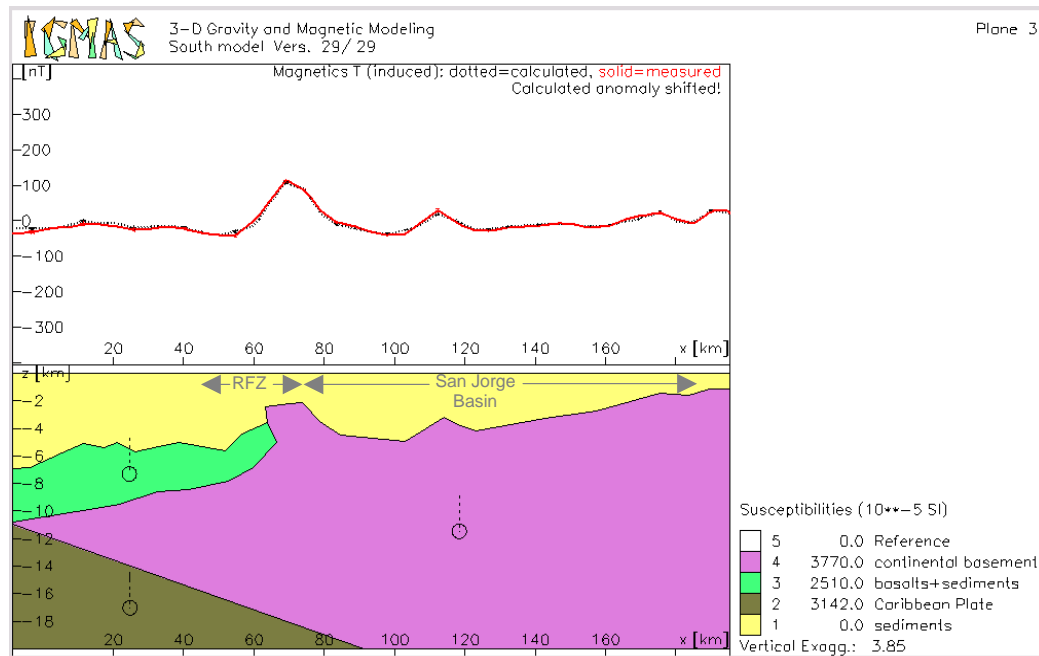

Figure 30: Plane 3 of south model (corresponding to plane 6 from 3D density model).

This also indicates here that this layer is deformed more complexly than in the 3D density model (Fig. 28). Unfortunately, IGMAS cannot resolve these small variations in the magnetic profile. Due to this, the layer appears less rough in Figure 30 than can be assumed from the magnetic profile in Figure 28. Approximately at the location of the magnetic anomaly 6-1-2 (south to Morrosquillo Gulf), a gravity high of 40 mGal is observed (Fig. 17) but which is not accompanied by any significant magnetic expression (Fig.15, 23, 25, 28 and 30). This may indicate a detached sedimentary uplift without an uplift of the underlying basement. A strike seismic line shows the presence of deep lateral ramps with N-NE and S-SW direction which cut the structural regional trend and which could control the Cenozoic sedimentation and recent deformation (Alfonso-Pava, personal communication).

The most prominent anomaly 6-2 is caused by the uplift of the basement along the Romeral Fault System. In contrast to the north model, it is modelled as a narrow fault zone as no low amplitude anomalies are identified on the western flank of this anomaly. The basement-surface geometry on its eastern part is consistent with the basement block configuration interpreted from the seismic images in this study (see Fig. 10) and other previous interpretations (e. g. ESRI-ILEX, 1995; ICP, 2000). These basement blocks (half-grabens) are limited by normal faults, some of which were inverted by compressive stress during the late Miocene (ESRI-ILEX, 1995; Reyes-Santos et al., 2000). Anomaly 6-3 is modelled by variation of the basement-surface only. This is supported by the identification of the basement-top from the seismic images (e.g. Fig. 10), where the late Eocene to early Miocene overlying sedimentary units are onlapping the basement towards the east. The slight increase of the magnetic values to the east of the profile can be fully explained by the rise of the basement towards the east. The depth of this part of the San Jorge Basin is based on seismic interpretation and on the crustal model derived from gravity modelling. However, a major difference occurs in the depth of the continental basement high at the Romeral Fault Zone as well as at the layer "basalts + sediments" because the modelled depth from the 3D density model is about 2 km deeper than the depth from the magnetic model. It must be considered that due to the poor seismic-imaging (e.g. Attachment 1) the contact between the basement and overlying sedimentary sequence west of the Romeral Zone cannot be identified. The residual map of the resultant 3D density model (Fig. 19 and 26) shows for this part of the model the highest differences. On the other hand, magnetic modelling is based on depth estimations from Peter's half-slope method and from the results of the 3D gravity modelling only. Without modern interpretation techniques and more seismic constraints, the observed depth difference cannot be explained.

Comparison between north and south magnetic models results in two characteristics of the crustal structure.

1) The first characteristic deals with the appearance of the Romeral Fault Zone (RFZ): At the southern part, the Romeral Fault Zone is very well defined as a relatively narrow fault zone, whereas in the north-model Romeral appears as a broad zone which extends into the San Jacinto Fold Belt. Further to the north,

the fault zone is extended to the magnetic anomaly "Cartagena onshore" (Fig. 15, 23 and 25). It can be assumed that the Romeral Fault System is trending almost N-S rather than SW-NE as assumed in several publications (Chapters 2.2 and 2.3). It appears that the lateral extension of this fault system is increasing from south to north. Reyes-Santos et al. (2000) suggest that toward the south the compressive component along this fault system is more dominant, while toward the north the lateral movement has a larger contribution.

2) The second characteristic is caused by the different explanation of the observed anomalies within the continental basement of the San Jorge-Plato Basin. Although the profiles are very similar, the anomaly is caused by a suprabasement feature in the case of the south model and by an intrabasement feature in the case of the north model. Both features are not recorded by the gravity data.

6.3.4 Correlation between the gravity and magnetic models

Qualitative and quantitative magnetic evaluation is consistent with the results of the 3D density model. Because magnetic anomalies are more sensitive to lateral and depth-variations of causative bodies, location of intrabasement structures are resolved more accurately than with the gravity data. Furthermore, with the application of enhanced filter methods, the location of main fault zones as well as the classification of observed anomalies to geologic sources is achieved. In the case of the Romeral Fault Zone, which does not show a strong gravity signature (Fig. 12, 17, 22a, 22b and 22c), basement type along this fault zone as well as basement depth are confirmed by the magnetic modelling. Moreover, according to the magnetic modelling, the Romeral Fault Zone does not represent the limit between continental and oceanic crust. Quantitative depth estimations from magnetic data almost coincide with depth estimations of the 3D density model for the larger geologic units. Results of modelling of magnetic suprabasement features are consistent with seismic interpretation in the San Jorge-Plato Basin and provide an acceptable approximation of the basement configuration in the San Jacinto Fold Belt where seismic coverage is either not available or poor in resolution. Thus, 3D gravity modelling complemented with 3D magnetic modelling of two small areas along the RFZ enhanced the large-scale tectonic understanding of the Colombian Caribbean margin.

7. INTEGRATION OF RESULTS AND DISCUSSION

Based on the integrated analysis of the 2D seismic reflection and potential field data, the structural architecture of the Colombian Caribbean margin (Morrosquillo area) has been examined. The four main aspects of the results in this study are discussed in the following.

7.1 Crustal structure

An accretion-dominated subduction model is proposed for the Colombian Caribbean margin. The major tectonic features of the margin are shown in Figure 31.

The gravity modelling defines the Caribbean Plate as an 11 km thick slab which is subducting beneath NW Colombia in an E-SE direction. The dip angle of the plate is 2.5° between the deformation front and the outer high, reaching more than 4° beneath the San Jorge-Plato Basin. The Colombian Basin extends seaward from the structural front of the accretionary prism as the model shows that the incoming plate is covered by more than 6 km of pre-Oligocene to Plio-Pleistocene sediments.

The active accretionary prism is defined by Byrne et al. (1993) as the material accreted relatively recently to a backstop of stronger rocks. In this model, the active prism corresponds to the external part of the Sinú-Colombia Accretionary Wedge. The development of seaward-vergent thrusting and accretionary ridges in the frontal part of the margin indicates that the accretion is ongoing.

The outer high domain includes the major structural complex formed by the easternmost part of the Sinú-Colombia Accretionary Wedge and the San Jacinto Fold Belt (SJFB). The outer high results from the gradual increase in both strength and bulk density as the material is compacted with depth and distance from the deformation front (Byrne et al., 1993). Thus, this domain represents the fossil part of the accretionary prism which acts as a dynamic backstop to the frontal active accretionary prism. This backstop is named dynamic according to the definition of Kopp and Kukowski (2003) because its trenchward termination progresses seaward as new material is frontally accreted and lithified. Seaward of the outer high, normal faulting, growth folding and mud diapirism can be well identified. As noted in the images of Chapter 3, the depth of the seismic data and its resolution are decreasing landward of this structural complex. Consequently, the detailed configuration of the pre-Oligocene units cannot be resolved.
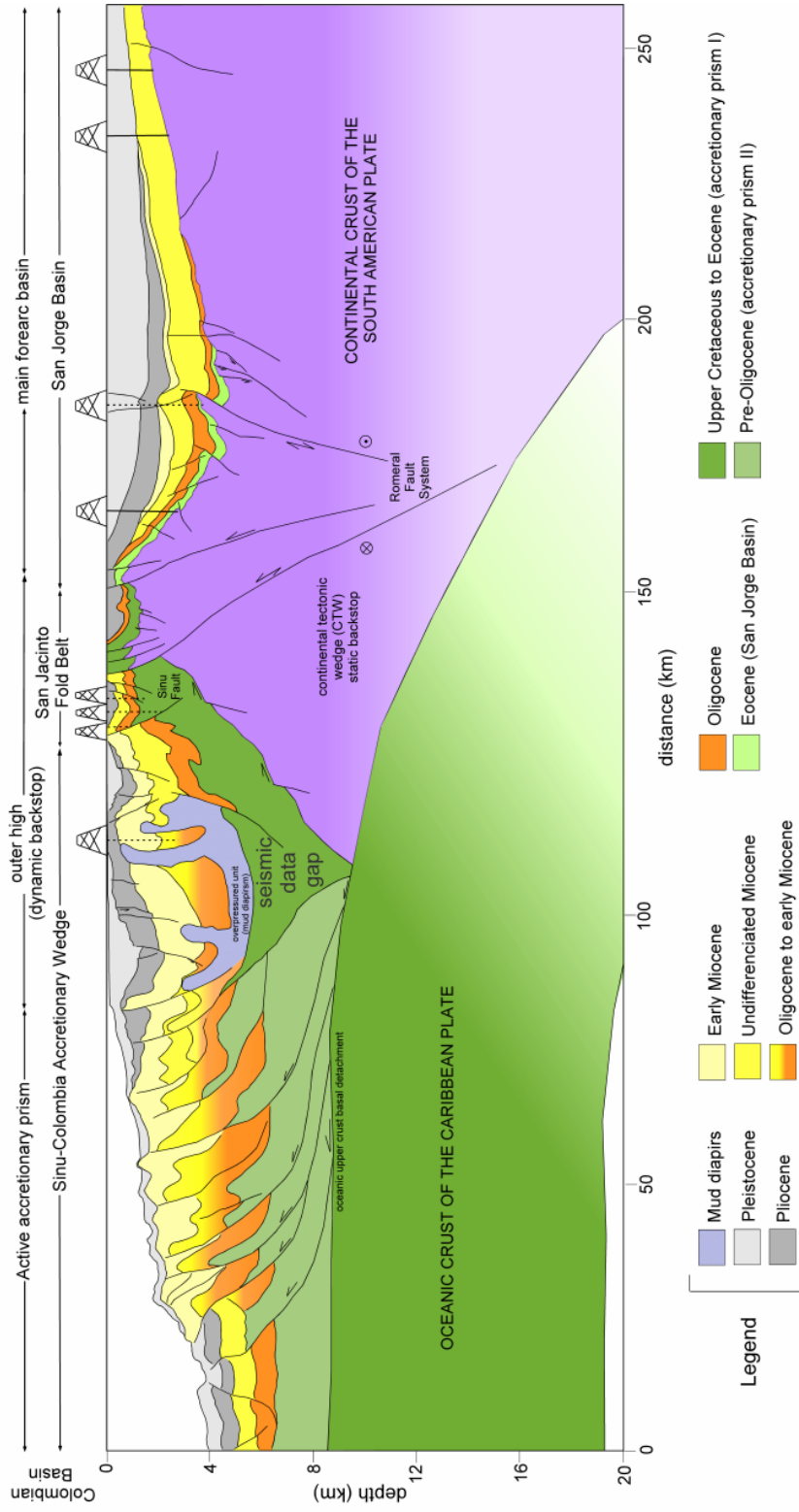
Figure 31: Major tectonic features of the Colombian Caribbean margin (Morrosquillo area). The accretionary system between the forearc region and deformation front is divided into two zones (active accretionary prism and outer high) with different morphological and structural characteristics. The outer high initially evolved by accretion against the static backstop (continental crust of the arc framework). Later, the outer high acted as a dynamic backstop for the younger accretionary prism that remains active to the present day.

The Sinú Fault has been interpreted as the boundary between the early-middle Eocene San Jacinto and middle Miocene to recent Sinú-Colombia accretionary prisms. However, from the examination of the density model (Fig. 22a, b and c) as well as the Bouguer anomaly Map (Fig. 12) it can be observed that the fault zone does not correspond to a sharp lateral density contrast as would be expected at the limit between two distinct units accreted in different events. In this study, the outer high is considered to be the result of a continuous accretion from upper Cretaceous to late Miocene time, when the plate convergence changed from oblique to orthogonal, leading to the development of the accretionary prism active today. Therefore, it can be concluded that this fault has no regional tectonic significance.

The limit between the active accretionary prism and the outer high domain corresponds to a structural backstop, whose definition is commonly based on strong acoustic reflectors and zones of higher seismic velocity. These geometries are well documented by Silver et al. (1985), Brandon (1986), Byrne and Hibbard (1987), Byrne et al. (1993), Davis (1996) and others. In the proposed model, this boundary is interpreted as the structurally higher zone which coincides with a more elevated zone and the slope break at the seafloor. This zone, which is characterized by a west-vergent imbricate thrust system and by a backward breaking out-of-sequence thrust, suggests a landward-dipping geometry for the dynamic backstop. This geometry corresponds to a backstop Type II of Byrne et al. (1993) which implies that much of the deformation involved dragging of weaker material beneath the backstop. The density model (Fig. 22a, b and c) shows that the lower end of the limit between the active accretionary prism and the outer high domain coincides with the seaward termination of the oceanic "basement complex" present in the San Jacinto Fold Belt. The downward limit of the dynamic backstop (outer high) is marked by the subducting Caribbean Plate, while its landward termination is provided by the continental basement of the overriding South American Plate.

Even today, the composition of the basement at the outer high domain is discussed controversially. Basalts of upper Cretaceous age are exposed together with ocean-floor sediments in fault slices and have also been drilled by some wells in the onshore area of the San Jacinto Fold Belt. Although the contact of this "basement complex" with the overlying sedimentary strata is impossible to identify from the existent seismic data, the 3D gravity and magnetic modelling supports the presence of an oceanic affinity unit which includes a mixture of the basalt and sediments (ρ = 2.70 x 10^3 kg/m^3 and k = 2.51 x 10^{-2} SI units). The oceanic "basement complex" of the outer high is underlain by a continental tectonic wedge (CTW), which is modelled with a density of 2.80 x 10^3 kg/m^3 and a susceptibility of 3.77 x 10^{-2} (SI units), and which is interpreted to be part of the South American margin.

According to the proposed model, the continental basement of the arc framework provides the static backstop against which the material of the dynamic backstop was previously accreted. While a static backstop supports most of the plate boundary stress, a region of low stress has developed above it (Byrne et al. 1993). This

explains the moderate deformation undergone by the overlying Plio-Pleistocene forearc basin infill which fossilizes most structures of the outer high domain.

The forearc domain exhibits several sub-basins filled by Plio-Pleistocene deposits. Seaward, these post-kinematic deposits fossilize the complexly deformed outer high. The landward part of the forearc domain comprises the bulge generated by the Romeral Fault System which represents a structural break between the smaller and mud-diapirism-deformed basins to the west and the main and deeper forearc San Jorge Basin to the east.

The geometry of the static backstop in the study area is impossible to determine from the available seismic data due to its limited depth. However, a seaward-dipping geometry of the static backstop can be interpreted from the density model (Fig. 22a, b and c). This geometry indicates a backstop Type I of Byrne et al. (1993) whose toe is located on the top of the Caribbean Plate approximately 130 km from the trench. In this static backstop Type I much of the weaker rock lies above the backstop where it forms a large outer arc high and a forearc basin. Byrne et al. (1993) suggest that the understuffing of wedge sediments beneath the high causes a slight landward tilt of the outer high which initially developed as a relatively symmetric pop-up structure over the toe of the static backstop.

7.2 Emplacement of the oceanic "basement complex"

The emplacement mechanism of mafic and ultramafic rocks along western Colombia is still a subject of discussion. Besides the units here termed collectively oceanic "basement complex" (basalts plus deep ocean sediments), isolated bodies of ultramafic rocks are also exposed in the southern part of the San Jacinto Fold Belt (Fig. 3). These rocks, which contain the main iron-nickel ore deposits in Colombia, have been interpreted (i.e. Mejia and Durango, 1981) to be part of the ophiolite sequences located along the Romeral mélange zone to the west of the Central Cordillera (see Fig. 2). The rocks located in the Romeral mélange were accreted during the Aptian - Albian collision of the Romeral terrane (Cediel et al., 2004; Amaime terrane in Pindell publications) with the Colombian Central Cordillera. However, as mentioned in Chapter 2.2, the San Jacinto Fold Belt (west of the Romeral North Fault Zone) does not exhibit evidence of a tectonic mélange similar to that of the Romeral mélange zone.

Although peridotites and ultramafic to mafic sequences are found in the San Jacinto Fold Belt (i.e. Ortiz, 2004), most of the members of an ophiolite suite (Coleman, 1977) are missing and contacts between its members are not well understood due to strong tectonic deformation. The oceanic "basement" of the San Jacinto Fold Belt is only defined by thrust sheets or blocks of oceanic sediments, basalts and mafic to ultramafic rocks which are intercalated within the accretionary prism. The lack of a complete ophiolite trinity (e.g. ultramafic rocks - layered gabbros and pillow basalts - pelagic sediments) supports the assumption that these complexes cannot be interpreted as evidence for obduction of oceanic crust, but represent offscraped

material from an oceanic crust during subduction. Offscraping is defined as the removal of topographic highs from the upper part of a downgoing oceanic slab. Ultramafic rocks within accretionary prisms may be offscraped remnants of peridotite-cored uplifts at ridge-transform intersections (Coleman, 2000).

Palinspastic reconstructions (Tectonic Analysis Inc., 1995; Pindell and Tabbutt, 1995) suggest that after accretion of the Amaime (Romeral) terrane the convergence of the South American and Caribbean plates in the northern Andes was accommodated by the initiation of the east-dipping subduction of the Caribbean crust beneath the Amaime terrane and the rest of Colombia. This subduction led to the westward emplacement of offscraped upper Caribbean crust onto the Amaime terrane to the south (Dagua terrane) and on top of the continental crust (CTW) along the NW Colombian margin. Thus, the presence of oceanic affinity rocks over continental basement (CTW: current static backstop) is interpreted here as material detached from the downgoing Caribbean slab by backthrusting which has developed in the internal part of the prism as a result of the oblique convergence.

7.3 Romeral Fault System and ocean-continent crust boundary

As mentioned in Chapters 5.4 and 6.3.4, the existence of a continental tectonic wedge (CTW) beneath the oceanic "basement complex" in the San Jacinto Fold Belt (east of the Romeral Zone) indicates that the Romeral Fault System does not represent a paleo-suture or tectonic boundary between oceanic crust to the west and continental crust to the east. The reasons why this interpretation had been proposed and for many years accepted are described in detail in Chapter 2.3.4. Summarizing here, the presence of upper Cretaceous basalts in the San Jacinto Fold Belt (east to the Romeral Zone) is cited frequently to be the evidence for this interpretation. However, the results of 3D gravity and magnetic modelling suggest that the Romeral Fault System originated within the block of continental crust on which the San Jacinto Fold Belt was formed. The absence of oceanic "basement complex" units (present in the San Jacinto Fold Belt) east of the Romeral north zone (western flank of the San Jorge-Plato Basin) is explained by their erosion due to tectonic uplift along the Romeral Fault Zone before the sedimentation of the middle(?)-late Eocene units. A clear characteristic, which can be observed in Figure 31, is the configuration of the Romeral Fault System as a positive flower structure along which blocks of continental crust have been displaced following the major fault rise. Thus, in view of today, the Romeral North Fault Zone (San Jacinto of Cediel et al., 2004) and its associated structures are interpreted here as a transcurrent fault system developed on the continental side of the forearc domain (static backstop) as a result of the oblique collision between the Caribbean and South American plates. The evolution of transcurrent fault systems in zones of oblique convergence is amply discussed by Fitch (1972). Calassou et al. (1993) presented analogue experiments that show strike-slip faulting developing flower structures near the static backstop.

It should be noted that the Colombian continental margin has a long and complex history of evolution. From south to north Colombia, the Romeral-Peltetec-San Jacinto

Fault System has been considered as the continental margin along which Jurassic (?) and Cretaceous oceanic rocks were accreted. However, Cediel et al. (2004) highlight the differences in style and associated characteristics observed in the Romeral-Peltetec System (Romeral South) and the San Jacinto Fault System (Romeral North). The migration of the Caribbean Plate along the northern margin of the South American craton during the Cretaceous-Cenozoic is documented by the transpressive strike-slip movement along the Romeral-Peltetec and San Jacinto faults accompanied by the east-west growth of the Oca–El Pilar transform system (Pindell, 1993; Cediel et al., 1994; Maresch et al., 2000). Since Miocene time, collision of the Panama Arc (Cañas Gordas and Baudó terranes) with NW Colombia has truncated the southern San Jacinto System and the faults of the Romeral-Peltetec system (Cediel et al., 2004).

The new interpretation of the Romeral Fault System as discussed above implies a new definition of the ocean-continental crust boundary. Two tectonic limits are identified from the proposed crustal model: an upper one, which represents the westward dipping contact between the continental tectonic wedge (CTW) and oceanic basalts detached from the downgoing slab, and a lower one which represents the eastward dipping boundary between the downgoing Caribbean Plate and the overriding South American Plate. The exact architecture of the upper ocean-continental crust boundary is difficult to define from this model. New, higher resolution seismic data and detailed modelling along this zone applying modern interpretation techniques, which allow the loading of the seismic data as a backdrop during the gravity and magnetic modelling, are necessary to distinguish the basement features and structures confined to the sedimentary cover. The lower ocean-continental crust boundary can be identified in the resultant model where a density contrast between the subducted Caribbean Plate and the crust of the overriding South American Plate (static backstop) occurs. In the modelled region, this zone is approximately 180 km long and starts at a depth of 14km until the crust-mantle transition at a depth of 24 km.

7.4 Tectonic evolution

The analysis of the crustal model proposed above and the northern South America-Caribbean plate interaction history suggest four major evolutionary stages for NW Colombia (Fig. 32).

7.4.1 Upper Cretaceous to middle Eocene

The Cenozoic evolution of the Colombian Caribbean margin must be understood at least since the Aptian (120 Ma), when a reversal of the subduction-direction between the Americas occurred (see Chapter 2.1). This polarity reversal led to the formation of a transform fault zone with dextral strike-slip motion-characteristics between Ecuador-Colombia and the Caribbean Plate (Pindell and Kennan, 2001). The transform fault separated the Greater Antilles trench, where west-dipping subduction of the Proto-Caribbean beneath the Caribbean Plate occurred, from the western

Colombian trench, where east-dipping subduction of the Caribbean Plate beneath NW South America took place (see Attachment 1).
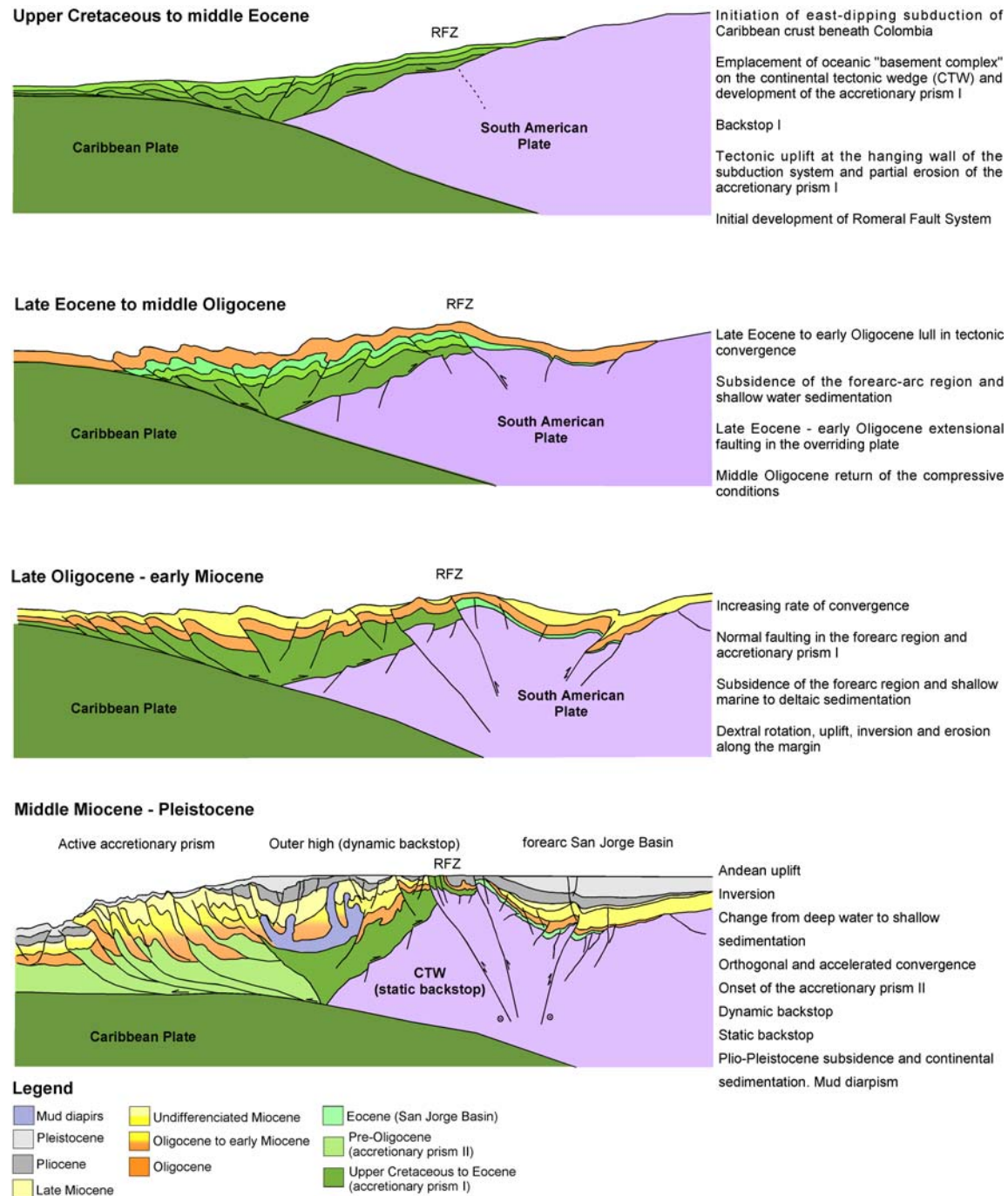
Figure 32: Sketch with the major stages of evolution of the accretionary prisms and forearc basin.

The continued N-NE migration of the Caribbean Plate led to a progressive lengthening of this transform fault zone along NW South America. The trace of this transform zone corresponds to the San Jorge-Plato Basin margin, the NW edge of the Santa Marta area, and NW Guajira margin (Tectonic Analysis Inc., 1995). By the end of the Cretaceous (100 Ma), closure of the Andean back-arc basin led to the overthrusting of the Amaime terrane onto the Colombian Central Cordillera (Pindell and Kennan, 2001) which consists of the Andean back-arc basalts as well as the southern part of the Greater Antilles Arc.

The east-dipping subduction of the Caribbean Plate beneath Colombia started in the Campanian (84 Ma) in the south, and in the Maastrichtian (72 Ma) in the north (Tectonic Analysis Inc., 1995) with the change of the relative motion of the Caribbean Plate from N-NE to E-W when the spreading of the proto-Caribbean ceased (Chapter 2.1). The oblique subduction of Caribbean lithosphere created the first accretionary prism on the leading edge of the overriding continental plate and led to the development of the paleo-forearc basin in NW Colombia. Offscraped upper Caribbean Plate materials (basalts, ultramafic rocks and pelagic sediments of upper Cretaceous age) and late Paleocene to middle Eocene continental turbidites initially built the prism (here called Accretionary Prism I). The continental basement of the South American Plate acted as a rigid backstop for the accreted units. The partial emplacement of the accreted units on top of the backstop must have been achieved by a major east-directed backthrust.

Due to the relatively rapid advance of the Caribbean crust beneath western Colombia and Venezuela, the Accretionary Prism I and the westernmost part of the forearc region (paleo-San Jorge-Plato Basin) were uplifted and partially eroded. The middle Eocene unconformity has been commonly interpreted as a record of this event.

Due to the oblique subduction it is probable that since this time dextral strike-slip faulting has developed on the continental side of the NW Colombian margin.

7.4.2 Late Eocene to middle Oligocene

A major tectonic event occurred in the late Eocene when Cuba collided with the Bahamas platform which led to the change from a north-easterly to an easterly directed movement of the Caribbean Plate with respect to South America. This event also terminated the northward migration of the Panamá triple junction (Farallón-Caribbean-South American plates) along the Colombian trench which remained fixed for the rest of the Tertiary at a point west of central Colombia (Pindell and Kennan, 2001).

In the early Oligocene slowing of the South American westward drift with respect to the Caribbean Plate caused a decrease of the subduction rate (about half the previous convergence rate) generating subsidence and westward prograding deposition in the forearc region (Pindell et al., 1998). The cease of the westward movement of South America allowed the rollback of the Caribbean Plate, which led to

reduced compression and induced extensional faulting in the overriding plate. It appears that this period was short because renewed thrusting is already observed in the middle to late Oligocene units of the inter-Andean basins. Thus, it can be suggested that compressive arc conditions returned in the middle Oligocene (Tectonic Analysis Inc., 1995).

Due to the strong younger overprint, the Paleogene to middle Oligocene deformational events are difficult to recognize in the Accretionary Prism I and western forearc region, but some of the normal faults identified in the San Jacinto Fold Belt were developed during the late Eocene-early Oligocene extensional phase.

7.4.3 Late Oligocene to early Miocene

The doubling of the South American-Caribbean plate convergence rate in late Oligocene time from 10 mm/yr to 20 mm/yr terminated the lull in convergent tectonism which characterized the late Eocene-middle Oligocene period (Tectonic Analysis Inc., 1995; Pindell et al., 1998). The increase of the convergence is attributed to acceleration of the South American Plate's absolute motion, rather than by an acceleration of the Caribbean Plate into the trench.

In the late Oligocene the uplift of the Sierra de Perijá, Santander Massif and Santa Marta Massif was initiated. Slip on the Oca and Santa Marta faults led to the isolation of the Santa Marta Massif. ICP (2000) suggests that strike-slip movement on the Bucaramanga-Santa Marta, Romeral and Palestina faults resulted in the clockwise rotation of the Santa Marta Massif, generating in the San Jorge-Plato Basin (forearc region) a series of transtensional and rotating basins which today exhibit a configuration of local basement highs and depocenters limited by normal faults. The strike-slip, which is accompanied by extension, does not only generate the normal faulting, but also subsidence. The late Oligocene-early Miocene sediments of shallow marine to deltaic environment were deposited in the formed half-graben structures.

During the early Miocene the plate convergence was directed NW-SE, essentially perpendicular to the trend of the Andes belts. Entry of the Panama Arc into the Colombian trench influenced the relative westward drift of South America (Tectonic Analysis Inc., 1995).

The early Miocene unconformity represents a regional erosional event which partially fossilized the previous structures (ICP, 2000). Rotation, uplift and erosion along the Romeral Zone are evidenced by the thinning of the early Miocene strata towards the western flank of the San Jorge-Plato Basin. The inversion structures observed in the westernmost part of the San Jorge Basin, which do not cut the middle Miocene unconformity, indicate that the early Miocene compression had a more important effect in the forearc region than the compression undergone during the final phase of the Andean Orogeny (middle Miocene-Recent).

The E-NE migration of the Caribbean Plate and subsequent subduction have produced up until this time strike-slip fault systems, lateral displacements and inversion as the Accretionary Prism I has developed.

7.4.4 Middle Miocene to Pleistocene

Since middle Miocene time the Andean Orogeny intensified leading to the development of the present-day Andean Colombian relief. The progressive decrease in the age of crust entering the trench along the length of the Andes, which caused resistance to subduction, and the rapidly increasing rates of subduction of the Nazca Plate in the Miocene appear to be the more important factors that have driven the Andean uplift (Pindell and Tabbutt, 1995).

The Andean uplift produced stronger erosion which in turn deposited a thick section of middle Miocene to Pleistocene molassic deposits across the Colombian Andean region. The middle Miocene regional unconformity marks the change from deep water to shallow water sedimentary environments along the Colombian Caribbean margin (ICP, 2000). The Andean Orogeny culminated during the Pliocene and generated an intra-Pliocene regional unconformity on which mainly continental sediments were deposited (ESRI-ILEX, 1995).

Since the late Miocene (10 Ma), the relative motion between South American and Caribbean plates has been directed E-W, resulting in an acceleration of the convergence. The collision of the buoyant Chocó Arc (Panama, including the Cañas Gordas and Baudó terranes) with western Colombia has increased Andean east-west contraction causing the underthrusting of the Caribbean Plate along the Oca-El Pilar fault system and the relative northwest migration of the Maracaibo block (Pindell et al., 1998).

The faster convergence could be the cause of the onset of the second accretionary prism. The piggy-back basins developed in the frontal thrust-sheets suggest a late Miocene to Pliocene age for the main accretion episode. The accreted and consolidated first accretionary prism was uplifted and partially eroded, forming an outer high which acted as a dynamic backstop for the younger accreted sediments (Accretionary Prism II). The accretionary ridges located at the frontal part of the active prism and extensional faulting reaching the seafloor support the assumption that accretion and crustal deformation is active today.

On the continental shelf and onshore part of the Sinú Fold Belt, mud diapirs have evolved from the overpressured Oligocene-early Miocene units as response to lateral compressional stresses (Duque-Caro, 1979).

The deepening and subsidence of the San Jorge-Plato Basin (main forearc basin) cannot be explained only by the outer high (Accretionary Prism I) uplift and loading effect of the sedimentary infill. Although sedimentary infill together with isostatic

adjustment can increase basin-subsidence, crustal extension of the backstop or localized tectonic erosion should be additionally considered (Larroque et al., 1995).

Due to the continued convergence (oblique and later orthogonal) between the Caribbean and South American plates, it can be assumed that compressive deformation dominated the structural development along the margin. Nevertheless, an extensional episode occurred between the late Eocene and early Oligocene in the arc framework (overriding plate). The inversion during the deposition of the late Miocene to early Pliocene units is evident along the Romeral Zone. In spite of continued and complex deformation undergone by the Romeral Fault system, it can be assumed that it has evolved as a transcurrent, mainly dextral transpressive fault system. The pronounced doming and the strong eastward-tilting of the hanging wall (westernmost part of the San Jorge Basin) suggest that it constantly behaved as a structural high.

8. SOME CONSIDERATIONS OF THE CRUSTAL MODEL FOR HYDROCARBON MATURATION

8.1 Characteristics of source rocks in NW Colombia

The components of a petroleum system are a source rock, a reservoir rock, a seal, a trapping mechanism, migration pathways and timing. The generation of hydrocarbons (oil and gas) depends on the quantity, quality and thermal maturity of the kerogen and expulsion efficiency of the source rocks. The minimum quantity of total organic content (TOC) which must be present in source rocks to produce commercially relevant petroleum deposits is 0.5% in shales and 0.3% in limestones. Organic matter will mostly be converted to kerogen, which produces hydrocarbons upon heating with deeper burial. The nature of organic matter will determine the type of kerogen, which will in turn control the type of hydrocarbon produced: terrestrial and marine organic matter produce gas-prone and oil-prone source rocks, respectively. Vitrinite reflectance (Ro%) and maximum pyrolysis temperature (Tmax) are widely used to estimate the maturity level of organic components. Depending on the burial history, and therefore on the rate, duration and extent of heating, different types and amounts of hydrocarbon can be produced (e.g. between 60° and 120 °C thermogenic oil and above 120 °C wet and dry gas are generated).

Geochemical analyses (BP Exploration, 1993; ESRI-ILEX, 1995; TEPMA, 2002) indicate that sediments of upper Cretaceous and late Oligocene to early Miocene age possess the best characteristics as hydrocarbon-source rocks in NW Colombia (Colombian Caribbean area).

The upper Cretaceous (Coniacian-Campanian) abyssal pelagic sediments (Cansona Formation) include marine black shales intercalated with cherts, limestones and some sandstones which were probably accumulated on the Caribbean Plate, off to the west from the NW South American margin, under productivity conditions enhanced by upwelling. Under such conditions (Pindell and Tabbutt, 1995), world class source rocks such as the La Luna Formation of the Catatumbo Basin in Colombia and the Maracaibo Basin in Venezuela were deposited. It must be noted, however, that according to paleographic reconstructions (e.g. Pindell and Kennan, 2001), these rocks have no relationship to the source rocks of the northern margin of South America. Later accretion of the upper Cretaceous oil-source rocks together with basalts from the upper part of the Caribbean Plate occurred along the present-day San Jacinto and Sinú folds belts. The source rocks are exposed in the San Jacinto Fold Belt and were penetrated by DSDP wells in the Colombian Basin and Costa Rica. Kerogen-type I and II with 2-15% TOC, a hydrogen index of 260 – 800 mg/g TOC and 417-450°C Tmax have been reported.

The late Oligocene to early Miocene section is represented by fine-grained facies of the Ciénaga de Oro, Porquero Inferior, Carmen Inferior and Perdices formations in the San Jorge-Plato Basin, San Jacinto Fold Belt and Maralú as well as the Pavo and Floresanto formations in the Sinú Fold Belt. A variable lithology characterizes these

units (see Chapter 2.4) which include mainly clastic material derived from the continent (shallow marine to deltaic deposits). This assemblage shows a gas-prone character, with Kerogen Types II, III and IV, containing up to 11% TOC. The hydrogen index is 20-280 mg/g TOC and Tmax is 417-436°C.

8.2 Heat flow in NW Colombia

Temperature and geothermal heat flow are critical parameters as they directly control hydrocarbon maturation and the physical properties of sediments and fluids. Modelling of the thermal and compaction history requires a detailed knowledge of sedimentation history, thermal properties of the sediments and the geodynamic evolution including also the effects of hydrothermal processes or local isostatic response.

Geothermal heat flow is one of the few constraints of thermal modelling that can be measured directly. Based on the available data, I have created a present-day heat flow distribution map for NW Colombia (Figure 33). Values from 50 to 59 mW/m^2 are observed for the major part of the Caribbean Plate which are in accordance with the heat flow characteristics of an oceanic plate older than 100 Ma (Stein, C. A. and S. Stein, 1992). Higher values from 60 to 120 mW/m^2 appear only in the western and northern part of the map, which may be explained by the Hess escarpment and the Beata ridge. The South American continental plate, which underlies the forearc region, is characterized by surface heat flows of 40 to 60 mW/m^2 which are typical for the stable continental crust (Demetrescu et al., 1989; Gordienko et al., 2001), but low with respect to the worldwide mean value for continental crust (65 mW/m^2, Pollack et al., 1993). Characteristic of the study area are the extremely low surface heat flow values along the deformation front of the Sinú-Colombia accretionary wedge, ranging from 30 to 38 mW/m^2 only, which indicates a disturbance of the heat flow from the Caribbean Plate to the surface. This is caused by the thermal blanketing effect of the thick sediment layer above the Caribbean oceanic crust at the active accretionary prism: a portion of the heat is consumed to warm up and thermally equilibrate the incoming sediments which are transported into the trench by the still ongoing subduction process since late Miocene. The outer high shows heat flows of 60 to 65 mW/m^2 (based on two values from wells). The higher values may be explained by the uplift of deeper and therefore hotter rocks nearer to the surface or by the expulsion of hot water from the dewatering of sediments (Yamano et al., 1992). Both the presence of mud diapirism and the results from the proposed crustal model (Chapter 7) support the presence of higher heat flows in the westernmost part of the Sinú Fold Belt and San Jacinto Fold Belt.

In contrast to extensional sedimentary basins, where crustal stretching and subsidence rates are important factors, the velocity of the subducting plate and uplift episodes of the outer high control the forearc sedimentation and burial maturation at convergent margins. At the NW margin of Colombia four different stages of subduction were identified in which convergence rates and heat flow have changed. The thermal history of accretionary prisms is mainly controlled by the heat flow from

the underlying oceanic plate. Variations of surface heat flow through time are due to changes of the convergence rate and varying inputs of young, cold sediments into the wedge. Heat-transfer from the oceanic plate to the overlying sediments is assumed to be constant since Maastrichtian (see above). The possibly hot-spot related formation of the plateau basalts 90 to 80 Ma ago contributes only to local changes of the heat flow from the oceanic plate. Low surface heat flows in the range from 25 to 35 mW/m^2 can be assumed, when fast subduction of the Caribbean Plate (>20mm/yr) occurred during upper Cretaceous to middle Eocene, late Oligocene to early Miocene and late Miocene to Pliocene. A recovery of the heat flow to the normal value of 50 to 59 mW/m^2 may have occurred between late Eocene and early Oligocene when the subduction rate decreased due to the collision of the Caribbean Plate with the North American Plate.
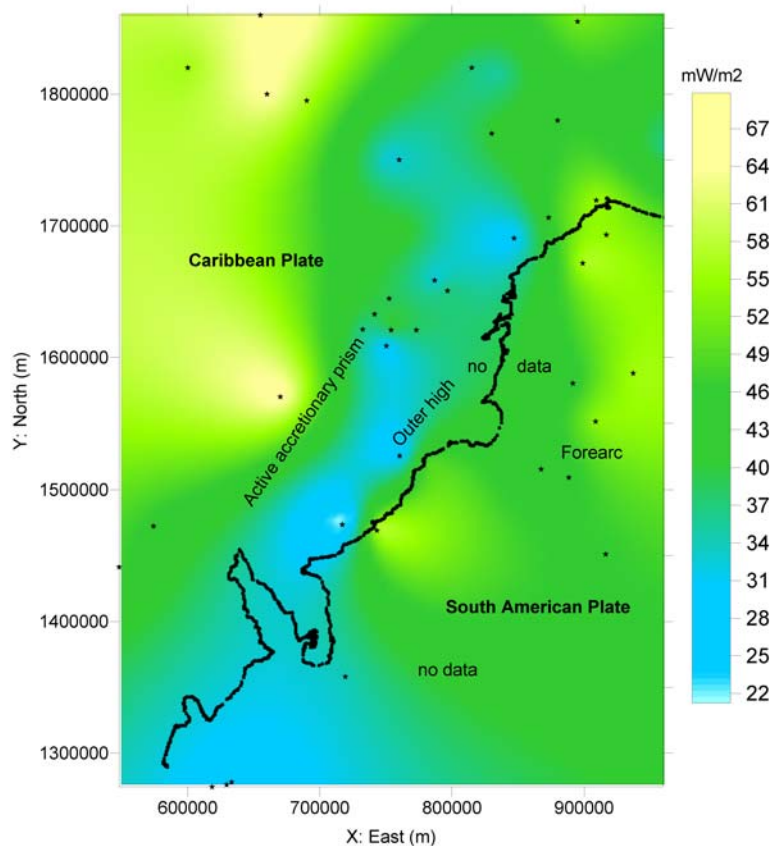

Figure 33: Heat flow map of NW Colombia (data compiled from BP Exploration, 1993; ESRI-ILEX, 1995; Hamza and Muñoz, 1996; TEPMA, 2002; Blackwell and Richards, 2004). Stars indicate the location of the measured heat flow data.

At active subduction zones, hydrocarbon accumulation is generally associated with forearc basins or intra-arc rifting. Deposits in such environments are strongly dependent on tectonic uplift, sedimentation supply and subsidence by loading. Changes of uplift and subsidence accompanied by the above mentioned changes of

the heat flow conditions complicate the evaluation of the thermal history of sediments especially present in the outer high as shown by the analyses of ESRI-ILEX, 1995 and TEPMA, 2002. As mentioned above, the state of hydrocarbon maturation can be estimated from vitrinite reflectance which indicates the degree of organic maturation. Several kinetic models for the calculation of vitrinite reflectance (Ro%) as a function of time and temperature exist in the literature. In order to achieve an estimation of the degree of organic maturation in the study area, the Easy% Ro-model of Sweeney and Burnham (1990) was selected where the vitrinite transformation is described by 20 parallel first-order Arrhenius reactions. A VBA software application was created, using the Easy% Ro algorithm as described by Sweeney and Burnham (1990). Input parameters include the estimation of the heat flow with time considering different convergent rates, variation of temperature with depth and two distinct starting times: $t_0 1$ at 72 Ma (initial development of the accretionary prism I) and $t_0 2$ at 27 Ma (initial development of the accretionary prism II). Heat-flows at recent subduction zones as well as at passive continental margins were used to estimate the impact of different subduction convergent rates on the surface heat-flow with time. Constant rock heat-conductivity through time was assumed.

Figures 34 and 35 show the variation of Ro% as a function of depth and time for sediments which were deposited at the accretionary wedge 83 to 72 Ma (Fig. 34), and 30 – 27 Ma ago (Fig. 35). The time-temperature profiles reflect different stages of the subduction process, considering a lull of convergence between late Eocene and early Oligocene time accompanied by a recovery of the thermal heat flow to the normal geothermal gradient (i.e. $\approx$ 30°C/km) and an acceleration of the subduction in late Oligocene, resulting in a low heat flow regime due to the transport of cold and water-rich sediments into the wedge. Because it is beyond the purpose of this study to develop a concrete reconstruction of the time-dependent burial of sediments, only general assumption on the maturation stage of the rocks present in the accretionary prisms are outlined.

Current depths of upper Cretaceous to Paleocene rocks vary from 10 km (according to the density model) to near-surface (results from wells) which reflects the complex burial history due to imbricate thrust faulting within the accretionary prisms I and II. It can be derived from Figure 34 that the oil-generation window (Ro%: 0.65 – 1.1: peak oil generation, Waples, 1980) started at a depth of 6 to 4 km in late Eocene time and moved to 4.8 to 3.4 km in recent time. Sediments within this time-depth range would be mature and based on measured TOC content of upper Cretaceous rocks, as mentioned above, it is possible that oil has been generated from these rocks since late Eocene time. Nevertheless, most of the upper Cretaceous to Paleocene sediments are now at depths deeper than 6 km and are therefore over-mature. Subsidence and exhumation paths are shown and explained in Figure 34.
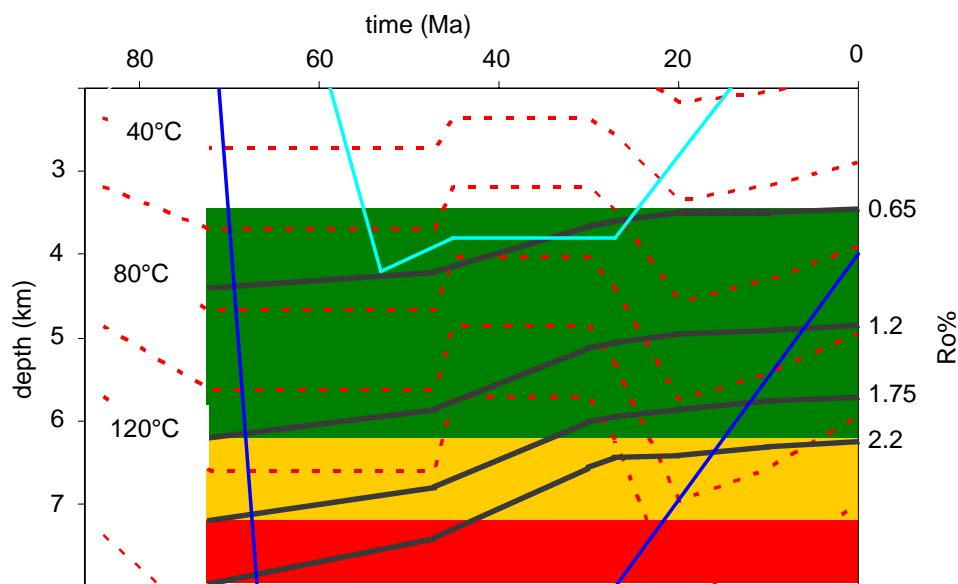
Figure 34: Depth-time plot and reconstruction of the maturation conditions for sediments with $t_0(1)$ = 72 Ma. Red lines indicate isotherms, black lines iso-Ro% values. Ro%-range of 0.65 and 1.2 is shown as green (oil window), of 1.2 to 1.75 as yellow (limit of 50° API oil) and of 1.75 to 2.2 as red area (limit for wet gas); red lines are isotherms in 20 K distances. Blue lines indicate estimated subsidence and exhumation paths for Cretaceous sediments for two cases: Dark blue line: subduction of upper Cretaceous sediments starts at 72 Ma with a subsidence rate of 0.45 km/Ma; light blue line: subduction of upper Cretaceous sediments starts at 62 Ma with a subsidence rate of 0.45 km/Ma; for both cases, exhumation starts by thrust imbrications, when sediments enter the continental wedge. Final depth of 4 km (case 1) and 0 km (case 2) are derived from present depths of Cretaceous sediments in the San Jacinto Fold Belt area. Based on these depths, an exhumation rate of 0.14 km/Ma is calculated for both cases. Depending on the time when these sediments entered the subduction zone, Cretaceous sediments are either overmature (subducted before 62 Ma) or mature to immature (subducted after 62 Ma). Because thickness of Cretaceous sediments on the Caribbean Plate decreases with increasing distance from the South American continent, it can be assumed that most of the Cretaceous sediments are over-mature today.

Eocene to Miocene sediments are found at depths between 0 and 6 km (based on wells). The oil-generation window started at a depth from 5.3 to 3.8 km in Oligocene and is located at 5 to 3.6 km in recent times. Sediments deposited in Eocene to late Oligocene would be situated now well within the oil-generation window, but due to low TOC content it seems unlikely that oil was generated (ESRI-ILEX, 1995).
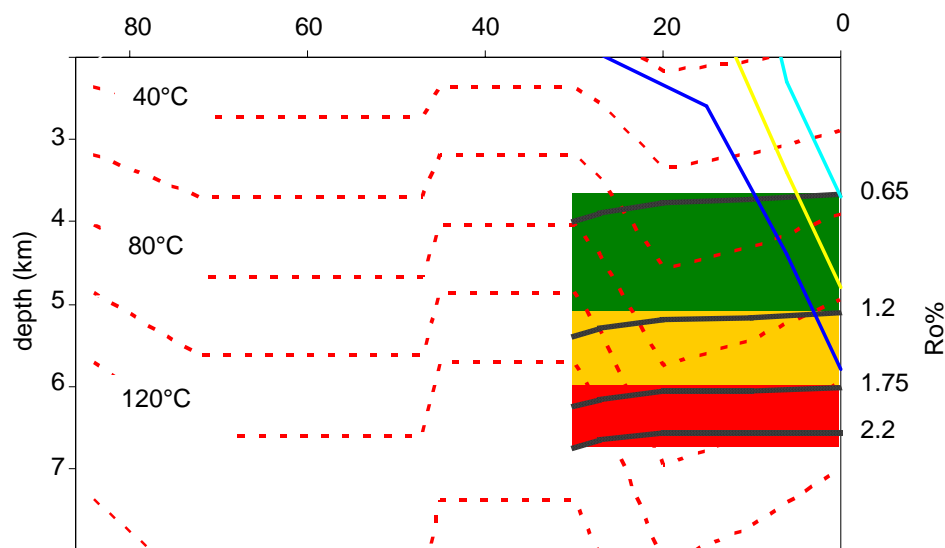
Figure 35: Depth-time plot and reconstruction of the maturation conditions for sediments with $t_0(2)$ = 30 Ma; refer to Figure 34 for further details. Dark blue, yellow and light blue lines indicate subsidence paths as observed for sediments in the Sinú Fold Belt area (dark blue: upper Cretaceous; yellow: late Oligocene; light blue: middle Miocene). According to this, sediments of Oligocene to Miocene age are within the oil generating window today.

Another possible source can be found in late Oligocene to late Miocene sediments as the TOC content is at 11%. As shown in Figure 35, it is likely that these sediments entered the oil generating field during fast subduction (Chapter 7.4) coeval with the likely onset of rapid thrust-imbrication in the accretionary prism in middle to late Miocene time. Miocene rocks at depths of 2 to 4 km are immature, having Ro% values of 0.3 to 0.6 (Figure 35). This is comparable to measured values of Vitrinite Reflectance on such sediments (e.g. 0.5 to 0.67 for Tertiary rocks at 3.5 km, BP Exploration, 1993; TEPMA, 2002).

From the general calculation of the time-temperature maturation process above it is possible to generate oil from both late Oligocene to late Miocene and upper Cretaceous source rocks. Based on the results of the density model and from well-data, it can be concluded that the major part of the upper Cretaceous to Paleocene rocks are over-mature, whereas Miocene sediments at a depth from 2 to 4 km did not reach the mature stage until today. Nevertheless, it must be considered that several assumptions were made for these two models. Other scenarios for the evolution of the geothermal heat flow with time and depth could lead to significantly different results. Also, the pressure regime within the accretionary wedge can influence oil generation, and finally, the intense deformation and thrusting can disrupt the burial history of hanging-wall strata and induce rapid exhumation within the considered time frame.

9. CONCLUSIONS

The following main conclusions can be drawn from the geological interpretation of the different geophysical methods applied in this study:

- The present-day crustal structure of the Colombian Caribbean margin is a result of the East-Northeast migration of the Caribbean Plate and its subsequent subduction beneath Colombia which has generated strike-slip fault systems, lateral displacements, rotation and inversion during the Cenozoic.

- 3D gravity modeling defines a shallow dipping Caribbean Plate that subducts at ~ 5° beneath northwest Colombia.

- The continued Caribbean-South American plate convergence since Upper Cretaceous has formed two accretionary prisms: the fossil accretionary prism (outer high), which includes the easternmost part of the Sinú-Colombia Accretionary Wedge and the San Jacinto Fold Belt, is assumed of Upper Cretaceous to middle Miocene age, and the active frontal accretionary prism of late Miocene to recent age, which corresponds to the external part of the Sinú-Colombia Accretionary Wedge.

- A seaward-vergent imbricate thrust system, which is developed in the frontal prism by the active deformation and strong shortening, is well defined in the seismic data.

- The older (fossil) accretionary prism is initially formed by upper Cretaceous basalts and ocean-floor sediments detached from the downgoing Caribbean Plate and subsequently emplaced on top of the continental basement of the South American Plate through backthrusting. Blocks of this oceanic "basement complex" are exposed and have been drilled in the San Jacinto Fold Belt. Occurrence of ultramafic rocks to the south of the San Jacinto Fold Belt is interpreted to be scraped-off remnants of peridotite-cored uplifts but not obducted oceanic crust.

- The older prism becomes an outer high as it grows and uplifts. Seaward, the outer high is characterized by normal faulting, growth folding and mud diapirism. Landward, the insufficient seismic coverage and its decreasing resolution do not allow determining the configuration of the pre-Oligocene units.

- The continental crust of the overriding South American Plate acted as a static-rigid backstop for the accreted older prism. 3D gravity and magnetic modelling suggest a seaward-dipping geometry for the static backstop.

85

- The complexly deformed outer high, which is approximately 80 km wide and more than 10 km deep, behaves as the dynamic backstop for the younger accretionary prism. A landward-dipping limit between the active and fossil (dynamic backstop) accretionary prisms is inferred from the seismic data.

- The Sinú Fault does not represent a limit between two distinct units accreted in different events because no sharp lateral density contrast from the 3D density model can be identified.

- The San Jorge-Plato Forearc Basin is formed between the older accretionary complex and arc framework. Some small depocenters developed behind the modern accretionary prism in the shelf sector are also interpreted as part of the forearc domain. The transition between outer high and the main forearc basin is marked by the kilometer-wide Romeral Fault Zone, which represents a structural break between the smaller and by mud diapirism deformed basins that fossilizes the outer high to the west and the main San Jorge Forearc Basin to the east. The evolution of the forearc basins is controlled by the tectonic uplift, sediment supply and basement subsidence by loading. Tectonic subsidence mechanisms, which were not discussed in this study, could be related to crustal extension of the static backstop or localized tectonic erosion.

- 3D gravity and magnetic modelling indicate that the Romeral Fault System involves continental basement-type along the transition from San Jorge-Plato Basin to San Jacinto Fold Belt, which allows the conclusion that the Romeral does not represent a boundary between ocean and continental crust. The Romeral and its associated structures form an intra-continental dextral transpressive fault system which has developed as a result of the oblique convergence between Caribbean and South American plates.

- From the proposed crustal model, two ocean-continental crust boundaries can be identified: an upper one, which represents the highly deformed east-vergent backthrust that emplaced the oceanic material onto the continental basement of the arc framework, and a lower one, which represents the eastward dipping boundary between the downgoing Caribbean Plate and the overriding South American Plate.

- The heat-flow distribution in NW Colombia reflects the strong control by continued uplift and subsidence phases during the development of the accretionary complex which makes the determination of the burial and thermal history very difficult. Based on general calculations of the Vitrinite Reflectance, it can be speculated that the oil-generation window has been at depths from 6 to 3 km since Maastrichtian time indicating that a major part of the upper Cretaceous source rocks are over-mature, whereas a part of the Miocene rocks has not yet reached the mature stage.

REFERENCES

Alfonso, C. A., Sacks, P. E., Secor D. T; Rine, J. and Pérez V., 1994: A Tertiary fold and thrust belt in the Valle del Cauca Basin, Colombia Andes, Journal of South American Earth Sciences 7 (3–4): 387 – 402.

Aubouin, J., Baltuck, M., Arnott, R.J., Bourgois, J., Filewiez, M., Helm, R., Kvenvolden, K. A., Lienert, B., Mc Donald, T., Mc Dougall l. K., Ogawa, Y., Taylor, E. and Winsborough, B., 1982: Leg 84 of the Deep Sea Drilling Project, subduction without accretion, Middle America Trench off Guatemala, Nature 297: 458–460.

Ball, M.M., Harrison, C.G.A. and Supko, P.R., 1969: Atlantic opening and the origin of the Caribbean, Nature 223: 167–168.

Barrero, D., Alvarez, J., and T. Kassem, 1969: Actividad ígnea y tectónica en la Cordillera Central, Boletín Geológico de INGEOMINAS 17 (1-3): 145-173.

Bermúdez, A., and Acosta, R., 1978: Mapa gravimétrico anomalías de Bouguer simples de Colombia, paper presented at 2nd Congreso Colombiano de Geología – INGEOMINAS, Bogotá, Colombia.

Bird, D., 1997: Interpreting magnetic data: online presentation from two articles by same author, entitled "Primer: Interpreting Magnetic Data" in Geophysical Corner, AAPG Explorer, May, 1997, and "Geology Should Rule Interpretation" in Geophysical Corner, AAPG Explorer.

Blackwell, D. and M. Richards, 2004: Geothermal map of North America, published by AAPG, website: http://bookstore.aapg.org/

Bonini, W. E., Garing, J. D. and Kellog, J. N., 1980: Late Cenozoic uplifts of the Maracaibo - Santa Marta Block, slow subduction of the Caribbean plate and results from a gravity study, 9th Trans. Caribbean Geol. Conference: 99 - 105.

Bowland, C. L., 1993: Depositional history of the western Colombian, Caribbean Sea, revealed by seismic stratigraphy, GSA Bulletin 105: 1321 – 1345.

Bowin, C., 1976: The Caribbean: Gravity Field and Plate Tectonics, Special Papers Geological Society of America 169: 79 p.

BP Exploration, 1993: Source risk in the Sur del Caribe Area, North-West Colombia, Technical Report 3276 of ECOPETROL S.A: 51-54.

Brandon, M. T., Johnson, S. Y., Stewart, R. J., McClain, K. J. (1984): Cross section B-B'-B", western Washington, in Ocean Margin Drilling Program, Regional Atlas Series 1, edited by L. D. Kulm et al., Marine Science International Woods Hole, Mass.: 19-20

Brown, L. F., 1985: Seismic Stratigraphic Interpretation and Petroleum Exploration. Continuing Education Course Note Series 16, AAPG Department Education: 3-4.

Burke, K., Fox, P.J. and Sengör, A.M.C., 1978: Buoyant ocean floor and the evolution of the Caribbean,. Journal Geophysics Research 83: 3949–3954.

Burke, K., 1988: Tectonic evolution of the Caribbean: Annual Revue of Earth and Planetary Sciences 16: 201-230.

Byme, T., Hibbard, J., 1987: Landward vergence in accretionary prisms: The role of the backstop and thermal history, Geology 15: 1163-1167.

Byrne, D. E., Wang, W. and Davis, D., 1993: Mechanical role of backstops in the growth of forearcs, Tectonics 12 (1): 123 – 144.

Callasou, S., Larroque, C., and Malavieille, J., 1993: Transfer zones of deformation in thrust wedges: an experimental study, Tectonophysics, 221: 325-344.

Campbell, C. J. 1968: The Santa Marta wrench fault of Colombia and its regional setting. Trans. IV Caribbean Geol. Conf., Trinidad: 247 – 261.

Case, J. E, Duran, L. G., Lopez, A. and Moore, W. R., 1971: Tectonic Investigations in Western Colombia and Eastern Panama, GSA Bulletin 83: 2685 – 2712.

Case, J. E. and McDonald, W. D., 1973: Regional Gravity Anomalies and Crustal Structure in Northern Colombia. GSA Bulletin 84: 2905-2916.

Case, J. E., 1974: Major Basins along the Continental Margin of Northern South America: In Burk, C. A, and C. L. Drake, eds., The Geology of Continental Margins, New York Springer-Verlag: 733 – 742.

Case, J. E., Holcome, T. L. and Martin, R. G., 1984: Map of geologic provinces in the Caribbean region, in The Caribbean-South America Plate Boundary and Regional Tectonics, edited by Bonini W. E, Hargraves R. B. and Hagam R.: 1-30.

Case, J. E., Shagam, R., and Giegengack, R. F., 1990: Geology of the northern Andes; an overview, in G. Dengo and J. E. Case, eds., The Caribbean region: GSA, The geology of North America H: 177-200.

Cediel, F., Etayo, F., and Cáceres, C., 1994: Facies Distribution and tectonic setting through the Phanerozoic of Colombia: INGEOMINAS, ed., Geotec Ltd., Bogotá (17 time-slices/maps in scale 1:2000.000).

Cediel, F., Shaw, R. and Cáceres, C., 2003: Tectonic Assembly of the Northern Andean Block., in C. Bartolini, R.T. Buffer, and J. Blickwede, eds., The Circum-Gulf of

Mexico and the Caribbean: Hydrocarbon habitats, basin formation, and plate tectonics: AAPG Memoir 79: 815-848.

Cediel, F., and Cáceres, C., 2000. Geological Map of Colombia, Third Edition: Geotec Ltd., Bogota, digital format with legend and tectonostratigraphic chart.

Cerón, J., 2002: Evaluación Regional de la Cuenca Caribe – Offshore Colombia, Technical Report of ECOPETROL: 33 p.

Cerón, J. and Kellog, J. 2005: The geometry of the basement in NW Colombia: Implications in the evolution of the Colombian basin, 17th Caribbean Geological Congress, San Juan, Puerto Rico.

Christofferson, E. 1973: Linear magnetic anomalies in the Colombia Basin, Central Caribbean Sea, GSA Bulletin 84: 3217 – 3230.

Coleman, R.G., 1977: Ophilolites: ancient oceanic lithosphere? (Mineral and rocks). Springer Verlag, 229 p.

Coleman, R.G., 2000: Prospecting for ophiolites along the California continental margin. In: Dilek, Y. D., Moores, E. M., Elthon, D. and Nicolas, A. (eds) Ophiolites and Oceanic Crust: New Insights from Field Studies and the Ocean Drilling program. GSA, Special Papers 349: 351-364.

Cortes, M and Angelier, J., 2005: Current states of stress in the northern Andes as indicated by focal mechanisms of earthquakes, Tectonophysics 403: 29-58.

Davis, D. M., 1996: Accretionary mechanics with properties that vary in space and time, in Subduction: Top to Bottom, Geophysics Monogr. Series (edited by G. E. Bedout et al., AGU, Washignton) 96: 39-48.

Demetrescu, C., Ene, M., Andreescu, M., and Burst, D., 1989: On the geothermal regime of the Moesian Platform and Getic depression, Tectonophysics 164: 281–287.

Dickinson, W. R., 1973: Widths of modern arc-trench gaps proportional to past duration of igneous activity in associated magmatic arcs, Journal Geophysical Research, 78: 3376-3389.

Dickinson, W. R., 1974: Plate tectonics and sedimentation. In: Tectonics and Sedimentation (Ed. By W. R. Dickinson), Soc. Econ. Paleont. Miner. Spec. Pub., 22: 1-27.

Dobrin, M. B., 1976: Introduction to Geophysical Prospecting, McGraw-Hill, Inc. Third Edition: 533 – 567.

Donnelly, T.W., 1985: Mesozoic and Cenozoic plate evolution of the Caribbean region, in: Stehli, F.G., Webb, S.D. (eds.), The Great American Biotic Interchange: 89–121.

Duque-Caro, H., 1972: Ciclos tectónicos y sedimentarios en el norte de Colombia y sus relaciones con la paleo-ecología: Boletín Geológico de INGEOMINAS 19 (3): 1–23.

Duque-Caro, H., 1973: The geology of the Montería area: Colombian Society of Petroleum Geologists and Geophysicists 14th Annual Field Conference, Guidebook, Bogotá, Colombia: 397–431.

Duque-Caro, H., 1975: Los foraminíferos planctónicos y el terciario de Colombia: Rev. Esp. Micropal. 7 (3): 403-427.

Duque-Caro, H., 1976: Características estratigráficas y sedimentarias del Terciario marino de Colombia: Memorias del 2nd Congreso Latinoamericano de Geología, Caracas, 1973: 945-964.

Duque-Caro, H., 1979: Major structural elements and evolution of northwestern Colombia, in J. S. Watkins, L. Montadert, and P. W. Dickerson, eds., Geological and geophysical investigations of continental margins, AAPG Memoir 29: 329–351.

Duque-Caro, H., 1984: Structural Style, diapirism and accretionary episodes of the Sinú-San Jacinto terrane, southwestern Caribbean borderland, GSA Memoir 162: 303-316.

Duque-Caro, H., 1990: The Chocó Block in the northwestern corner of South American: Structural tectonostratigraphic and paleographic implications, Journal of South American Earth Sciences 3: 71-84.
Edgar, T. N., Ewing J. and Hennion J., 1971: Seismic Refraction and Reflection in Caribbean Sea, AAPG Bulletin 55 (6): 833 -870.

Engebretson, D.C., Cox, A., Gordon, G.R., 1985: Relative plate motions between oceanic and continental plates in the Pacific basin, GSA Special Paper 206: 1–64.

ESRI (Earth Sciences Resources Institute at University of South Carolina) – ILEX Ltd., 1995: Evaluación Geológica Regional de la Cuenca de Sinú – San Jacinto, Technical Report 3851 of ECOPETROL S.A.

Finn, C.A., Pilkington, M., Miles, W., Hernandez, I., Cuevas, A., Velez, J., Sweeny, R., Kucks, R., Bankey, V. and Daniels, D., 2002: The new North American magnetic anomaly map, published by USGS. Gridded data: Online: http://pubs.usgs.gov/of/2002/ofr-02-414/

Fitch, T., 1972: Plate convergence, transcurrent faults, and internal deformation adjacent to Southeast Asia and the Western Pacific. Journal of Geophysical Research 77 (23): 4432 – 4460.

Flinch, J. F., M. V. Grand, and P. Casero, 2000: Accretion and obduction along the Sinú-Lower Magdalena area (Northern Colombia), Memorias VII Simposio Bolivariano, Exploración Petrolera en las Cuencas Subandinas, Sociedad Venezolana de Geólogos, Caracas, Venezuela, September, 2000: 218–229.

Flinch, J. F., Amaral J., Doulcet, A., Mouly, B., Osorio, C. Pince, J. M., 2003: Onshore-Offshore Structure of the Northern Colombia Accretionary Complex, Memory AAPG International Conference Barcelona, Spain, September, 2003: 1 – 5.

Flinch, J., Amaral, J., Doulcet, A., Mouly, B., Osorio, C. and Pince, J. M., 2003: Structure Of The Offshore Sinú Accretionary Wedge, Northern Colombia, Memorias VIII Simposio Bolivariano - Exploración Petrolera en las Cuencas Subandinas, Asociación Colombiana de Geólogos y Geofísicos del Petróleo, Cartagena, Colombia, September, 2003: 76-83.

Flinch, J. F., 2003: Structural Evolution of the Sinú-Lower Magdalena Area (Northern Colombia), in C. Bartolini, R. T. Buffler, and J. Blickwede, eds., The Circum-Gulf of Mexico and the Caribbean: Hydrocarbon habitats, basin formation, and plate tectonics: AAPG Memoir 79: 776–796.

Freymüller, J., Kellog, J. and Vega, V., 1993: Plate Motions in the North Andean Region, Journal of Geophysical Research 98 (B12): 21,853-21,863.

Frisch, W., Meschede, M., Sick, M., 1992: Origin of the Central American ophiolites: evidence from paleomagnetic results. GSA Bulletin 104 (10): 1301–1314.

GETECH (Geophysical Exploration Technology Ltd. – School of Earth Sciences at University of Leeds), 2001: Colombia Satellite Gravity and Bathymetry (Atlantic Region), Technical Report of ECOPETROL S.A: 30 p.

Gordienko, V. V., Gordienko, I. V., Zavgorodnjaja, O. V., and Usenko, O. V., 2001: Heat flow map of Ukraine and Moldova, in: Gordienko, V. V. and Tarasov, V. N. (Eds.): Recent activization and He-isotopy of Ukrainian territory, (in Russian), Znanie, Kiev: 12p.

Götze, H.J. and Lahmeyer, B., 1988: Application of three-dimensional interactive modelling in gravity and magnetics, Geophysics 53 (8): 1096-1108.

Schmidt, S. and Götze, H. J., 1995: IGMAS 3D Gravity and Magnetic Modeling Program. Publication on the internet at: http://userpage.fu-berlin.de/~sschmidt/Sabine_IGMAS.html

Grosse, E., 1926: Estudio Geológico del Terciario Carbonífero de Antioquia en la parte occidental de la Cordillera Central de Colombia, entre el río Arma y Sacaojal, ejecutado en los años de 1920 - 1923: Berlín, Dictrich Reimer: 361 p.

Hamza, V. M., and Muñoz, M., 1996: Heat flow map of South America, Geothermics 25 (6): 596-646.

Hayes, D. E., 1966: A Geophysical Investigation of the Perú – Chile Trench, Marine Geology 4: 309 – 351.

Hofmann, Y., Jahr, T. and Jentzsch, G., 2003: Gravimetric modelling and studies of the gravity field of the Vogtland area and its surroundings, Journal of Geodynamics 35 (1-2): 209 – 220.

ICP (Instituto Colombiano del Petroleo – ECOPETROL S.A.), 2000: Evaluación Regional Integrada Cuenca Valle Inferior del Magdalena, Technical Report of ECOPETROL S.A (CDROM 2).

Instituto Geográfico Agustín Codazzi – IGAC, 1959: Mapa Gravimétrico de la Republica de Colombia. R. M. Slinkard, principal compiler.

INGEOMINAS, 1988: Mapa Geológico de Colombia, scale: 1.500.000, compiled by Vargas, R., Espinosa, A., Núñez, A., González, H., Orrego, A., Etayo, F, Duque-Caro, H., Mendoza, H., and Paris, P.

INGEOMINAS, 1997: Atlas Geológico Digital de Colombia, scale 1:500.000, plates 1, 3, 4 and 6.

James, K. H., 2002: Cretaceous-Eocene flysch deposits of the Caribbean area: Chronological record of discussions and implications for tectonic history and early phases of hydro-carbon generation, 16th Caribbean Geological Conference, Barbados, Abstracts.

James, K. H., 2006: Arguments for and against the Pacific origin of the Caribbean Plate: discussion, finding for an inter-American origin, Geologica Acta 4 (1-2): 279-302.

Karig, D. F., and Sharman, G. F., 1975: Subduction and accretion at trenches, Bulletin Geological Society of America, 86: 377-389.

Kellog, J. N., 1980: Cenozoic basement tectonics of the Sierra de Perijá Venezuela and Colombia, 9th Caribbean Geological Conference.

Kellog, J. and Bonini, W. E., 1982: Subduction of the Caribbean Plate and basement uplifts in the overriding South America Plate, Tectonics 1: 251 – 276.

Kellog, J, N., Godley, V. M., Ropain, C., and Bermúdez, A., 1983: Gravity anomalies and tectonic of northwestern South America, 10th Caribbean Geological Conference.

Kellog, J. N., 1984: Cenozoic tectonic history of the Sierra de Perijá and adjacent basins, in Bonini, W. E., Hargraves, R. B., and Shagam, R., eds., Caribbean-South American plate boundary and regional tectonics, GSA Memoir 162: 239 – 261.

Kellog, J. and Vega, V., 1995: Tectonic development of Panama, Costa Rica, and Colombian Andes: Constrain from Global positioning System geodetic studies and gravity, Mann Paul (editor), Geologic and Tectonic Development of the Caribbean Plate boundary in southern Central America, GSA Special Paper 295: 75 – 90.

Kerr, A. C., Taney, G. F., Marriner, F., Nivia, A., Klaver, G. T., and Saunders, A. D., 1996: The geochemistry and tectonic setting of late Cretaceous Caribbean and Colombian volcanism: Journal of South America Earth Sciences 9: 111-120.

Kerr, A.C., Tarney, J., 2005: Tectonic evolution of the Caribbean and northwestern South America: The case for accretion of two Late Cretaceous oceanic plateaus, Geology 33 (4): 269-272.

Klitgord, K. and Schouten, H., 1986: Plate kinematics of the central Atlantic. In: Tucholke, B.E., Vogt, P.R. (eds.), The Western Atlantic Region (The Geology of North America, M), GSA, Boulder, Colorado: 351–378.

Kopp, H., Flueh, E. R., Klaeschen, D., Bialas, J., and Reichert, C., 2001: Crustal Structure of the central Sunda margin at the onset of oblique subduction, Geophysical Journal International, 147: 449-474.

Kopp, H. and Kukowski, N. 2003: Backstop geometry and accretionary mechanics of the Sunda margin, Tectonics 22: 11-1 – 11-15.

Land and Marine Gravity CD-ROMs, 1999: Compiled by David Dater, Dan Metzger, and Allen Hittelman: U.S. Department of Commerce, National Oceanic and Atmospheric Administration, National Geophysical Data Center, Boulder, CO. Gravity 1999 Edition on 2 CD-ROMs.

Larroque, C., Calassou, S., Malavielle, J. and Chaniert, F., 1995 : Experimental modelling of the forearc basin development during accretionary wedge growth, Basin Research 7: 255-268.

Laverde, F., 2000: The Caribbean Basin of Colombia, a composite Cenozoic Accretionary Wedge with Under-Explored Hydrocarbon Potential, Memorias del VII Simposio Bolivariano de Exploración Petrolera en Cuencas Subandinas, Caracas, Venezuela, September, 2000: 394 – 410.

Lu, R. S and McMillen, K. J., 1982: Multichannel Seismic Survey of the Colombia Basin and Adjacent Margins, in Watkins, J. S and Drake, C. L., eds, Studies in Continental Margin Geology: AAPG Memoir 34: 395 – 410.

Luna, O., Manrique, M., Laverde, F., Buchelli, F., Rueda. M. C., 2001: Informe Geologico Regional de la Provincia Petolífera del Noroccidente Colombiano, Technical Report of ECOPETROL S.A: 133 p.

Malavé, G. and Suárez, G., 1995: Intermediate-depth seismicity in northern Colombia and western Venezuela and its relationship to Caribbean Plate subduction, Tectonics 14: 617-628.

Malfait, B.T., Dinkelman, M.G., 1972: Circum-Caribbean tectonic and igneous activity and the evolution of the Caribbean plate, GSA Bulletin 83: 251–272.

Maresch, W. V., Stoeckhert, B., Baumann, A., Kaiser, C., Kluge, R., Krueckhans-Lueder, G., Brix, M. R., and Thomson, M., 2000: Crustal history and plate tectonic development in the southern Caribbean: Zeitschrift für Angewandte Geologie, 1: 283-289.

McCourt, W. J., and Apsden, J. A., 1983: Modelo Tectónico de Placas para la Evolución Fanerozoica de Colombia Central y del Sur. X Conferencia del Caribe, Cartagena, Colombia: 27 p.

McCourt, W. J., and Millward, D. 1983: Fallas principales de acreción de las placas en el Valle del Cauca, Suroccidente de Colombia, IV Congreso Colombiano de Geología, Cali, Colombia: 7 p.

Mejía V. M. and Durango, J.R., 1981-1982: Geología de las lateritas niquelíferas de Cerromatoso, Boletín de Geología de la Universidad Industrial de Santander 15 (29): 117-123.

Meschede, M., Frisch, W., Herrmann, U.R., Ratschbacher, L., 1997: Stress transmission across an active plate boundary: an example from southern Mexico, Tectonophysics 266: 81–100.

Meschede, M and Frisch, W., 1998: A plate-tectonic model for the Mesozoic and Early cenozoic history of the Caribbean Plate, Tectonophysics 296: 269 – 291.

Mountney, N. P and Westbrook, G., 1997: Quantitative analysis of Miocene to recent forearc basin evolution along the Colombian convergent margin, Basin Research 9: 177-196.

Nasu, N., 1982: Multi-channel seismic reflection data across the Nakai Through. IPOD-Japan Basic Data Series, 4, Ocean Research Insitute, University of Tokio.

Nettleton, L. L., 1971: Elementary Gravity and Magnetics for Geologists and Seismologists. Monograph Series (Wuenschel, P. C., Editor) Number 1, Society of Exploration Geophysicists, 121 p.

Ortiz, F., 2004: Guías para la localización de metales preciosos en ofiolitas colombianas, Informe de Avance Proyecto CYTED XIII.1. Ofiolitas: Características mineralógicas y petrográficas del Yacimiento de Níquel de Cerro Matoso. Dyna, Medellín, Colombia, Año 71 (142): 11 – 23.

Pennington, W. D., 1981: Subduction of the Eastern Panama Basin and Seismotectonics of Northwestern South America. Journal of Geophysical Research 86 (B11): 10753-10770.

Peters, L. J., 1949: The direct approach to magnetic interpretation and its practical application: Geophysics 14: 290 – 320.

Pindell, J.L., Dewey, J.F., 1982: Permo-Triassic reconstruction of western Pangea and the origin of the Gulf of Mexico/Caribbean region. Tectonics 1: 179-212.

Pindell, J., 1985: Alleghanian reconstruction and subsequent evolution of the Gulf of Mexico, Bahamas and Proto-Caribbean, Tectonics 4: 1 – 39.

Pindell, J., Cande, S. C, et al., 1988: A plate-kinematic framework for models of the Caribbean evolution, in, C. R. Scotese and W. W. Sager, eds., Mesozoic and Cenozoic plate reconstructions, Tectonophysics 155: 121-138.

Pindell, J.L., Barrett, S.F., 1990: Geological evolution of the Caribbean region; a plate-tectonic perspective, in: Dengo, G., Case, J.E. (eds.), The Caribbean Region, The Geology of North America, GSA H: 405-432.

Pindell, J. L., 1993: Regional synopsis of Gulf of Mexico and Caribbean evolution: Gulf Coast Section, Society for Sedimentary Geology (SEPM), 13th Annual Research Conference Proceedings: 251-274.

Pindell, J., and Erikson, J.P., 1994: Sub-surface Jurassic shelf ?, NE Venezuela and Trinidad: Petroleum Exploration in the Subandean Basins, V Simposio Bolivariano, Venezuelan Geology Society: 244 – 262.

Pindell, J. L., and Tabbutt, K. D., 1995: Mesozoic-Cenozoic Andean paleogeography and regional controls on hydrocarbon systems, in A. J. Tankard, R. Suárez S., and H. J. Weisink, Petroleum basins of South America: AAPG Memoir 62: 101-128.

Pindell, J.., Higgs, R. and Dewey, J. F., 1998: Cenozoic palinspastic reconstruction, paleogeographic evolution, and hydrocarbon setting of the northern margin of South America, in J. L. Pindell and C. L. Drake, eds., Palaeogeographic Evolution and Non-

glacial Eustasy, northern South America: Special Publication, SEPM (Society for Sedimentary Geology): 45-86.

Pindell, J. and Kennan, L., 2001: Kinematic evolution of the Gulf of Mexico and Caribbean, in petroleum system of deep-water basins: Global and Gulf of Mexico experience, Proceedings, Gulf Coast Section, SEPM, 21st Annual Research Conference, December 2-5: Houston, Texas, Society for Sedimentary Geology (SEPM):193-220.

Pindell, J., Kennan, L., 2002a: Critical assessment of Caribbean seismic tomography (Hilst, 1990) in light of Caribbean kinematic evolution, 16th Caribbean Geological Conference, Barbados, Abstracts, 97p.

Pindell, J., Kennan, L., 2002b: Palinspastic paleogeographic evolution of Eastern Venezuela and Trinidad. 16th Caribbean Geological Conference, Barbados, Abstracts, 99p.

Pindell, J., Kennan, L., 2003: Synthesis of Gulf of Mexico and Caribbean Tectonic Evolution: Pacific Model for Caribbean Lithosphere. AAPG International Meeting, Barcelona, Abstracts.

Pindell, J., Kennan. L., Stanek, K.P, Maresch, W.V. and Draper, G., 2006: Foundations of Gulf of Mexico and Caribbean evolution: eight controversies resolved. Geologica Acta, Vol. 4, No. 1-2, p. 303-341.

Reyes-Harker, A., G., Montenegro-Buitrago, and Gómez, G. D., 2000: Evolución Tectonoestratigrafica del Valle Inferior del Magdalena, Colombia, Memorias VII Simposio Bolivariano, Exploración Petrolera en las Cuencas Subandinas, Sociedad Venezolana de Geólogos, Caracas, Venezuela, September 2000: 293–309.

Reyes-Santos, J. P., Mantilla, M. and González, J. S., 2000: Regiones Tectono-Sedimentarias del Valle Inferior del Magdalena, Colombia, Memorias VII Simposio Bolivariano, Exploración Petrolera en las Cuencas Subandinas, Sociedad Venezolana de Geólogos, Caracas, Venezuela, September 2000: 310– 333.

Ross, M.I., Scotese, C.R., 1988: A hierarchical tectonic model of the Gulf of Mexico and Caribbean region, in: Scotese, C.R., Sager, W.W. (eds.), Mesozoic and Cenozoic Plate Reconstructions, Tectonophysics 155: 139–168.

Ruiz, C., Davis, N., Bentham, P., Price, A. and Carvajal, D., 2000: Structure and tectonic evolution of the South Caribbean Basin, southern offshore Colombia: A progressive accretionary system, Memorias VII Simposio Bolivariano, Exploración Petrolera en las Cuencas Subandinas, Sociedad Venezolana de Geólogos, Caracas, September 2000: 334–355.

Schmidt, S. and Götze, H. J., 1995: IGMAS 3D Gravity and Magnetic Modelling Program, Publication on the internet at: http://userpage.fu-berlin.de/~sschmidt/Sabine_IGMAS.html

Sheriff, R. E., 1984: Encyclopedic Dictionary of Exploration Geophysics, Society of Exploration Geophysicists, Second Edition.

Silver, E.A., Ellis, M. J., Breen, N. A., Shipley, T. H., 1985: Comments on the growth of accretionary wedges, Geology 13: 6-9

Stein, C. A. and Stein, S., 1992: A model for the global variation in oceanic depth and heat flow with lithospheric age, Nature 359: 123–129.

Stern, R. J., 1998: A Subduction Primer for Instructors of Introductory – Geology Courses and Authors of Introductory – Geology Textbooks. Journal of Geoscience Education 46: 221 – 228.

Stephan, J.F., Mercier de Lepinay, B., Calais, E., Tardy, M., Beck, C., Carfantan, J.-C., Olivet, J.-L., Vila, J.-M., Bouysse, P., Mauffret, A., Bourgois, J., Thery, J.-M., Tournon, J., Blanchet, R., Dercourt, J., 1990: Paleogeodynamic maps of the Caribbean: 14 steps from Lias to Present. Bull. Soc. Géol. Fr. 8 (6): 915–919.

Sharma, P. V., 1997: Environmental and engineering geophysics. Cambridge University Press, First Edition: 83-94.

Sykes, L.R., Mc Cann, W.R., Kafka, A.L., 1982: Motion of the Caribbean plate during the last 7 million years and implications for earlier Cenozoic movements. Journal Geophysical Research 87: 10656–10676.

Sweeney J.J and Burkan, A. K., 1990: Evolution f o simple model of Vitrinite reflectance based on chemical kinetics. AAPG Bulletin 74 (10): 1159-1570.

Taboada, A., Rivera, L. A., Fuenzalida, A., Cisternas, A., Philip, H., Bijwaard, H., Olaya, J., and Rivera, C., 2000: Geodynamics of the northern Andes: Subductions and intracontinental deformation (Colombia), Tectonics 19 (5): 787 – 813.

Tectonic Analysis Inc., 1995: The paleographic evolution of Colombia: implications for hydrocarbons, Technical Report of ECOPETROL S.A.

TEPMA, 2002: Informe Técnico Anual – Año 2002, Technical Report of ECOPETROL S.A: 127 p.

Toto, E. A. and Kellog, J., 1992: Structure of the Sinú – San Jacinto Fold Belt – An Active Accretionary Prism in Northern Colombia. Journal of South America Earth Sciences 5 (2): 211 – 222.

Van der Hilst, R., 1990: Tomography with P, PP and pP delay-time data and three-dimensional mantle structure below the Caribbean region: Doctoral Dissertation, Institute of Earth Sciences, University of Utrecht, Netherlands, No. 67, 257 p.

Van der Hilst, R., and P. Mann, 1994: Tectonic implications of tomography images of subducted lithosphere beneath northwestern South America: Geology 22: 451–454.

Vernette, G., 1986: LE DiAPIRISME ARGILEUX ET SES CONSEQUENCES SUR LES CARACTERES MORPHOLOGIQUES ET SEDIMENTAIRES DE LA MARGE COLOMBIENNE DES CARAIBES. Bull. Inst. Géol. Bash d'Aquiíah,Bordeaux 40: 35-51.

Vernette, G., Mauffret, A., Bobier, C., Briceño, l. And Gayet, J., 1992: Mud diapirism, fan-sedimentation and strike-slip faulting, Caribbean Colombian margin, Tectonophysics 202: 335-349.

Waples, D.W., 1980: Time and temperature in petroleum generation – an application of Lopatin`s technique to petroleum exploration, American Association of Petroleum Geologists Bulletin 64: 916-926.

Wilson, J.T., 1965: Submarine fracture zones, aseismic ridges, and the international council of scientific unions line: proposed western margin of the East Pacific Ridge. Nature 207: 907– 911.

Yamano, M., J.-P. Foucher, M. Kinoshita, A. Fisher, R.D. Hyndman and ODP Leg 131 Shipboard Scientific Party 1, 1992: Heat flow and fluid flow regime in the western Nankai accretionary prism. Earth and Planetary Science Letters 109: 451-462.

ACKNOWLEDGMENTS

The development of this project would not have been possible without financial support from German Academic Exchange Service (DAAD). I am extremely grateful to this institution and to their support, especially from Dr. Eckhard Schmidt, Angelika Hennecke and Arpe Caspary, who I had the pleasure to meet, and also Hilde Mönch, Elke Massa Miranda, Maria Luisa Nünning and Michael Eschweiler.

I am very much indebted to Prof. Dr. Gerhard Jentzsch for inviting me to do my PhD thesis at Friedrich-Schiller University, for his help to address objectives and his patience for clarifying the gravity and magnetic concepts to me. His critical comments about the thesis manuscript are greatly appreciated.

I am very grateful to Prof. Dr. Jonas Kley for his constant advice, enthusiastic and enjoyable discussions on tectonic interpretation of northern Andes-Caribbean region and for his dedication to review the manuscript of this thesis.

This paragraph is too short to express my gratitude to Dr. Carlos Alfonso-Pava, co-adviser of this thesis, for his constant support throughout my work. I am especially grateful to him, because since 1997 he has showed me the fantastic world of structural interpretation of seismic data and structural modelling, and he also taught me how to develop a regional geological model; sharing his professional and personal experiences with me enriched my life.

Special thanks also to John Cerón. He supplied me with the gravity and magnetic grid-data and kindly responded to all my questions on the telephone and by e-mail during the gravity modelling. His expertise working with potential field data in the oil and gas industry motivated me to start this challenge.

Dr. Yvonne Hofmann introduced me to the IGMAS software and philosophy of 3D gravity modelling. She became a good friend, helping me even in personal matters. Her stimulation and assistance still continued after her departure from Jena. I have happy memories of our friendship and all the pleasant shared moments with her family in Ernstroda.

Dr. Sabine Schmidt is kindly thanked for her orientation by e-mail with IGMAS software and to solve some of my questions about 3D gravity modelling.

The idea to develop this project was born when I worked at INGEOMINAS. Dr. Adolfo Alarcón and Dr. Georgina Guzmán are acknowledged for their institutional support. Also special thanks to Eduardo López, Wilson Quintero and Carlos Rey for their support and technical suggestions.

Dr. Fabio Cediel and Dr. Carlos Cáceres encouraged me to complete my education in Germany. I thank their trust as well as the opportunity to have access to geological

SELBSTSTÄNDIGKEITSERKLÄRUNG

Ich erkläre, dass ich die vorliegende Arbeit selbstständig und unter Verwendung der angegebenen Hilfsmittel, persönlichen Mittteilungen und Quellen angefertigt habe.

Adriana Mantilla P.

Jena, 5. Juni 2007   Unterschrift der Verfasserin

CURRICULUM VITAE

Born: 7 February 1971, Bucaramanga (Colombia).

University Education

2007   Dr.rer.nat at Friedrich-Schiller-Universität Jena (Germany).

Dissertation: Crustal Structure of the Southwestern Colombian Caribbean margin: A geological interpretation of geophysical data.

Supervisors: Prof. Dr. Gerhard Jentzsch, Prof. Dr. Jonas Kley (Friedrich-Schiller-Universität Jena) and Dr. Carlos Alfonso-Pava (ECOPETROL S.A).

1998   Diploma in Geology at Universidad Industrial de Santander.

Diploma thesis: Balanced cross-section across the Middle Valley Basin, Eastern Cordillera and Llanos Basin (Colombia).

Supervisors: Prof. Ricardo Mier-Umaña (Universidad Industrial de Santander) and Dr. Carlos Alfonso-Pava (ECOPETROL S.A).

Professional Career

Since 2008   Geoscientist at Fugro-Robertson (Fugro Middle East).

1998-2002   Consultant Geologist on a variety of projects developed for the Colombian Oil Company (ECOPETROL S.A), Colombian Petroleum Institute (ICP) and Colombian Geological Survey (INGEOMINAS).

**1997**   Internship at ECOPETROL S.A.

Crustal Structure of the Southwestern Colombian Caribbean Margin
by Adriana Maria Mantilla Pimiento

Attachment 1: Model for the evolution of the Caribbean region from early Jurassic to late Miocene (Pindell and Kennan, 2001). NOAM – North America: SOAM – South America; CAR – Caribbean Plate; FAR – Farallon Plate; KUL – Kula Plate; NAM – North American Plate; SAm – South American Plate; HS – hotspot; RRF – ridge-ridge fault; V – volcanic; Oc – oceanic; CAY – Cayman; CC – Central Cordillera; DR – Dominican Republic; EC – Eastern Cordillera; ESC – Escambray; HA – Haiti; HUAL – Huallaga Basin; MAR – Margarita; MOC – Mocoa; Muertos Shelf; NC – Northern Cordillera; OCA – Oca Fault; PI – Isle of Pines or Isle of Youth; PR – Puerto Rico; SANT – Santiago Basin; SWH – Southwest Haiti; SMB – Santa Marta-Bucaramanga Fault; TOB – Tobago; VIR – Virgin Islands.

From Chapter 2.1, "Caribbean tectonic overview"

Crustal Structure of the Southwestern Colombian Caribbean Margin
by Adriana Maria Mantilla Pimiento

Attachment 2: Seismic composite profile (central cross-section) displays the typical morphological elements and tectonic domains of the subduction complex along the Southwestern Colombian Caribbean Margin. See Figure 4 for location.

From Chapter 3, "2D Structural Configuration"